第 21 屆教育部國家講座成果報告表

第 1 年：107 年 2 月 1 日至 108 年 1 月 31 日

國立交通大學應用數學系

賴明治 教授

中華民國 108 年 2 月 11 日

賴明治　　教授執行　107　年度國家講座成果報告表

該學年度國家講座執行情形：
一、教學課程綱要
1 偏微分方程導論(大學部一學期必修，90 人選此門課) Heat equation: derivation of the conduction of heat in a 1D rod, boundary conditions and physical meanings, Method of separation of variables for heat equation and Laplace equation, Fourier series and its convergence, Wave equation: vibrating strings and membranes, Non-homogeneous problems: heat flow with sources and non-homogeneous boundary conditions; Higher-dimensional PDEs 2 流體界面專題(研究生選修) Immersed boundary method and applications to the interfacial flows, Immersed interface method and its implementations, Interfacial flows with insoluble and soluble surfactant: mathematical models, numerical schemes and applications; Vesicle or inextensible interface problem: mathematical models, numerical schemes and applications 3 科學計算導論(研究生一學期必修，14 人選此門課) Finite difference approximations, Steady states and boundary value problem, Consistency, stability and convergence in L2 norm and maximum norm, Two-point boundary value problem with delta function singularity, Discrete delta function and interpolating accuracy, Elliptic equations and finite difference schemes, Fast elliptic solvers, Parabolic equations and finite difference schemes, von Neumann stability analysis, Hyperbolic equations and finite difference schemes
二、研究重點及方向
今年的的研究重點及方向，主要還是延續流體界面的問題，特別是在有界面活性劑及囊泡問題更深一層的研究。首先，我們分別發展了 level set method, immersed boundary method, grid based particle method 去研究三維可溶性與不可溶性界面活性劑的數值方法，這是將我們過去的研究成果做完全三維的推廣。在囊泡問題上面，我們將原來的囊泡在牛頓流體的問題推廣至非牛頓流體上面，我們很驚奇的發現囊泡在 shear flow 底下的穩定型態有負的傾斜角，這跟在牛頓流體有完全不一樣的現象，我們希望這個結果可作為日後實驗的驗證題材。另外，我也提出了一個有關不可延展介面的數學理論問題，給定一個外力，在二維 Stokes 方程底下的不可延展問題，證明解的適應性，也就是解是否存在及唯一的問題。我的猜測是當界面非圓時，速度場及未知張力是唯一決定的而壓力是唯一但 up to a constant，我們數值的結果驗證了我的猜測。另外，用沉浸邊界法有限差分去直接離散方程，我們可以獲得在速度場及未知張力一階收斂(L2 norm)的結果，而在壓力則是得到半階收斂的結果，目前我們尚未有嚴格理論上的證明，這也將是未來一年的研究方向。針對有 bending 的 non-stationary 二維 Stokes 方程底下的不可延展問題，我們發展了一套能量完全無條件穩定的數值方法，不僅可以嚴格證明其能量穩定性，數值上也驗證了其能量遞減的特性，未來也將朝如何用 fractional step 的技巧去有效解此線性方程組。

三、學校資源配合狀況

（一）學校對於講座主持人教學研究各項資源配合內容

本校除提供相關的各項資源配合主持人的開課要求外，亦提供彈性薪資獎勵與補助與國際高引用學者合作的相關費用，在此感謝本校的各項配合措施。

（二）國家講座開設跨校性選修課程、辦理全國巡迴講座並宣揚研究教學成果情形

在執行國家講座期間，主持人已在全國多所學校做最新研究議題及研究成果的巡迴演講，包含清華大學，高雄大學，中原大學等，其中清華大學演講內容已錄影存檔(見附件)，中原大學的錄影檔也可在 https://drive.google.com/file/d/.1_mehO8FBM1fB3CISZYFOd4LI_u1-y8z9/view?usp=drive_web獲得。對大學部開設的偏微分方程課程亦有外校學生來選課。此外，為推廣數學建模的重要性，主持人擔任理事長的台灣工業與應用數學會，協助成功大學舉辦高中數學建模黑克松活動，本人並於比賽中擔任評審並與高中生參賽者分享數學的重要性與實際的應用性。

四、執行效益自我評估

主持人在執行國家講座期間，在教學方面，第一學期所開設大學部的基礎課程”偏微分方程導論”，就吸引了 90 位學生(礙於上課教室的選課人數上限)來選課，除應用數學系的學生外，尚有其他電機，材料，光電，土木，電子物理等本校不同科系的學生來選課，顯現主持人在開設基礎課程方面有一定的吸引力，教學內容以數學模型為前導，再配合如何求解方程式，最後再以解釋其物理意義，深入淺出的方式成為上課的主軸。另外，在研究所課程中，除平常作業外也加上了實際寫程式的訓練，並於期末分組做專題報告，學生能獲得較完整的學習。就研究成果方面而言，在執行講座期間，2018 年共有 6 篇 SCI 文章發表，另外有 2 篇正在付梓中，3 篇在審議中，整體研究成果豐碩。此外，再加上各校巡迴的專題演講，執行講座效益個人認為還算符合預期。

五、檢討與建議

未來希望能夠在碩博士生前沿研究議題的課程提供跨校系的選修，這方面比較可行的方式是於暑期利用國家理論科學研究中心的資源開設短期課程，或於學期中在 Taiwan Mathematical School 的架構下開設專題課程進行遠距教學，讓更多的學生能夠受益。在研究方面，希望在目前所研究的計算流體力學的議題中加入探討 machine learning 的元素，目前已有初步的想法。此外，未來一年也打算至國內較為偏遠(如花東地區)或資源較缺乏的數學系或應用數學系進行專題演講。

附件	☐成果報告 1 冊（含實施計畫、課程講義、回饋分析表或相關佐證資料）及成果電子檔 1 份 ☐收支結算表 1 份(填列附件)

填表人： 賴明治 （簽章）

填表日期：　2019　年　1　月　31　日

出席國際會議心得報告

報告人: 賴明治

日期: 2018/5/13-2018/5/17

地點: 國立新加坡大學

這次主要是應國立新加玻大學 Institute for Mathematical Sciences 的邀請去參加其舉辦的 Workshop on Modeling and Simulations of Interface Dynamics in Fluid/Solids and Applications，本人獲邀在此彥講會給了一個 45 分鐘的演講，這是一個高水準的研討會，參與的人多是在界面流體研究的國際專家，我們也有充分的討論時間，也獲得了不少研究新領域的資訊。特別是認識了在英國 University of Warwick 的 Charlie Elliott 教授，由於我們雙方都讀過彼此的論文，我也請教了他一些我們正在處理的研究問題，雙方相談甚歡，我也打算找時間請他訪問台灣，總體而言，此次會議收穫甚豐。

出席國際會議心得報告

報告人: 賴明治

日期: **2018/06/03-2018/06/07**

地點: 香港城市大學

這次主要是應香港城市大學 Qiang Zhang 教授的邀請去參加在其校舉辦的兩年一度的 International Conference on Applied Mathematics 2018，這是個大型的應用數學研討會，台灣受邀的學者有兩人而本人為其中之一，在會議中個人發表最新的研究成果，也就是有關囊泡問題在非牛頓流體下的形變問題，聽眾反應還算熱烈，也問了不少問題，特別是在牛頓流體與非牛頓流體的差異，囊泡有不同的表現行為，這當中有不少有趣的物理問題可探究，可以當作未來的研究方向。另外，個人也聽了不少有趣的演講，值得一提的便是 UT-Austin Thomas Hughes 的 Isogeometric Analysis，他在演將中提到一些離散曲面的方法，似乎可以應用到目前我們的問題上面，總括的來說，這次參與國際會議獲益良多。

出席國際會議心得報告

報告人: 賴明治

日期: 2018/06/22-2018/06/26

地點: 日本東京大學

這次主要是去參加一年一度的東亞工業與應用數學會(EASIAM)的年會，本次會議的主辦單位為日本東京大學，本人為該會的執行委員會成員(Executive Committee member)並擔任一個邀請演講的主持人。在會議期間，我們召開了執行委員會議，本人被推舉為顧問委員會的成員，從明年一月起任期為四年，由於這次台灣去參加此次會議的成員有 32 位之多，參加人數居除主辦單位之冠，因此我們在該學會的影響力也逐漸加大。除一些專業演講外，我也認識了大會主講 Ohio State University 的 Martin Golubitsky，我們也討論了一些 EASIAM 未來的發展及對 SIAM 的影響，他建議我們除了固定的年會之外，應該舉辦一些高水準的研究型的 activity group 的 workshop 以增加這個學會的能見度與影響力，目前我們傾向朝此方向發展，整體而言，這次參與國際會議獲益良多。

出席國際會議心得報告

報告人: 賴明治

日期: **2018/12/15-2018/12/18**

地點: 泰國曼谷

這次主要是應泰國 Mahidol University 大學 Yongwimon Lenbury 教授的邀請去參加其舉辦的 International Conference in Mathematics and Applications，並於會中發表個人最近的研究成果，也就是有關 Unconditionally energy stable schemes for inextensible interface with bending 的成果。基本上聽眾的反應較不熱烈，可能是因為這並非以小型演講論壇的形式展現，所以參加者的領域背景不盡相同。此行的另一收穫便是聽到不少有關深度學習及其應用的演講，目前我們也想利用深度學習做些有關流體控制的問題。

移地研究心得報告

報告人: 賴明治

日期: 2018/04/24-2018/04/27

地點: 香港

這次主要是應香港理工大學 Zhonghua Qiao 教授的邀請去參加移地研究，主要是討論有關 Cahn-Hilliard 方程式在不可延展界面條件下的數值方法的發展，及其在流體力學的應用。初步的構想是利用 convex splitting method 再做更深入的分析，再配合 phased field method 去模擬 vesicle problem，但這需要解決如何處理界面不可延展的條件，我與喬教授在這方面有充分的討論，也有一些新的想法，也討論了一些新的文獻。此外，在數學理論上面，我們討論了不可延展界面解的適應性問題，其唯一性可以證明，但存在性卻尚未解決，這些都是目前尚須持續研究的議題。總之，此次移地研究收獲不少。

移地研究心得報告

報告人: 賴明治

日期: 2018/07/24-2018/07/27

地點: 深圳

這次主要是應中國大陸深圳南方科技大學張振 Zhen Zhang 教授的邀請去參加移地研究，主要是討論有關界面活性劑問題如何在 phase field 方法底下的數學模型及數值方法。我們也討論了一些應用在液滴對撞的數值模擬的設定問題，及有移動接觸線的物理數學模型。此外，我還建議了他可以發展 Cahn-Hilliard 方程式在不可延展界面條件下的數值方法，及其在流體力學的應用。初步的構想是利用 phased field method 去模擬 vesicle problem，但這需要解決如何處理界面不可延展的條件，我與張教授在這方面有充分的討論，也有一些新的想法，也討論了一些新的文獻。總之，此次移地研究收獲不少。

移地研究心得報告

報告人: 賴明治

日期: 2018/09/04-2018/09/09

地點: 北京

這次主要是應中國大陸北京大學張平文 Pingwen Zhang 教授的邀請去參加移地研究，主要是討論有關複雜流體的數學模型及數值方法。我們討論了一些在液晶問題上面的數值模擬及其可能的應用，基本上我想用沉浸邊界法去模擬液晶問題，並與他討論可能碰到的問題。此外，由於大陸計算數學在這幾年進步相當快速，今年的國際數學家大會在計算方面的邀請演講者在大陸工作的有兩人(張教授為其一)，另外還有兩位是大陸在美工作的華人，張教授與我交換了發展應用數學的心得及如何推廣計算數學在各學科的影響力，我與張教授在這方面有充分的溝通與討論。總之，此次移地研究收獲不少。

移地研究心得報告

報告人: 賴明治

日期: 2018/11/7-2018/11/11

地點: 日本京都

這次主要是應京都大學 Yuusuke Iso 教授的邀請去參加移地研究，主要是討論有關不可延展界面條件下的數值方法的發展，及其在多精度運算的可行性。我們找到了二維固定曲線的 Stokes 方程的解析解，並在他們的數值分析專題討論會上報告這方面的最新進度，獲得不錯的回響。在數學理論上面，我們討論了不可延展界面解的適應性問題，其唯一性可以證明，但存在性卻尚未解決，這些都是目前尚須持續研究的議題。總之，此次移地研究收獲不少。

移地研究心得報告

報告人: 賴明治

日期: 2018/12/4-2018/12/7

地點: 廈門

這次主要是應廈門大學Chuanju Xu教授的邀請去參加移地研究，主要是討論合作有關有限元素法在不可延展界面條件下的 Stokes 方程數值方法的發展，及其在流體力學的應用。目前我們已經有設計好解析解，Xu 教授的博士生已著手寫有限元素法的程式，初步已經獲得一些結果，但是是在解光滑下的結果，而且 LBB 的條件也未能證明出來，表示這類問題的確有相當的困難度須解決，我們傾向先證明速度場的一街收斂性之後，再來看其他如壓力及張力的收斂性。總之，此次移地研究收獲不少。

移地研究心得報告

報告人: 賴明治

日期: 2019/1/13-2019/1/20

地點: 香港

這次是應香港大學 Xiaoming Yuan 教授的邀請去參加移地研究，主要是討論合作有關最佳化理論與機器學習的教學與研究議題。機器學習目前可說是相當熱門的議題，表現在諸多應用當中，即便在傳統的應用數學領域，如計算流體力學也有相當的應用議題可發揮。此次與 Yuan 教授討論最佳化入門的教課書，本人計畫在新的國家講座計畫的一年中，在大學部開設最佳化的課程，目前課名定為應用數學導論。除此之外，在研究方面，我們想利用最佳化的方式去研究 phase field 方法的 asymptotic limit 的問題，希望可以驗證理論證明的結果。

Introduction to Scientific Computing/Finite Difference Methods for PDEs

Ming-Chih Lai

1 Introduction

Some Terms:

- Numerical mathematics or (computational mathematics) are a branch of applied math using computational method to solve math problem.
- Numerical analysis is mainly to consider the theoretical analysis of the methods.
- Scientific computing is to emphasis on getting computational results on realistic model.
  The justification of a valid method is either with rigorous theoretical proof or comparison with experiments or observed data or physical phenomenon.
  Be able to reproduce well-established results.

Numerical methods

Finite difference method : Easy to understand, regular domain and many package available.

Finite element method : Theoretical background, Sobolev space and irregular domain.

Finite volume method : The integral form of conservation law.

$$\frac{d}{dt}\int u dx = -f(u)|_{\partial\Omega}$$

.

Spectral method : Very accurate to linear problem. Fourier analysis, Chebyshev polynomials, pseudospectral method

Second-oder P.D.E

$$Pu = au_{xx} + bu_{xy} + cu_{yy} + du_x + eu_y + f = 0$$

Elliptic P.D.E : $b^2 + 4ac < 0$

Hyperbolic P.D.E : $b^2 + 4ac > 0$

Parabolic P.D.E : $b^2 + 4ac = 0$

Elliptic P.D.E

Laplace equation $\nabla^2 u = \frac{\partial^2 u}{\partial x^2} + \frac{\partial^2 u}{\partial y^2} = 0$

$$\nabla^2 = \Delta$$

Poisson equation $\nabla^2 u = f$

Helmholtz equation $\nabla^2 u + \lambda u = f$

Biharmonic equation

$$\nabla^4 u = \nabla^2(\nabla^2 u) = \frac{\partial^4 u}{\partial x^4} + 2\frac{\partial^4 u}{\partial x^2 \partial y^2} + \frac{\partial^4 u}{\partial y^4} = f$$

$$u|_{\partial\Omega} = g_1, \frac{\partial u}{\partial n}|_{\partial\Omega} = g_2$$

Cauchy-Riemann

$$\begin{cases} u_x - v_y = 0, \\ u_y + v_x = 0 \end{cases}$$

Stokes's equation

$$\begin{cases} -\nabla p + \nabla^2 \mathbf{u} = 0 \\ \nabla \cdot \mathbf{u} = 0 \end{cases}$$

where $\mathbf{u} = (u, v)$ is velocity and p is pressure.

Hyperbolic P.D.E

Linear advection equation $u_t + au_x = 0$

Wave equation $u_{tt} = u_{xx}$

Inviscid Burgers equation $u_t + u\, u_x = 0$

Hyperbolic conservation law $u_t + (f(u))_x = 0$

All equations must be accompanied with some sort of initial conditions.

Parabolic P.D.E

$$\text{Heat equation} \quad u_t = u_{xx} + f(x,t)$$

Navier-Stokes equations:

$$\begin{cases} u_t + (u\cdot\nabla)u + \nabla p = \nu\Delta u + f, \\ \hfill \nabla\cdot u = 0 \\ \hfill u(x,0): \quad \text{given} \\ \hfill u|_{\partial\Omega} = 0 \quad \text{no-slip conditions} \end{cases}$$

2. Steady States and Boundary Value Problems

The steady-state problem

Consider the one-dimensional heat equation

$$\begin{cases} u_t = u_{xx} - f(x), & x \in (0,l), \quad t > 0, \\ u(x,0) = u_0(x), \\ u(0,t) = u(l,t) = 0, \end{cases}$$

where $u(x,t)$ stands for the temperature. we expect the solution to eventually reach a *steady-state* i.e. $u_t \to 0$ as $t \to \infty$, so we obtain an ODE in x to solve $u(x)$. This problem is called a two-point boundary value problems (BVP) as following:

$$\begin{cases} u''(x) = f(x), & x \in (0,1) \\ u(0) = u(1) = 0. \end{cases}$$

The boundary condition $u(0) = u(1) = 0$ is called a *Dirichlet boundary condition.*

A simple finite difference method

We use the finite difference method to solve this BVP. First, give a uniform partition $0 = x_0 < x_1 < \cdots < x_{m+1} = 1$, where the *mesh grid* $\Delta x = x_{j+1} - x_j = h$ for $j = 0, 1, \cdots, m$. Define two grid functions $U(x)$ and $F(x)$ satisfied

$$U(x_j) \approx u(x_j) \quad F(x_j) = f(x_j) \;\text{ for } j = 0, 1, \cdots, m+1,$$

where $U(xj)$ is our numerical solution. For simplicity, we use the notations $U_j = U(x_j)$ and $u_j = u(x_j)$. Set $U_0 = u_0$ and $U_{m+1} = u_{m+1}$, so we have m unknowns to compute. Approximate u_j'' by the center difference approximation

$$u_j'' \approx \frac{U_{j-1} - 2U_j + U_{j+1}}{h^2} \;\text{ for } j = 1, \cdots, m.$$

So it is equivalent to solve a linear system as following:

$$A^h U = \frac{1}{h^2} \begin{bmatrix} -2 & 1 & & & \\ 1 & -2 & 1 & & \\ & \ddots & \ddots & \ddots & \\ & & 1 & -2 & 1 \\ & & & 1 & -2 \end{bmatrix} \begin{bmatrix} U_1 \\ U_2 \\ \vdots \\ U_{m-1} \\ U_m \end{bmatrix} = \begin{bmatrix} F_1 \\ F_2 \\ \vdots \\ F_{m-1} \\ F_m \end{bmatrix}$$

This tridiagonal linear system is nonsingular and can be easily solved.

Local truncation error

The local truncation error denoted by τ_j is

$$\begin{aligned}\tau_j &= \frac{u_{j-1} - 2u_j + u_{j+1}}{h^2} - f_j \\ &= \frac{h^2}{12} u_j'''' + O(h^4) \qquad \text{assum } u''''(x) \text{ exist and use Taylor expansion}\end{aligned}$$

for $j = 1, 2, \cdots, m$. Define a grid function $\widehat{U}$ satisfied $\widehat{U}_j = u_j$ for all j and

$$E = U - \widehat{U},$$

E is said to be a *global error*.

Before we use this finite difference scheme in our computer, we have to introduce an important theorem which guarantees that our scheme is *convergent*.

Convergence

Definition. A method is *consistent* if $\|\tau\| \to 0$ as $h \to 0$.

Assume $|u_j''''| \leq M$, we have $|\tau_j| \leq \frac{Mh^2}{12}$ for all j. This implies $\tau_j = O(h^2)$, thus we have $\|\tau\|_\infty = O(h^2)$ and $\|\tau\|_2 = O(h^2)$. Hence, our finite difference scheme is certainly consistent.

Definition. A method is *convergent* if $\|E\| \to 0$ as $h \to 0$.

Since $A^h E = -\tau$, claim A^h is invertible, then we have $E = -(A^h)^{-1}\tau$. Assume $\|(A^h)^{-1}\| \leq C$ for some C, we have

$$\|E\|_2 = \| - (A^h)^{-1}\tau\|_2 \leq \|(A^h)^{-1}\|_2 \|\tau\|_2 \leq C\|\tau\|_2,$$

thus $\|E\|_2 = O(h^2)$. Finally, we have $\|E\|_2 \to 0$ as $h \to 0$.

Now we have to show that our claim is true. Since

$$\begin{aligned}\|A^h\|_2 &= \left(\lambda_{max}((A^h)^T A^h)\right)^{\frac{1}{2}} \\ &= \left(\lambda_{max}((A^h)^2)\right)^{\frac{1}{2}} \qquad \because A^h \text{ is symmertic} \\ &= \left((\lambda_{max}(A^h))^2\right)^{\frac{1}{2}} \qquad \because \lambda((A^h)^2) = (\lambda(A^h))^2 \\ &= \left|\left(\lambda_{max}(A^h)\right)\right|,\end{aligned}$$

if A^h is invertible, then

$$\|(A^h)^{-1}\|_2 = \left(\lambda_{min}(A^h)\right)^{-1}.$$

So all we have to show is all eigenvalues of A^h are not zero. Let u^p be a $m \times 1$ vector satisfied

$$u_j^p = \sin(p\pi jh) \qquad \text{for } j = 1, 2, \cdots, m,$$

then

$$\begin{aligned}
(A^h u^p)_j &= \frac{u_{j-1}^p - 2u_j^p + u_{j+1}^p}{h^2} \\
&= \frac{\sin(p\pi(j-1)h) - 2\sin(p\pi jh) + \sin(p\pi(j+1)h)}{h^2} \\
&= \underbrace{\frac{2}{h^2}(\cos(p\pi h) - 1)}_{\lambda_p} \underbrace{\sin(p\pi jh)}_{u_j^p}.
\end{aligned}$$

Hence, we can conclude that λ_p is eigenvalue of A^h respect to eigenvector u^p. Clearly, $\lambda_p \neq 0$ for $p = 1, 2, \cdots, m$, hence A^h is invertible. Moreover, λ_1 is the smallest value of all eigenvalues and

$$\begin{aligned}
\lambda_1 &= \frac{2}{h^2}(\cos(\pi h) - 1) \\
&= \frac{2}{h^2}\left(1 - \frac{(\pi h)^2}{2!} + O(h^4) - 1\right) \text{ by Taylor expansion} \\
&= -\pi^2 + O(h^2),
\end{aligned}$$

so $\|(A^h)^{-1}\|_2 = \frac{1}{|\lambda_1|}$ is bounded. This condition is said to be the *stability* condition.

In all process of proof, we arrive at the conclusion that

$$\text{consistency } + \text{ stability } \Rightarrow \text{ convergence}.$$

Next we introduce two methods about stability analysis.

Stability analysis by the energy method

Let U and V be two $m \times 1$ vectors, define an inner product by

$$\langle U, V \rangle = \sum_{j=1}^{m} U_j V_j h.$$

Remark. Suppose $\widehat{U}(x)$ is the exact solution of BVP as following

$$\begin{cases} u''(x) = f(x), & x \in (0,1) \\ u(0) = u(1) = 0. \end{cases}$$

Then

$$\begin{aligned}
\|\widehat{U}\|_{L^2} &= \left(\int_0^1 |\widehat{U}(x)|^2 \mathrm{d}x\right)^{\frac{1}{2}} \\
&\approx \left(h\sum_{j=0}^{m} \frac{\widehat{U}_{j+1}^2 + \widehat{U}_j^2}{2}\right)^{\frac{1}{2}} \qquad \text{by trapezodial rule} \\
&= \left[h\left(\frac{\widehat{U}_1^2 + \widehat{U}_0^2}{2} + \frac{\widehat{U}_2^2 + \widehat{U}_1^2}{2} + \cdots + \frac{\widehat{U}_m^2 + \widehat{U}_{m-1}^2}{2} + \frac{\widehat{U}_m^2 + \widehat{U}_{m+1}^2}{2}\right)\right]^{\frac{1}{2}} \\
&= \left(\sum_{j=1}^{m} \widehat{U}_j^2 h\right)^{\frac{1}{2}} \\
&= \|\widehat{U}\|_2 \qquad \text{in } \langle\cdot,\cdot\rangle \text{ defined above.}
\end{aligned}$$

So our stability analysis by energy method is in a viewpoint of discrete form.

Let U be the numerical solution of BVP above and L_h be a differential operator defined by

$$L_h U_j = \frac{U_{j-1} - 2U_j + U_{j+1}}{h^2} = D^+D^-U_j = D^-D^+U_j = F_j$$

Our goal is to show that

$$\|U\| \leq \frac{1}{2}\|F\|.$$

First we want to show that L_h is a self-adjoint operator i.e.

$$\langle L_h U, V\rangle = \langle U, L_h V\rangle \quad \forall\, U, V \in \mathcal{R}^m$$

and semi-negative definite operator i.e.

$$\langle L_h U, U\rangle \leq 0 \quad \forall\, U \in \mathcal{R}^m.$$

Given U and V satisfied $U_0 = U_{m+1} = V_0 = V_{m+1}$.

$$
\begin{aligned}
&\because U_{j+1}V_{j+1} - U_jV_j = (U_{j+1} - U_j)V_j + (V_{j+1} - V_j)U_{j+1} \\
&\Rightarrow \sum_{j=0}^{m}(U_{j+1} - U_j)V_j + \sum_{j=0}^{m}(V_{j+1} - V_j)U_{j+1} = \sum_{j=0}^{m}(U_{j+1}V_{j+1} - U_jV_j) = 0 \\
&\Rightarrow \sum_{j=0}^{m}(U_{j+1} - U_j)V_j = -\sum_{j=0}^{m}(V_{j+1} - V_j)U_{j+1} = -\sum_{j=1}^{m+1}(V_j - V_{j-1})U_j \\
&\Rightarrow \sum_{j=1}^{m}\frac{U_{j+1} - U_j}{h}V_j = -\sum_{j=1}^{m}\frac{V_j - V_{j-1}}{h}U_j \\
&\therefore \langle D^+U, V\rangle = -\langle U, D^-V\rangle \\
&\Rightarrow \langle L_hU, U\rangle = \langle D^+D^-U, U\rangle = -\langle D^-U, D^-U\rangle \leq 0
\end{aligned}
$$

and

$$
\begin{aligned}
\langle L_hU, V\rangle &= \langle D^+D^-U, V\rangle \\
&= -\langle D^-U, D^-V\rangle \\
&= \langle U, D^+D^-V\rangle \\
&= \langle U, L_hV\rangle
\end{aligned}
$$

Hence L_h is a self-adjoint and semi-negative definite operator.

$$
\begin{aligned}
&\because U_j = \left(\sum_{k=1}^{j}\frac{U_k - U_{k-1}}{h}\right)h \\
&\Rightarrow U_j^2 = \left(\sum_{k=1}^{j}\frac{U_k - U_{k-1}}{h}\right)^2 h^2 \leq jh^2\sum_{k=1}^{j}\left(\frac{U_k - U_{k-1}}{h}\right)^2 \\
&\Rightarrow h\sum_{j=1}^{m}U_j^2 \leq h^3\sum_{j=1}^{m}j\sum_{k=1}^{j}\left(\frac{U_k - U_{k-1}}{h}\right)^2 \leq h^2\sum_{j=1}^{m}j\sum_{k=1}^{m}\left(\frac{U_k - U_{k-1}}{h}\right)^2 h \\
&\Rightarrow \|U\|^2 \leq h^2\frac{m(m+1)}{2}\sum_{k=1}^{m}\left(\frac{U_k - U_{k-1}}{h}\right)^2 h \leq \frac{1}{2}\|D^-U\|^2
\end{aligned}
$$

Since

$$
\begin{aligned}
\|D^-U\|^2 = |\langle L_hU, U\rangle| &= |\langle F, U\rangle| \\
&\leq \|F\|\|U\| \qquad \text{by Cauchy-Schwarz inequality,}
\end{aligned}
$$

finally we have $\|U\| \leq \frac{1}{2}\|F\|$.

Green's functions and max-norm stability

Consider the BVP

$$\begin{cases} u''(x) = f(x), \quad x \in (0,1) \\ u(0) = u(1) = 0. \end{cases}$$

Integrate both side from 0 to x, we have

$$u'(x) = \underbrace{\int_0^x f(s)\mathrm{d}s}_{F(x)} + u'(0).$$

Integrate again, we have

$$\begin{aligned} u(x) - u(0) &= \int_0^x F(t)\mathrm{d}t + u'(0)x \\ &= tF(t)|_0^x - \int_0^x tF'(t)\mathrm{d}t + +u'(0)x \\ &= xF(x) - \int_0^x tf(t)\mathrm{d}t + +u'(0)x \\ &= x\int_0^x f(t)\mathrm{d}t - \int_0^x tf(t)\mathrm{d}t + u'(0)x \\ &= \int_0^x (x-t)f(t)\mathrm{d}t + u'(0)x. \end{aligned}$$

By the boundary condition, we have

$$u(1) - u(0) = 0 = \int_0^1 (1-t)f(t)\mathrm{d}t + u'(0),$$

thus $u'(0) = -\int_0^1 (1-t)f(t)\mathrm{d}t$. So our solution becomes

$$\begin{aligned} u(x) &= \int_0^x (x-t)f(t)\mathrm{d}t - \int_0^1 x(1-t)f(t)\mathrm{d}t \\ &= \int_0^x (x-t)f(t)\mathrm{d}t - \left(\int_0^x x(1-t)f(t)\mathrm{d}t + \int_x^1 x(1-t)f(t)\mathrm{d}t\right) \\ &= \int_0^x t(x-1)f(t)\mathrm{d}t - \int_x^1 x(1-t)f(t)\mathrm{d}t \\ &= \int_0^1 G(x,t)f(t)\mathrm{d}t, \end{aligned}$$

where $G(x,t) = \begin{cases} t(x-1) & 0 \le t \le x, \\ x(t-1) & x \le t \le 1, \end{cases}$ which is called the *Green's function*. Since

$$\begin{aligned}
|u(x)| &= \left| \int_0^1 G(x,t) f(t) \mathrm{d}t \right| \\
&\le \int_0^1 |G(x,t)||f(t)| \mathrm{d}t \\
&\le \|f\|_\infty \int_0^1 |G(x,t)| \mathrm{d}t \\
&= \|f\|_\infty \frac{x(1-x)}{2} \qquad \text{for } x \in [0,1] \\
&\le \frac{1}{8} \|f\|_\infty,
\end{aligned}$$

finally we have

$$\|u\|_\infty \le \frac{1}{8} \|f\|_\infty.$$

Neumann boundary condition

How to solve the equation with Neumann boundary such as

$$\begin{cases} u'' = f \\ u(0) = u'(1) = 0 \end{cases}$$

Using the same centered difference formula,

$$\frac{U_{i+1} - 2U_i + U_{i-1}}{h^2} = f_i$$

we need the boundary value U_N, when $i = N - 1$. How can we provide such numerical boundary value?

Method 1:(first-order accurate)
Since $u'(1) = 0$, $\frac{U_N - U_{N-1}}{h} = 0$ then $U_N = U_{N-1}$

$$\begin{bmatrix} \frac{-2}{h^2} & \frac{1}{h^2} & & & 0 \\ \frac{1}{h^2} & \frac{-2}{h^2} & \frac{1}{h^2} & & \\ & \cdots & \cdots & & \\ & & \cdots & \cdots & \\ & & \frac{1}{h^2} & \frac{-2}{h^2} & \frac{1}{h^2} \\ 0 & & & \frac{\mathbf{1}}{h^2} & \frac{\mathbf{-1}}{h^2} \end{bmatrix} \begin{bmatrix} U_1 \\ U_2 \\ \vdots \\ U_{N-1} \end{bmatrix} = \begin{bmatrix} f_1 - \frac{u_0}{h^2} \\ f_2 \\ \vdots \\ f_{N-1} \end{bmatrix}.$$

Method 2(ghost point method):(second-order accurate)
Since $u'(1) = 0$, $\frac{U_{N+1} - U_{N-1}}{2h} = 0$ then $U_{N+1} = U_{N-1}$

$$\begin{bmatrix} \frac{-2}{h^2} & \frac{1}{h^2} & & & 0 \\ \frac{1}{h^2} & \frac{-2}{h^2} & \frac{1}{h^2} & & \\ & \cdots & \cdots & & \\ & & \cdots & \cdots & \\ & & \frac{1}{h^2} & \frac{-2}{h^2} & \frac{1}{h^2} \\ 0 & & & \frac{\mathbf{2}}{h^2} & \frac{\mathbf{-2}}{h^2} \end{bmatrix} \begin{bmatrix} U_1 \\ U_2 \\ \vdots \\ U_N \end{bmatrix} = \begin{bmatrix} f_1 - \frac{u_0}{h^2} \\ f_2 \\ \vdots \\ f_N \end{bmatrix}.$$

Compact difference scheme

Now we will introduce a compact (three-point stencil) fourth-order accurate method for the model problem. Here, we give some difference notation

$$\delta_+ u_i = \frac{u_{i+1} - u_i}{h}, \quad \delta_+ u = \frac{du}{dx} + O(\Delta x), O(\Delta x) \leq C\Delta x$$

$$\delta_- u_i = \frac{u_i - u_{i-1}}{h}, \quad \delta_- u = \frac{du}{dx} + O(\Delta x), O(\Delta x) \leq C\Delta x$$

$$\delta_0 u_i = \frac{u_{i+1} - u_{i-1}}{2h}, \quad \delta_0 u = \frac{du}{dx} + O(\Delta x^2), O(\Delta x^2) \leq C\Delta x^2$$

$$\delta^2 u_i = \frac{u_{i+1} - 2u_i + u_{i-1}}{h^2}, \quad \delta^2 u = \frac{d^2 u}{dx^2} + O(\Delta x^2)$$

Next we will find a better method(4-th order method) to solve the problem,

$$u'' = f, \quad u(0) = u(1) = 0$$

$$u(x_i+h) = u(x_i)+u'(x_i)h+\frac{u''(x_i)h^2}{2!}+\frac{u'''(x_i)h^3}{3!}+\frac{u''''(x_i)h^4}{4!}+\frac{u^(5)(x_i)h^5}{5!}+O(h^6)\ldots(1)$$

$$u(x_i-h) = u(x_i)-u'(x_i)h+\frac{u''(x_i)h^2}{2!}-\frac{u'''(x_i)h^3}{3!}+\frac{u''''(x_i)h^4}{4!}-\frac{u^(5)(x_i)h^5}{5!}+O(h^6)\ldots(2)$$

(1)+(2)

$$\begin{aligned}
\frac{u(x_i+h) - 2u(x_i) + u(x_i-h)}{h^2} &= u''(x_i) + \frac{u''''(x_i)h^2}{12} + O(h^4) \\
&= f_i + \frac{h^2}{12}\left(\frac{d^2 f_i}{dx^2}\right) + O(h^4) = f_i + \frac{h^2}{12}\delta^2 f_i + O(h^4)
\end{aligned}$$

Since $\frac{d^2 f_i}{dx^2} = \delta^2 f + O(h^2)$, we then have

$$\frac{U_{i+1} - 2U_i + U_{i-1}}{h^2} = f_i + \frac{h^2}{12}\frac{f_{i+1} - 2f_i + f_{i-1}}{h^2} = \frac{f_{i+1} + 10f_i + f_{i-1}}{12}$$

. The resultant linear equations has the form

$$\begin{bmatrix} -2 & 1 & & & & \\ 1 & -2 & 1 & & & \\ & \cdots & \cdots & & & \\ & & \cdots & \cdots & & \\ & & 1 & -2 & 1 & \\ & & & 1 & -2 & \end{bmatrix} \begin{bmatrix} U_1 \\ U_2 \\ \vdots \\ U_{N-1} \end{bmatrix} = \frac{h^2}{12} \begin{bmatrix} f_0 + 10f_1 + f_2 \\ f_1 + 10f_2 + f_3 \\ \vdots \\ f_{N-2} + 10f_{N-1} + f_N \end{bmatrix}.$$

This is called **4**-order compact scheme which involves solving the same tri-diagonal linear system as the second-order centered difference method.

3 Finite difference method for 1D Parabolic equation

Now let us consider the numerical method for 1D heat equation.

$$\begin{cases} u_t = u_{xx} \\ u(0,t) = u(1,t) = 0 \\ u(x,0) = f(x) \end{cases}$$

This equation serves as a model problem for the finite difference scheme of the parabolic equation. Since the problem is simple enough, one can write down the exact solution immediately.

$$u(x,t) = \sum_{n=1}^{\infty} a_n e^{-(n^2+\pi^2)t} \sin n\pi x, \text{ where } \quad a_n = 2\int_0^1 f(x) \sin n\pi x dx$$

The solution of heat equation satisfies the following properties

(1) Energy dissipation

$$\begin{aligned} \int_0^1 u u_t dx &= \int_0^1 u u_{xx} dx \\ \frac{d}{dt}\int_0^1 \frac{u^2}{2} &= \int_0^1 u u_{xx} dx = u u_x|_0^1 - \int_0^1 u_x u_x dx \\ \Rightarrow \frac{d}{dt}\int_0^1 \frac{u^2}{2} &= -\int_0^1 u_x^2 dx \\ \Rightarrow \int_0^1 \frac{u^2(x,t)}{2} dx &\leq \int_0^1 \frac{f^2(x)}{2} dx \end{aligned}$$

(2) Maximum principle(extreme value only occur on boundary or initial conditions)

Proof: Suppose not, for example, the maximum occurs at (x_0, t_0), then we have

$$\begin{cases} u_t(x_0,t_0) > 0 \\ u_{xx}(x_0,t_0) < 0 \end{cases} \Rightarrow \text{don't satisfy} \quad u_t = u_{xx}.$$

Thus, this leads to a contradiction.

3.1 Explicit scheme

Define the mesh points or gird points as

$$x_j = j\Delta x, t_n = n\Delta t, j = 0, 1, \ldots N, \Delta x = \frac{1}{N}.$$

We seek approximation of the solution at those mesh grids i.e $U_j^n \approx u(x_j, t_n)$

$$u_t = \frac{\partial u(x_j, t_{n+1})}{\partial t} \approx \frac{u(x_j, t_n + \Delta t) - u(x_j, t_n)}{\Delta t}$$
$$u_{xx} = \frac{\partial^2 u}{\partial x^2} \approx \frac{u(x_j + \Delta x, t_n) - 2u(x_j, t_n) + u(x_j - \Delta x, t_n)}{\Delta x^2}$$
$$\frac{U_j^{n+1} - U_j^n}{\Delta t} = \frac{U_{j+1}^n - 2U_j^n + U_{j-1}^n}{\Delta x^2}$$
$$U_j^{n+1} = U_j^n + \frac{\Delta t}{\Delta x^2}(U_{j+1}^n - 2U_j^n + U_{j-1}^n)$$
$$= (1 - 2\beta)U_j^n + \beta U_{j+1}^n + \beta U_{j-1}^n, \quad \text{where } \beta = \frac{\Delta t}{\Delta x^2}.$$

$$U_j^0 = f(x_j) \quad \text{initial condition.}$$
$$U_0^n = U_N^n = 0 \quad \text{boundary condition.}$$

Note that this scheme is the first-order accurate in time and second-order in space, since the truncation error is $O(\Delta t) + O(\Delta x^2)$

$$\tau(x,t) = \frac{u(x_j, t_n + \Delta t) - u(x_j, t_n)}{\Delta t} - \frac{u(x_j + \Delta x, t_n) - 2u(x_j, t_n) + u(x_j - \Delta x, t_n)}{\Delta x^2}$$

.

Exercise: Write a matlab program to solve the 1D heat equation using the above scheme with

$$f(x) = \begin{cases} 2x, & 0 \le x \le \frac{1}{2} \\ 2 - 2x, & \frac{1}{2} \le x \le 1 \end{cases} \qquad \text{N=20, } \Delta x = 0.05$$

Choose two different Δt, $\Delta t = 0.0012$ and $\Delta t = 0.0013$, you will find they lead to two different results.

From the above numerical experiment, we simply observe that when the time step $\Delta t = 0.0012$, the computed solution becomes very large in a few time steps and soon the result becomes overflow. This has something to do with the stability of the method. In other words, in order to have a successful computation, one must choose the time step carefully. Let us pay another visit about this situation.

$$f(x) = \epsilon \cos \frac{\pi x}{\Delta x}, \quad f(x_j) = \epsilon \cos \frac{\pi x_j}{\Delta x} = \epsilon \cos j\pi = \epsilon(-1)^j$$

$$U_j^{n+1} = (1 - 2\beta)U_j^n + \beta U_{j+1}^n + \beta U_{j-1}^n, \quad U_j^0 = \epsilon(-1)^j$$
$$U_j^1 = (1 - 2\beta)\,\epsilon(-1)^j + \beta\,\epsilon(-1)^{j+1} + \beta\,\epsilon(-1)^{j-1}$$
$$U_j^n = (1 - 4\beta)^n\,\epsilon(-1)^j$$

$$|f(x)| = |u(x,0)| \leq \epsilon$$

By maximum principle we have $|U_j^n| \leq \epsilon$. So if

$$|1-4\beta| \leq 1 \Rightarrow \beta \leq \frac{1}{2},$$

we can have such bound for $|U_j^n|$. However, if it is violated, then the solution is growing without bounds so we are unable to obtain a reasonable solution. The above constraint is called the stability constraint.

Convergence of the explicit scheme

Truncation error analysis

$$\begin{aligned}
\tau(x,t) &= \frac{u(x_j, t_n+\Delta t) - u(x_j,t_n)}{\Delta t} - \frac{u(x_j+\Delta x, t_n) - 2u(x_j,t_n) + u(x_j-\Delta x, t_n)}{\Delta x^2} \\
u(x,t+\Delta t) &= u(x,t) + u_t \Delta t + \frac{u_{tt}(x,\zeta)\Delta t^2}{2!} \\
u(x+\Delta x,t) &= u(x,t) + u_x\Delta x + \frac{u_{xx}\Delta x^2}{2!} + \frac{u_{xxx}\Delta x^3}{3!} + \frac{u_{xxxx}(\xi_1,t)\Delta x^4}{4!} \\
u(x-\Delta x,t) &= u(x,t) - u_x\Delta x + \frac{u_{xx}\Delta x^2}{2!} - \frac{u_{xxx}\Delta x^3}{3!} + \frac{u_{xxxx}(\xi_2,t)\Delta x^4}{4!}
\end{aligned}$$

$$\Rightarrow \frac{u(x_j+\Delta x, t_n) - 2u(x_j,t_n) + u(x_j-\Delta x, t_n)}{\Delta x^2} = u_x x + \frac{u_{xxxx}(\xi,t)\Delta x^2}{12}$$

then

$$\tau(x,t) = \frac{u_{tt}(x,\zeta)\Delta t}{2} - \frac{u_{xxxx}(\xi,t)\Delta x^2}{12}, \quad O(\Delta t) + O(\Delta x^2)$$

$$|\tau(x,t)| \leq \frac{M_{tt}\Delta t}{2} + \frac{M_{xxxx}\Delta x^2}{12} = \frac{\Delta t}{2}(M_{tt} + \frac{1}{6\beta}M_{xxxx}), \quad \beta = \frac{\Delta t}{\Delta x^2},$$

where M_{tt} is a bound for $|u_{tt}|$ and M_{xxxx} is a bound for $|u_{xxxx}|$. For a fixed ratio β, $|\tau(x,t)|$ behaves like $O(\Delta t)$ as $\Delta t \to 0$ i.e. $|\tau(x,t)| \to 0$ as $\Delta t \to 0$.

Definition: We say that a scheme is convergent if for any fixed point (x^*, t^*) in the domain $(0,1)\times(0,T)$ as $x_j \to x^*, \quad t_n \to t^*$, we have $U_j^n \to u(x_j,t_n)$.

Theorem: If $\beta \leq \frac{1}{2}$, then the explicit scheme is convergent.
Proof: We denote e by the error $U-u$ in the approximation $e_j^n := U_j^n - u(x_j,t_n)$.
Claim :

$$e_j^{n+1} = (1-2\beta)e_j^n + \beta e_{j+1}^n + \beta e_{j-1}^n - \tau_j^n \Delta t$$

$$\|e^n\|_\infty = \{|e_j|, j=0,1\ldots N\}$$

If $\beta \le \frac{1}{2}$, then

$$|e_j^{n+1}| \le |(1-2\beta)||e_j^n| + \beta|e_{j+1}^n| + \beta|e_{j-1}^n| + |\tau_j^n|\Delta t$$
$$|e_j^{n+1}| \le |(1-2\beta)|\|e^n\|_\infty + \beta\|e^n\|_\infty + \beta\|e^n\|_\infty + |\tau_j^n|\Delta t$$

then

$$\|e^n\|_\infty \le \|e^n\|_\infty + \tau\Delta t \le \|e^{n-1}\|_\infty + 2\tau\Delta t$$
$$\|e^n\|_\infty \le \|e^0\|_\infty + n\tau\Delta t$$

Since $e^0 \equiv 0$ is the initial data,

$$\|e^n\|_\infty \le \frac{\Delta t}{2}(M_{tt} + \frac{1}{6\beta}M_{xxxx})T$$

as $\Delta t \to 0$ we have $\|e^n\|_\infty \ \to 0$.
Note that we have here required that these bounds M_{tt} and M_{xxxx} hold for uniformly on the whole region $(0,1)\times(0,T)$.

von Nenmann analysis

$$U_j^n = g^n e^{ik(j\Delta x)}, \quad g(k) = 1 - 4\beta\sin^2\frac{k\Delta x}{2}$$

where $g(k)$ is the amplification factor. Need $|g(k)| \le 1 + K'\Delta t$ or $|g(k)| \le 1$.

Theorem(von Neumann condition): A necessary condition for stability is that there exists a constant K' s.t

$$|g(k)| \le 1 + K'\Delta t \quad \text{for all } k \text{ and } n\Delta t \le T\ .$$

3.2 First-order implicit scheme

The stability limit $\Delta t \le \frac{\Delta x^2}{2}$ is a very severe restriction for the explicit scheme, we now find other difference scheme to avoid such restriction.
Let us replace the explicit scheme by

$$\begin{aligned}
\frac{U_j^{n+1} - U_j^n}{\Delta t} &= \frac{U_{j+1}^{n+1} - 2U_j^{n+1} + U_{j-1}^{n+1}}{\Delta x^2} \\
U_j^{n+1} - U_j^n &= \frac{\Delta t}{\Delta x^2}(U_{j+1}^{n+1} - 2U_j^{n+1} + U_{j-1}^{n+1}) \\
(1+2\beta)U_j^{n+1} &= U_j^n + \beta U_{j+1}^{n+1} + \beta U_{j-1}^{n+1}
\end{aligned}$$

$$\Rightarrow -\beta U_{j-1}^{n+1} + (1+2\beta)U_j^{n+1} - \beta U_{j+1}^{n+1} = U_j^n$$

$$U_0^{n+1} = U_N^{n+1} = 0 \quad \text{are boundary condition.}$$

At each time step, given U_j^n, we need to find U_j^{n+1}. This involves solving a tridiagonal linear system of equation for U_j^{n+1} i.e $Av = b$ where

$$A = \begin{bmatrix} 1+2\beta & -\beta & & & & \\ -\beta & 1+2\beta & -\beta & & & \\ & \cdots & \cdots & & & \\ & & \cdots & \cdots & & \\ & & -\beta & 1+2\beta & -\beta & \\ & & & -\beta & 1+2\beta & \end{bmatrix} \quad v = \begin{bmatrix} U_1^{n+1} \\ U_2^{n+1} \\ \vdots \\ U_{N-1}^{n+1} \end{bmatrix} \quad b = \begin{bmatrix} U_1^n \\ U_2^n \\ \vdots \\ U_{N-1}^n \end{bmatrix}.$$

Next we use maximum principle to check if we have avoided the restriction

$$(1+2\beta)U_j^{n+1} = U_j^n + \beta U_{j+1}^{n+1} + \beta U_{j-1}^{n+1}$$

$$(1+2\beta)|U_j^{n+1}| \leq |U_j^n| + \beta|U_{j+1}^{n+1}| + \beta|U_{j-1}^{n+1}|$$

$$(1+2\beta)\|U_j^{n+1}\|_\infty \leq \|U^n\|_\infty + 2\beta\|U^{n+1}\|_\infty$$

$$\Rightarrow \|U^{n+1}\|_\infty \leq \|U^n\|_\infty$$

Question: Why maximum principle is relevant to established stability?

$$(1+2\beta)g^{n+1}e^{ijk\Delta x} = g^n e^{ijk\Delta x} + \beta g^{n+1}e^{i(j+1)k\Delta x} + \beta g^{n+1}e^{i(j-1)k\Delta x}$$

$$(1+2\beta)g = 1 + \beta g e^{ik\Delta x} + \beta g e^{-ik\Delta x}$$

$$g(1+2\beta-2\beta\cos k\Delta x) = 1 \quad \text{then } g = \frac{1}{1+4\beta\sin^2\frac{k\Delta x}{2}}$$

Since $|g| \leq 1$ therefore this method is **unconditionally stable**.

3.3 Crank-Nicholson scheme

$$\frac{du}{dt} = f(u), \quad \frac{u^{n+1}-u^n}{\Delta t} = \frac{1}{2}(f(u^{n+1}) + f(u^n)) + O(dtd^2)$$

$$\frac{U_j^{n+1}-U_j^n}{\Delta t} = \frac{1}{2}\left(\frac{U_{j+1}^{n+1} - 2U_j^{n+1} + U_{j-1}^{n+1}}{\Delta x^2} + \frac{U_{j+1}^n - 2U_j^n + U_{j-1}^n}{\Delta x^2}\right) \approx O(\Delta t^2) + O(\Delta x^2)$$

This is a second-order in time and space method.

Again, we need to solve a tridiagonal linear system using eg. **Thomas algorithm**.

The Thomas algorithm

If

$$-a_jU_{j-1} + b_jU_j - c_jU_{j-1} = d_j, \quad j = 0, 1, \ldots \text{with } U_0 = U_N = 0$$

we assume that $a_j > 0$, $b_j > 0$, $c_j > 0$ and $d_j > a_j + c_j$.
The matrix is diagonally dominant and suppose that the first k equations have been reduced to

$$U_j - e_jU_{j+1} = f_j, \quad j = 1, 2, \ldots, k.$$

The last equation is $U_k - e_kU_{k+1} = f_k$

$$-a_{k+1}U_k + b_{k+1}U_{k+1} - c_{k+1}U_{k+2} = d_{k+1}$$

It is easy to eliminate U_K from these equation, giving a new equation involving U_{k+1} and U_{k+2},

$$\Rightarrow \quad U_{k+1} - \frac{c_{k+1}}{b_{k+1} - a_{k+1}e_k}U_{k+2} = \frac{d_{k+1} + a_{k+1}f_k}{b_{k+1} - a_{k+1}e_k}$$

$$\begin{cases} e_j = \frac{c_j}{b_j - a_je_{j-1}} \\ \\ f_j = \frac{d_j + a_jf_{j-1}}{b_j - a_je_{j-1}}, \quad j = 1, 2, \ldots, N \end{cases}$$

And $U_0 = 0$ for $j = 0$, $r_0 = f_0 = 0$.
Use these recurrence relation to find the coefficients, the value of U_j are easily obtained by beginning the operation values $U_N \to U_{N_1} \to U_{N-2} \ldots \to U_1$. Operation counts is $O(N)$ operation.

Maximum principle

$$(1+\beta)U_j^{n+1} + \beta U_j^n = U_j^n + \frac{\beta U_{j+1}^{n+1}}{2} + \frac{\beta U_{j-1}^{n+1}}{2} + \frac{\beta U_{j+1}^n}{2} + \frac{\beta U_{j-1}^n}{2}$$

If $\beta \leq \frac{1}{2}$

$$(1+\beta)|U_j^{n+1}| \leq (1-\beta)|U_j^n| + \frac{\beta}{2}|U_{j+1}^{n+1}| + \frac{\beta}{2}|U_{j-1}^{n+1}| + \frac{\beta}{2}|U_{j+1}^n| + \frac{\beta}{2}|U_{j-1}^n|$$

$$(1+\beta)|U_j^{n+1}| \leq \beta\|U^{n+1}\|_\infty + \|U^n\|_\infty$$

$$\Rightarrow (1+\beta)\|U^{n+1}\|_\infty \leq \beta\|U^{n+1}\|_\infty + \|U^n\|_\infty$$

Hence $\|U^{n+1}\|_\infty \leq \|U^{n+1}\|_\infty$.

von Neumann analysis

$$(1+\beta)U_j^{n+1} - \frac{\beta U_{j+1}^{n+1}}{2} - \frac{\beta U_{j-1}^{n+1}}{2} = (1-\beta)U_j^n + \frac{\beta U_{j+1}^n}{2} + \frac{\beta U_{j-1}^n}{2}$$

$$(1+\beta)g - \frac{\beta g e^{ik\Delta x}}{2} - \frac{\beta g e^{-ik\Delta x}}{2} = (1-\beta) + \frac{\beta(e^{ik\Delta x} + e^{-ik\Delta x})}{2}$$

$$\Rightarrow g(1 + 2\beta \sin^2 \frac{k\Delta x}{2}) = 1 - 2\beta \sin^2 \frac{k\Delta x}{2}$$

$$g = \frac{1 - 2\beta \sin^2 \frac{k\Delta x}{2}}{1 + 2\beta \sin^2 \frac{k\Delta x}{2}} \quad \Rightarrow |g| \leq 1.$$

Therefore the scheme is unconditionally stable.

3.4 The weight average method

$$\frac{U_j^{n+1} - U_j^n}{\Delta t} = \theta \frac{U_{j+1}^{n+1} - 2U_j^{n+1} + U_{j-1}^{n+1}}{\Delta x^2} + (1-\theta)\frac{U_{j+1}^n - 2U_j^n + U_{j-1}^n}{\Delta x^2}$$

$$\begin{aligned} \theta &= 0 \quad \text{explicit scheme} \\ \theta &= 1 \quad \text{first-order implicit scheme} \\ \theta &= \frac{1}{2} \quad \text{Crank-Nicholson scheme} \end{aligned}$$

If $\beta(1-\theta) \leq \frac{1}{2}$, then the maximum principle holds. The maximum principle means that maximum norm stable.

More general boundary condition

$$\frac{\partial u}{\partial x} = \alpha(t)u, \quad \alpha(t) \text{ is given at } x = 0$$

$$\frac{U_1^n - U_0^n}{\Delta x} = \alpha^n U_0^n$$

$$\Rightarrow U_0^n(1 + \alpha^n \Delta x) = U_1^n$$

$$\Rightarrow U_0^n = \frac{U_1^n}{(1 + \alpha^n \Delta x)}$$

More general linear problems

$$\frac{\partial u}{\partial x} = a(x,t)\frac{\partial^2 u}{\partial x^2}, \quad a(x,t) > 0$$

Explicit scheme

$$\frac{U_j^{n+1} - U_j^n}{2\Delta t} = a_j^n \frac{U_{j+1}^n - 2U_j^n + U_{j-1}^n}{\Delta x^2}$$

$$U_j^{n+1} = U_j^n + \beta a_j^n (U_{j+1}^n - 2U_j^n + U_{j-1}^n), \quad \text{where } a_j^n = a(x_j, t_n)$$

Maximum principle if $\beta\, max|a_j^n| \leq \frac{1}{2}$.

4 The 1D convection-diffusion equation

$$u_t + au_x = \nu u_{xx}$$

Forward time central space scheme

$$\frac{U_j^{n+1} - U_j^n}{2\Delta t} + a\frac{U_{j+1}^n - U_j^n}{2\Delta x} = \nu\frac{U_{j+1}^n - 2U_j^n + U_{j-1}^n}{\Delta x^2}$$

$$U^{n+1_j} = (1-2\beta)U_j^n + (\beta - \frac{\lambda}{2})U_{j+1}^n + (\beta + \frac{\lambda}{2})U_{j-1}^n$$

where $\lambda = \dfrac{a\Delta t}{\Delta x}, \beta = \dfrac{\nu\Delta t}{\Delta x^2}$ and $\lambda :$ CFL(courant-Friedrich-Lewy) condition.

The scheme satisfies the maximum principle if $\lambda \leq 2\beta \leq 1$

$$|U_j^{n+1}| \leq (1-2\beta)|U_j^n| + (\beta - \frac{\lambda}{2})|U_{j+1}^n| + (\beta + \frac{\lambda}{2})|U_{j-1}^n|$$

Hence $\|U^{n+1}\|_\infty \leq \|U^n\|_\infty$. That is, we have

$$\frac{2\nu\Delta t}{\Delta x^2} \leq 1 \quad \frac{a\Delta t}{\Delta x} \leq \frac{2\nu\Delta t}{\Delta x^2}$$

$$\Rightarrow Rc = \frac{a\Delta x}{\nu} \leq 2 \quad \Delta x \leq \frac{2\nu}{a}, \text{ where } Rc \text{ is cell Reynolds number.}$$

$Rc \leq 2$ is rather severe on the mesh width when ν is small. This is called the cell Reynolds number constraint. This causes the consequence that the time step must be chosen as

$$\lambda \leq 1, \quad \frac{a\Delta t}{\Delta x} \leq 1, \quad \Delta t \leq \frac{\Delta x}{a} \leq \frac{2\nu}{a^2}.$$

This explains why the forward time central space for $u_t + au_x = \nu u_{xx}$ is unstable when $\nu = 0$.

von Neumann analysis

$$|g(k)^2| \leq 1 - 4(2\beta - \lambda^2)\sin^2\frac{k\Delta x}{2} + 4(4\beta^2 - \lambda^2)\sin^4\frac{k\Delta x}{2}$$

Thus, we need $\lambda^2 \leq 2\beta \leq 1$

$$(\frac{a\Delta t}{\Delta x})^2 \leq \frac{2\nu\Delta t}{\Delta x^2} \quad \Rightarrow \quad \Delta t \leq \frac{2\nu}{a^2}$$

So we can summarize the stability constraint of the explicit scheme for linear convection-diffusion equation is

$$\Delta t \leq \frac{2\nu}{a^2}.$$

Now suppose we treat the diffusion term implicitly, and keep the convection term explicitly. The von Neumann analysis gives the amplification factor,

$$|g(k)^2| = \frac{1 + 4\lambda^2 \sin^2 \frac{k\Delta x}{2} \cos^2 \frac{k\Delta x}{2}}{(1 + 4\beta \sin^2 \frac{k\Delta x}{2})^2}.$$

The stability condition is

$$|g(k)^2| \leq 1 \text{ if } \lambda^2 \leq 2\beta \quad \Rightarrow \quad \Delta t \leq \frac{2\nu}{a^2}.$$

So the constraint derived from the cell Reynolds number constraint remains even thought we discretize the diffusion term implicitly. That is the reason why at high Reynolds number flow, most of stability problems come from the convection term, and the diffusion term does not help too much to stabilize it.

5 Hyperbolic equation in 1D

The simple 1D linear advection equation is written as

$$\begin{cases} u_t + au_x = 0 \\ u(x,0) = u_0(x), \quad -\infty < x < \infty, x > 0 \end{cases}$$

The method of characteristics: The characteristics are the solution of the ordinary differential equation $\frac{dx}{dt} = a$ and along a characteristic curve the solution satisfies

$$\frac{du(x(t),t)}{dt} = u_t + u_x \frac{dx}{dt} = u_t + au_x = 0$$

This, the characteristics are curve in the $x - t$ plane satisfying the O.D.E $x'(t) = a, \quad x(0) = x_0$ and the solution u is constant along these characteristics. More generally $u_t + (a(x)u)_x = 0$ where $a(x)$ is a smooth function.

$$u_t + a(x)u_x = -a'(x)u$$

$$\Rightarrow (\frac{\partial}{\partial t} + a(x)\frac{\partial}{\partial x})u = -a'(x)u.$$

It follows that evolution of u along any curve $x(t)$ satisfying

$$\begin{cases} x'(t) = a(x(t)) \\ x(0) = x_0, \end{cases} \qquad \text{satisfies a simple O.D.E} \qquad \frac{du(x(t),t)}{dt} = -a'(x(t))u(x(t),t)$$

In this case, the solution $u(x,t)$ is not a constant along these curve, but can be easily determined by solving two sets of O.D.E .

Two ideas need to be mentioned: Domain of dependence and Range of influence.

Hyperbolic conservation law: $u_t + f(u)_x = 0$ where $f(u)$ is a nonlinear function of u. We will assume that $f(u)$ in convex function, $f'(u) > 0$ for all u. The convexity assumption corresponds to genuine nonlinearity.

$$\text{inviscid Burgers equation:} \qquad u_t + uu_x = 0 \quad f(u) = \frac{u^2}{2}$$

$$\text{viscous Burgers equation:} \qquad u_t + uu_x = \epsilon u_{xx}$$

This is the simplest model that includes the nonlinear and viscous effects of fluid dynamics. **The viscous Burgers equation can be reduced to linear heat equation via Cole-Hopf transformation.**

Now consider the inviscid Burgers equation with smooth initial data. For small time, a solution can be constructed by the method of characteristics. It looks like an advection equation, but with the advection velocity u equation to the value of advected quantity. The characteristics satisfying $\frac{dx}{dt} = u(x(t), t)$ and along each characteristic u is a constant since $\frac{d}{dt}u(x(t), t) = \frac{\partial u}{\partial t} + \frac{dx}{dt}\frac{\partial u}{\partial t} = u_t + uu_x = 0$

Moreover, since u is constant on each characteristic, the slope $x'(t)$ is constant, so the characteristics are straight line determined by the initial data. If the initial data is smooth, then this can be used to determined the solution $u(x, t)$ for small enough time t, that characteristics don't cross. For each (x, t) we can solve the equation $x = \xi + u(\xi, 0)t$ for ξ and then $u(x, t) = u(\xi, 0)$.

Formation of shock

Consider the initial data

$$\begin{cases} u(x,0) = 1, & x < 0 \\ \qquad\quad 0, & x > 0 \end{cases}$$

Along the characteristic $\frac{dx}{dt} = 1$, the solution $u(x, t) = 1$, but along the characteristic $\frac{dx}{dt} = 0$, the solution $u(x, t) = 0$. Thus, the characteristics cross, and the wave breaks. That is, the discontinuous solution occurs and shock forms.

Question: How to determine the solution when this is happening?
Jump condition + entropy condition

$$u(x,t) = \begin{cases} 1, & x < st \\ 0, & x > st \end{cases} \qquad s = \frac{1}{2} \text{ is shock speed.}$$

6 Fast Poisson solver in polar coordinates

Many physical problems involve solving elliptic equations on polar or cylindrical domains. The first step is to transform the rectangular coordinate system into the convenient polar or cylindrical coordinates. Thus, we can rewrite the governing equations in those new coordinates. Let us consider Poisson equation on a unit disk $\Omega = \{(x, y) : x^2 + y^2 < 1\}$,

$$\frac{\partial^2 U}{\partial x^2} + \frac{\partial^2 U}{\partial y^2} = F \quad \text{in } \Omega, \tag{3}$$

with the Dirichlet $U = G$, or the Neumann $\frac{\partial U}{\partial \mathbf{n}} = G$ boundary conditions on $\partial\Omega$.

Applying the polar coordinate transformation, $x = r\cos\theta, y = r\sin\theta$, where $r = \sqrt{x^2 + y^2}$ and $\theta = \tan^{-1}(y/x)$, and setting $u(r, \theta) = U(r\cos\theta, r\sin\theta)$, $f(r, \theta) = F(r\cos\theta, r\sin\theta)$, and $g(\theta) = G(\cos\theta, \sin\theta)$, then Eq. (3) becomes

$$\frac{\partial^2 u}{\partial r^2} + \frac{1}{r}\frac{\partial u}{\partial r} + \frac{1}{r^2}\frac{\partial^2 u}{\partial \theta^2} = f(r, \theta) \quad 0 < r < 1,\ 0 \le \theta < 2\pi, \tag{4}$$

with $u(1, \theta) = g(\theta)$ (Dirichlet), or $\frac{\partial u}{\partial r}(1, \theta) = g(\theta)$ (Neumann).

Eq. (4) has an apparent singularity at the origin $r = 0$. It is important to realize that the cause of singularity is due to the representation of the governing equation in polar coordinate system. Thus, the solution itself is no way singular at the origin if f is smooth enough. In order to have the desired regularity and accuracy, the traditional finite difference scheme uses a uniformly integered grid with some condition at the origin. This pole condition acts as a numerical boundary condition at the origin which is needed in finite difference scheme. However, from the rectangular coordinate point of view, there is no need to impose any conditions.

In the following, we will present a finite difference discretization for Eq. (4) which is second-order accurate without imposing any pole conditions.

Finite difference discretization

Let us first consider the Dirichlet boundary problem. We choose a grid which the grid points are half-integered in radial direction and integered in azimuthal direction, that is,

$$r_i = (i - \frac{1}{2})\,\Delta r, \qquad \theta_j = (j - 1)\,\Delta\theta \tag{5}$$

where $\Delta r = \frac{2}{2N+1}$, $\Delta\theta = \frac{2\pi}{M}$, and $i = 1, 2, \ldots, N+1; j = 1, 2, \ldots, M+1$. Note that, by the choice of the radial mesh width, the boundary values are defined on the grid points. Let the discrete values be denoted by $u_{ij} \approx u(r_i, \theta_j)$, $f_{ij} \approx f(r_i, \theta_j)$, and $g_j = g(\theta_j)$. Using the centered difference method to discretize Eq. (4), for $i = 2, 3, \ldots, N, j = 1, 2, \ldots, M$ we have

$$\frac{u_{i+1,j} - 2\,u_{ij} + u_{i-1,j}}{(\Delta r)^2} + \frac{1}{r_i}\frac{u_{i+1,j} - u_{i-1,j}}{2\,\Delta r} + \frac{1}{r_i^2}\frac{u_{i,j+1} - 2\,u_{ij} + u_{i,j-1}}{(\Delta\theta)^2} = f_{ij}. \tag{6}$$

Among the above representations, the boundary values are given by $u_{N+1,j} = g_j$, and $u_{i0} = u_{i,M}, u_{i1} = u_{i,M+1}$ since u is 2π periodic in θ.

At $i = 1$, we have

$$\frac{u_{2j} - 2\,u_{1j} + u_{0j}}{(\Delta r)^2} + \frac{1}{r_1}\frac{u_{2j} - u_{0j}}{2\,\Delta r} + \frac{1}{r_1^2}\frac{u_{1,j+1} - 2\,u_{1j} + u_{1,j-1}}{(\Delta\theta)^2} = f_{1j}. \tag{7}$$

Since $r_1 = \frac{\Delta r}{2}$, we immediately observe that the coefficient of u_{0j} in Eq. (7) is zero. It turns out that the scheme does not need any extrapolation for u_{0j} so that there is no pole condition needed.

Let us order the unknowns u_{ij} by first grouping the same ray then moving counter-clockwise to cover the whole domain. Thus, the unknown vector v is defined by

$$v = \begin{bmatrix} u_1 \\ u_2 \\ \vdots \\ u_M \end{bmatrix}, \qquad u_j = \begin{bmatrix} u_{1j} \\ u_{2j} \\ \vdots \\ u_{Nj} \end{bmatrix}. \tag{8}$$

The remaining problem is to solve a large sparse linear system $Av = b$, where A can be written as ,

$$A = \begin{bmatrix} T-2D & D & & & & D \\ D & T-2D & D & & & \\ & \cdot & \cdot & \cdot & & \\ & & \cdot & \cdot & \cdot & \\ & & & D & T-2D & D \\ D & & & & D & T-2D \end{bmatrix}, \tag{9}$$

where $D = diag(\beta_1, \beta_2, \ldots, \beta_N)$ with $\beta_i = \frac{1}{(i-1/2)^2(\Delta\theta)^2}, 1 \le i \le N$, and

$$T = \begin{bmatrix} -2 & 1+\lambda_1 & & & & \\ 1-\lambda_2 & -2 & 1+\lambda_2 & & & \\ & \cdot & \cdot & \cdot & & \\ & & \cdot & \cdot & \cdot & \\ & & & 1-\lambda_{N-1} & -2 & 1+\lambda_{N-1} \\ & & & & 1-\lambda_N & -2 \end{bmatrix}, \tag{10}$$

with $\lambda_i = \frac{1}{2(i-1/2)}, 1 \le i \le N$. The known vector b is defined by

$$b = \begin{bmatrix} b_1 \\ b_2 \\ \vdots \\ b_M \end{bmatrix}, \qquad b_j = \begin{bmatrix} (\Delta r)^2\, f_{1j} \\ \vdots \\ (\Delta r)^2\, f_{N-1,j} \\ (\Delta r)^2\, f_{Nj} - (1+\lambda_N) g_j \end{bmatrix}. \tag{11}$$

Scaling the matrix A by the block diagonal matrix with block sub-matrix D^{-1}, the remaining linear equations can be solved by the famous cyclic reduction algorithm in $O(NM \log N)$ arithmetic operations. The matrix from the traditional finite difference scheme on a uniformly integered grid with the pole condition involves finding extra approximation at $r = 0$ which has one more row and column than A; thus, it cannot be solved directly by the Buneman algorithm. Although, our new scheme does not reduce significant amount of operation counts, the matrix of the new scheme has more succinct form than the traditional one. Furthermore, the discretization used here can be applied directly to the Helmholtz-type equation by just adding more terms in the diagonal part of the matrix A. The Helmholtz-type equation has applications from the numerical integration of time-dependent heat equation, reaction-diffusion equations, and fluid equations.

For the Neumann boundary problem, the grid points are located in the same way as the Dirichlet problem. The slight difference is the choice $\Delta r = \frac{1}{N}$. With this choice of radial mesh width, the discrete values of u are defined midway between boundary so that first derivatives can be centered on the grid points. That is, at $r = 1$,

$$\frac{\partial u}{\partial r} \approx \frac{u_{N+1,j} - u_{Nj}}{\Delta r}. \tag{12}$$

So the numerical boundary values $u_{N+1,j}$ can be approximated by $u_{Nj} + g_j \Delta r$. Therefore, we only need to modify T by

$$T = \begin{bmatrix} -2 & 1+\lambda_1 & & & & & \\ 1-\lambda_2 & -2 & 1+\lambda_2 & & & & \\ & \cdot & \cdot & \cdot & & & \\ & & \cdot & \cdot & \cdot & & \\ & & & \cdot & \cdot & \cdot & \\ & & & & 1-\lambda_{N-1} & -2 & 1+\lambda_{N-1} \\ & & & & & 1-\lambda_N & -1+\lambda_N \end{bmatrix}, \tag{13}$$

and b_j by

$$b_j = \begin{bmatrix} (\Delta r)^2 f_{1j} \\ \vdots \\ (\Delta r)^2 f_{N-1,j} \\ (\Delta r)^2 f_{Nj} - (1+\lambda_N)\, g_j \,\Delta r \end{bmatrix}. \tag{14}$$

It is important to note that the grid used for the Neumann problem turns out to be the popular staggered grid used for most of Neumann boundary problems [?].

7 Another simple FFT-based fast Poisson solver in polar coordinates

Let us consider the Poisson equation on a unit as in Eqn. (4) with the Dirichlet boundary value $u(1,\theta) = g(\theta)$, Neumann boundary value $\frac{\partial u}{\partial r}(1,\theta) = g(\theta)$, or the mixed Robin boundary condition $\frac{\partial u}{\partial r}(1,\theta) + \alpha u(1,\theta) = g(\theta), \alpha > 0$.

For the Neumann problem to have a solution, it is necessary that f satisfies the compatibility condition,

$$\int_0^{2\pi} \int_0^1 f(r,\theta)\, r\, dr\, d\theta = \int_0^{2\pi} g(\theta)\, d\theta. \tag{15}$$

7.1 Fourier mode equations

Since the solution u on a disk is periodic in θ, we can approximate it by the truncated Fourier series as

$$u(r,\theta) = \sum_{n=-N/2}^{N/2-1} u_n(r)\, e^{in\theta}, \tag{16}$$

where $u_n(r)$ is the complex Fourier coefficient given by

$$u_n(r) = \frac{1}{N} \sum_{j=0}^{N-1} u(r,\theta_j)\, e^{-in\theta_j}, \tag{17}$$

and $\theta_j = 2j\pi/N$, and N is the number of grid points along a circle. The above transformation between the physical space and Fourier space can be efficiently performed using the fast Fourier transform (FFT) with $O(N \log_2 N)$ arithmetic operations.

Substituting those expansions into Eq. (4) and equating the Fourier coefficients, $u_n(r)$ satisfies the ordinary differential equation

$$\frac{d^2 u_n}{dr^2} + \frac{1}{r}\frac{du_n}{dr} - \frac{n^2}{r^2} u_n = f_n, \quad 0 < r < 1, \tag{18}$$

with the Dirichlet boundary condition $u_n(1) = g_n$, the Neumann boundary condition $u_n'(1) = g_n$, or the mixed Robin condition $u_n'(1) + \alpha u_n(1) = g_n, \alpha > 0$. Here, the complex Fourier coefficients $f_n(r)$ and g_n are defined in the same manner as Eqs. (16)-(17). Eq. (18) is a singular equation in which the singularity occurs at the origin $r = 0$.

So far, the approach is in common with the spectral or pseudospectral methods. Next, we will introduce both second- and fourth-order finite difference discretizations to solve Eq. (18) without imposing any pole condition. The resulting linear system has a banded diagonal coefficient matrix. The inversion takes only $O(M)$ operations, where M is the number of the discretization points. The implementation of the present scheme is much simpler compared to the spectral methods which need to impose some pole conditions and also involve the fast cosine transform of $O(M \log_2 M)$ operations for solving Eq. (18). Nevertheless, the present scheme has roughly the same total computational costs ($O(NM \log_2 M)$ operations, including the costs of FFT in the beginning and the end) as the spectral methods. Besides, our finite difference scheme can be applied to different boundary including Dirichlet, Neumann and Robin problems without any difficulty.

7.2 Second-order method

Using a grid described in [?, 4] to avoid evaluating the value at the origin, we place the grid points at

$$r_i = (i - 1/2)\,\Delta r, \qquad i = 1, 2, \ldots M, M+1, \tag{19}$$

where the mesh width Δr will be specified later. From now on, we denote the discrete values $U_i \approx u_n(r_i)$ and $F_i \approx f_n(r_i)$.

First, we introduce a second-order centered difference scheme for the solution of Eq. (18) with the Dirichlet boundary value $u_n(1) = g_n$. We choose the mesh width $\Delta r = 2/(2M+1)$ so that $r_{M+1} = 1$, and the grid points are defined at the boundary. Applying the centered difference method to Eq. (18), we obtain

$$\frac{U_{i+1} - 2\,U_i + U_{i-1}}{(\Delta r)^2} + \frac{1}{r_i}\frac{U_{i+1} - U_{i-1}}{2\,\Delta r} - \frac{n^2}{{r_i}^2}\,U_i = F_i. \tag{20}$$

This is a tridiagonal linear system of equations for $U_i, i = 1, 2, \ldots M$, which can be solved by $O(M)$ arithmetic operations. In order to complete the linear system, the numerical boundary values U_0 and U_{M+1} should be supplied. When $i = 1$, the coefficient of U_0 in Eq. (20) equals to zero since $r_1 = \Delta r/2$; thus, no approximation for U_0 is needed. The other value U_{M+1} is given by the boundary value g_n. Note that, in [3], the author used the same scheme as (20) on an uniform grid without shifting half mesh so that some approximation at the origin is needed. It turns out that the matrix of the linear system is not as succinct as the one obtained from our approach.

For the Neumann ($\alpha = 0$) or Robin boundary problem, we still use the same grid described in (19) but with different choice of $\Delta r = 1/M$. With the choice of this mesh width, the discrete values of u are defined midway between boundary so that the first derivative can be centered on the grid points. This means, at $r = 1$, we have the approximation

$$\frac{\partial u}{\partial r} + \alpha\, u \approx \frac{U_{M+1} - U_M}{\Delta r} + \alpha\,\frac{U_{M+1} + U_M}{2} = g_n. \tag{21}$$

Therefore, the numerical boundary value U_{M+1} can be obtained in terms of U_M and g_n.

It is worth mentioning that the existence and uniqueness of the solution to Poisson equation with Neumann boundary can be explained by considering the zeroth Fourier mode equation

$$\frac{d^2 u_0}{dr^2} + \frac{1}{r}\frac{du_0}{dr} = f_0, \quad 0 < r < 1, \qquad u_0'(1) = g_0. \tag{22}$$

It is obvious that if the solution of the above equation exists, it is unique up to a constant. The existence of the solution is guaranteed by

$$\int_0^1 f_0(r)\, r\, dr = g_0, \tag{23}$$

which is an equivalent form of Eq. (15). The discrete analogue of (23) can be written as

$$\sum_{i=1}^{M} f_0(r_i)\, r_i\, \Delta r = g_0. \tag{24}$$

One should also note that the tridiagonal linear system resulting from the discretization of the zeroth Fourier mode equation is singular. If the discrete constraint (24) is satisfied, then the right-hand side vector falls into the range of the resulting matrix. Using Gauss elimination with pivoting, a zero pivot element is found for the last entry $i = M$ as well as the corresponding right-hand side of the zero pivot equation. The last element of the solution vector can be assigned to any value. This is the descrete analogue to the nonuniquess of the solution of the Neumann problem.

7.3 Fourth-order method

In this subsection, we use the same grid given in Eq. (19) with the choice of $\Delta r = 2/(2M+1)$. Before introducing the fourth-order scheme, we first write down the fourth-order five point difference operators for the first and second derivatives as

$$\begin{aligned} u'(r_i) &= \frac{-u_{i+2} + 8u_{i+1} - 8u_{i-1} + u_{i-2}}{12\,\Delta r} + O((\Delta r)^4), && (25)\\ u''(r_i) &= \frac{-u_{i+2} + 16u_{i+1} - 30u_i + 16u_{i-1} - u_{i-2}}{12\,(\Delta r)^2} + O((\Delta r)^4). && (26)\end{aligned}$$

The above approximations are defined at the interior points. For the boundary points, we use the following one-sided difference formulas given in [**?**]

$$\begin{aligned} u'(r_{M+1}) &= \frac{3u_{M+2} + 10u_{M+1} - 18u_M + 6u_{M-1} - u_{M-2}}{12\,\Delta r} + O((\Delta r)^4), && (27)\\ u''(r_{M+1}) &= \frac{11u_{M+2} - 20u_{M+1} + 6u_M + 4u_{M-1} - u_{M-2}}{12\,(\Delta r)^2} + O((\Delta r)^4). && (28)\end{aligned}$$

Now let us discretize Equation (18) using the fourth-order difference operators given in (25)-(26) at the interior points $i = 1, 2, \ldots, M$ as

$$\frac{-U_{i+2} + 16U_{i+1} - 30U_i + 16U_{i-1} - U_{i-2}}{12\,(\Delta r)^2} + \frac{-U_{i+2} + 8U_{i+1} - 8U_{i-1} + U_{i-2}}{12\, r_i\, \Delta r} - \frac{n^2}{r_i^2} U_i = F_i. \tag{29}$$

This is a pentadiagonal system for U_i. Solving (29) is a little more expensive than solving a tridiagonal system, but it still needs only $O(M)$ arithmetic operations.

Numerical boundary value

Again, in order to complete the system, we need to supply numerical boundary values such as U_{-1}, U_0, U_{M+1} and U_{M+2}. The inner numerical boundary values U_0, U_{-1} can be easily found by the symmetry constraint for polar coordinates as

$$\begin{aligned} U_0 &\approx u_n(r_0) = u_n(-\Delta r/2) = (-1)^n\, u_n(\Delta r/2) \approx (-1)^n\, U_1, \qquad (30)\\ U_{-1} &\approx u_n(r_{-1}) = u_n(-3\,\Delta r/2) = (-1)^n\, u_n(3\,\Delta r/2) \approx (-1)^n\, U_2. \qquad (31)\end{aligned}$$

The derivation of symmetry constraint is as follows. Let us first consider the transformation between Cartesian and polar coordinates as

$$x = r\cos\theta, \qquad y = r\sin\theta. \tag{32}$$

When we replace r by $-r$ and θ by $\theta+\pi$, the Cartesian coordinates of a point remains the same. Therefore, any scalar function $f(r,\theta)$ satisfies $f(-r,\theta) = f(r,\theta+\pi)$. Using this equality, we have

$$f(-r,\theta) = \sum_{n=-\infty}^{\infty} a_n(-r)\, e^{in\theta} = \sum_{n=-\infty}^{\infty} a_n(r)\, e^{in(\theta+\pi)} = \sum_{n=-\infty}^{\infty} (-1)^n\, a_n(r)\, e^{in\theta}.$$

Thus, when the domain of a function is extended to negative values of r, the nth Fourier coefficient of this function satisfies

$$a_n(-r) = (-1)^n a_n(r). \tag{33}$$

The outer numerical boundary value U_{M+2} can be obtained as follows. By requiring the equation (18) to be hold at the boundary $r_{M+1} = 1$ as well, we deduce

$$u_n''(r_{M+1}) + u_n'(r_{M+1}) = n^2\, u_n(r_{M+1}) + f_n(r_{M+1}). \tag{34}$$

Substituting the one-sided difference formulae (27)-(28) into the above equation, we obtain a formula for U_{M+2} in terms of $U_{M+1}, U_M, U_{M-1}, U_{M-2}$ and F_{M+1}. For the Dirichlet problem, the value U_{M+1} is known. As to the Neumann or Robin boundary, an approximation of U_{M+1} can be derived using the one-sided difference formula (27).

Summary:

Let us close this section by summarizing the algorithm and the operation counts in the following three steps:
1. Compute the Fourier coefficients for the right-hand side function as in (17) by FFT, which requires $O(MN\log_2 N)$ arithmetic operations.
2. Solve the tridiagonal (2nd-order) or pentadiagonal (4th-order) linear system for each Fourier mode. This requires $O(MN)$ operations.

3. Convert the Fourier coefficients as in (16) by FFT to obtain the solution, which requires $O(MN \log_2 N)$ operations.

The overall operation count is thus $O(MN \log_2 N)$ for $M \times N$ grid points. The method can be easily extended to the Helmholtz-type equation in a straightforward manner.

References

[1] R. J. LeVeque, Finite difference methods for differential equations, 1998.

[2] K. W. Morton and D. F. Mayers, Numerical solution of partial differential equations, Cambridge University Press, 1994.

[3] A. Iserles, A first course in the numerical analysis of differential equations, Cambridge University Press, 1996.

[4] M.-C. Lai, A note on finite difference discretizations for Poisson equation on a disk, Numer. Methods Partial Differential Eq., 17, 199–203, (2001).

[5] M.-C. Lai and W.-C. Wang, Fast direct solvers for Poisson equation on 2D polar and spherical geometries, Numer. Methods Partial Differential Eq., 18, 56–68, (2002).

Immersed boundary and immersed interface method for elliptic equations involving interfaces or irregular domains

Ming-Chih Lai
mclai@math.nctu.edu.tw

Department of Applied Mathematics
National Chiao Tung University
1001, Ta Hsueh Road, Hsinchu 30050
Taiwan

Outline of the talk

Motivation-Immersed Boundary Method

Poisson equation with jump discontinuities

- An IIM to incorporate the jumps in the normal direction
- An interpolation (grid to interface) formula for non-smooth functions
- Numerical examples

Stokes flow with singular forces

- Numerical scheme
- Numerical results

Poisson equation on an irregular domain

- Integral equation formulation approach
- Boundary value extrapolation method
- High-order compact scheme for Poisson equation on 2D irregular domain
- Numerical results

Immersed boundary method

Mathematical formulation:

- Treat the elastic material as a part of fluid
- The material acts force into the fluid
- The material moves along with the fluid

Numerical method:

- Finite difference discretization
- Eulerian grid points for the fluid variables
- Lagrangian markers for the immersed boundary
- The fluid-boundary are linked by a smooth version of Dirac delta function

Review: C.S. Peskin, Acta Numer., 11:479-517, 2002

Numerical issues of IB method

- Simple and easy to implement
- Embedding complex structure into Cartesian domain, no complicated grid generation
- Fast elliptic solver (FFT) on Cartesian grid can be applied
- Numerical smearing near the immersed boundary
- First-order accurate, accuracy of 1D IB model (Beyer & LeVeque 1992, Lai 1998), formally second-order scheme (Lai & Peskin 2000, Griffith & Peskin 2005, Griffith et al 2007), Immersed Interface Method (IIM, LeVeque & Li 1994)
- High-order discrete delta function in 2D, 3D
- Numerical stability tests, different semi-implicit methods (Tu & Peskin 1992, Mayo & Peskin 1993, Newren, Fogelson, Guy & Kirby 2007, 2008)
- Stability analysis (Stockie & Wetton 1999, Hou & Shi 2008)
- Convergence analysis (Y. Mori 2008)

Mathematical formulation

Consider a massless elastic membrane Γ immersed in viscous incompressible fluid domain Ω.

$$\Gamma : \qquad \boldsymbol{X}(s,t), \quad 0 \leq s \leq L_b \qquad L_b : \qquad \text{unstressed length}$$

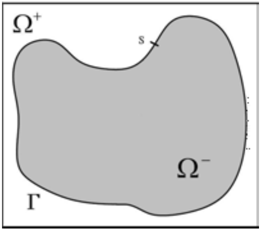

$$\rho\left(\frac{\partial \boldsymbol{u}}{\partial t} + (\boldsymbol{u}\cdot\nabla)\boldsymbol{u}\right) + \nabla p = \mu\Delta\boldsymbol{u} + \boldsymbol{f}$$

$$\nabla\cdot\boldsymbol{u} = 0$$

$$\boldsymbol{f}(\boldsymbol{x},t) = \int_\Gamma \boldsymbol{F}(s,t)\delta(\boldsymbol{x}-\boldsymbol{X}(s,t))ds$$

$$\frac{\partial \boldsymbol{X}(s,t)}{\partial t} = \boldsymbol{u}(\boldsymbol{X}(s,t),t) = \int_\Omega \boldsymbol{u}(\boldsymbol{x},t)\delta(\boldsymbol{x}-\boldsymbol{X}(s,t))d\boldsymbol{x}$$

$$\boldsymbol{F}(s,t) = \frac{\partial}{\partial s}(T\boldsymbol{\tau}), \quad T = \sigma(\left|\frac{\partial \boldsymbol{X}}{\partial s}\right|; s,t), \quad \boldsymbol{\tau} = \frac{\partial \boldsymbol{X}/\partial s}{|\partial \boldsymbol{X}/\partial s|}$$

FLUID		BOUNDARY	
$\boldsymbol{u}(\boldsymbol{x},t)$:	velocity	$\boldsymbol{X}(\boldsymbol{x},t)$:	boundary configuration
$\boldsymbol{p}(\boldsymbol{x},t)$:	pressure	$\boldsymbol{F}(\boldsymbol{x},t)$:	boundary force
ρ :	density	T :	tension
μ :	viscosity	$\boldsymbol{\tau}$:	unit tangent

Jump conditions, LeVeque & Li 1997 (2D), Lai & Li 2001 (3D)

Theorem (1)

The pressure and the velocity normal derivatives across the boundary satisfy

$$[p] = \frac{\boldsymbol{F} \cdot \boldsymbol{n}}{|\partial \boldsymbol{X} / \partial s|},$$

$$[\boldsymbol{u}] = 0,$$

$$\mu \left[\frac{\partial \boldsymbol{u}}{\partial \boldsymbol{n}} \right] = - \frac{\boldsymbol{F} \cdot \boldsymbol{\tau}}{|\partial \boldsymbol{X} / \partial s|} \boldsymbol{\tau}$$

Theorem (2)

The normal derivatives of the pressure across the boundary satisfies

$$\left[\frac{\partial p}{\partial \boldsymbol{n}} \right] = \frac{\frac{\partial}{\partial s} \left(\frac{\boldsymbol{F} \cdot \boldsymbol{\tau}}{|\partial \boldsymbol{X} / \partial s|} \right)}{|\partial \boldsymbol{X} / \partial s|}$$

A test example with known solutions

$$\frac{\partial \boldsymbol{u}}{\partial t} + (\boldsymbol{u} \cdot \nabla)\boldsymbol{u} + \nabla p = \Delta \boldsymbol{u} + \boldsymbol{f} + \boldsymbol{g}$$

$$\nabla \cdot \boldsymbol{u} = 0$$

$$\boldsymbol{f} = \int_\Gamma \boldsymbol{F}(s,t)\delta(\boldsymbol{x} - \boldsymbol{X}(s,t))ds$$

$$\frac{\partial \boldsymbol{X}(s,t)}{\partial t} = \boldsymbol{u}(\boldsymbol{X}(s,t),t)$$

$$\Omega = [0,1]\times[0,1], \qquad \Gamma = \{\big(X(s),Y(s)\big) = \big(0.5\cos s, 0.5\sin s\big), 0 \le s \le 2\pi\}$$

$$\left|\frac{\partial \boldsymbol{X}}{\partial s}\right| = 0.5$$

$$\boldsymbol{n} = \big(\cos s, \sin s\big), \quad \boldsymbol{\tau} = \big(-\sin s, \cos s\big)$$

$$u(x,y,t)=\begin{cases} e^{-t}\left(2y-\frac{y}{r}\right) & r\geq 0.5\\ 0 & r<0.5\end{cases}, \qquad \left[\frac{\partial u}{\partial \boldsymbol{n}}\right]=2e^{-t}\sin s$$

$$v(x,y,t)=\begin{cases} e^{-t}\left(-2x+\frac{x}{r}\right) & r\geq 0.5\\ 0 & r<0.5\end{cases}, \qquad \left[\frac{\partial v}{\partial \boldsymbol{n}}\right]=-2e^{-t}\cos s$$

$$p(x,y,t)=\begin{cases} 0 & r\geq 0.5\\ 1 & r<0.5\end{cases}, \qquad \left[\frac{\partial p}{\partial \boldsymbol{n}}\right]=-1$$

$$g_1(x,y,t)=\begin{cases} e^{-t}\left(\frac{y}{r}-2y-\frac{y}{r^3}\right)+e^{-2t}\left(\frac{4x}{r}-4x-\frac{x}{r^2}\right) & r\geq 0.5\\ 0 & r<0.5\end{cases}$$

$$g_2(x,y,t)=\begin{cases} -e^{-t}\left(\frac{x}{r}-2x-\frac{x}{r^3}\right)+e^{-2t}\left(\frac{4y}{r}-4y-\frac{y}{r^2}\right) & r\geq 0.5\\ 0 & r<0.5\end{cases}$$

$$F_{\boldsymbol{n}}=-0.5 \qquad F_1=-0.5\cos s-e^{-t}\sin s \qquad [\boldsymbol{g}\cdot\boldsymbol{n}]=0$$

$$F_{\boldsymbol{\tau}}=e^{-t} \qquad F_2=-0.5\sin s+e^{-t}\cos s$$

Numerical scheme

FLUID-Eulerian	BOUNDARY-Lagrangian
$N \times N$ lattice points $\boldsymbol{x} = (ih, jh)$	M moving points $\boldsymbol{X}_k$
$\boldsymbol{u}^n \approx \boldsymbol{u}(\boldsymbol{x}, n\Delta t)$,	$\boldsymbol{U}_k^n \approx \boldsymbol{u}(\boldsymbol{X}_k, n\Delta t)$
$\boldsymbol{f}^n \approx \boldsymbol{f}(\boldsymbol{x}, n\Delta t)$,	$\boldsymbol{F}_k^n \approx \boldsymbol{F}(\boldsymbol{X}_k, n\Delta t)$
$p^n \approx p(\boldsymbol{x}, n\Delta t)$,	

How to march $(\boldsymbol{X}^n, \boldsymbol{u}^n)$ to $(\boldsymbol{X}^{n+1}, \boldsymbol{u}^{n+1})$?

Step1 Compute the boundary force

$$T^n_{k+1/2} = \sigma(|D_s \boldsymbol{X}^n_k|), \quad \boldsymbol{\tau}^n_{k+1/2} = \frac{D_s \boldsymbol{X}^n_k}{|D_s \boldsymbol{X}^n_k|}, \quad \boldsymbol{F}^n_k = D_s(T\boldsymbol{\tau})^n_{k+1/2},$$

where $T^n_{k+1/2}$ and $\boldsymbol{\tau}^n_{k+1/2}$ are both defined on $s = (k + \frac{1}{2})\Delta s$, and $\boldsymbol{F}^n_k$ is defined on $s = k\Delta s$.

Step2 Apply the boundary force to the fluid

$$\boldsymbol{f}^n(\boldsymbol{x}) = \sum_k \boldsymbol{F}^n_k \delta_h(\boldsymbol{x} - \boldsymbol{X}^n_k)\Delta s.$$

Step3 Solve the Navier-Stokes equations with the force to update the velocity

$$\rho\left(\frac{\boldsymbol{u}^{n+1} - \boldsymbol{u}^n}{\Delta t} + \sum_{i=1}^{2} u^n_i D^{\pm}_i \boldsymbol{u}^n\right) = -D^0 p^{n+1} + \mu \sum_{i=1}^{2} D^+_i D^-_i \boldsymbol{u}^{n+1} + \boldsymbol{f}^n,$$
$$D^0 \cdot \boldsymbol{u}^{n+1} = 0,$$

where $T^n_{k+1/2}$ and $\boldsymbol{\tau}^n_{k+1/2}$ are both defined on $s = (k + \frac{1}{2})\Delta s$, and $\boldsymbol{F}^n_k$ is defined on $s = k\Delta s$.

Step4 Interpolate the new velocity on the lattice into the boundary points and move the boundary points to new positions

$$\boldsymbol{U}_k^{n+1} = \sum_{\boldsymbol{x}} \boldsymbol{u}^{n+1} \delta_h(\boldsymbol{x} - \boldsymbol{X}_k^n) h^2$$

$$\boldsymbol{X}_k^{n+1} = \boldsymbol{X}_k^n + \Delta t \boldsymbol{U}_k^{n+1}$$

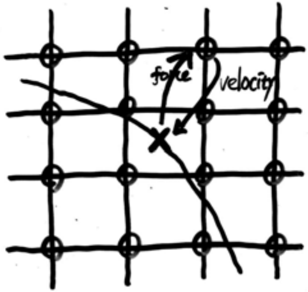

Discrete delta function δ_h

$\delta_h(\boldsymbol{x}) = \delta_h(x)\delta_h(y)$

1. δ_h is positive and continuous function.
2. $\delta_h(x) = 0$, for $|x| \geq 2h$.
3. $\sum_j \delta_h(x_j - \alpha)h = 1$ for all α.
   $\left(\sum\limits_{j \text{ even}} \delta_h(x_j - \alpha)h = \sum\limits_{j \text{ odd}} \delta_h(x_j - \alpha)h = \frac{1}{2}\right)$
4. $\sum_j (x_j - \alpha)\delta_h(x_j - \alpha)h = 0$ for all α.
5. $\sum_j \left(\delta_h(x_j - \alpha)h\right)^2 = C$ for all α.
   $\left(\sum_j \delta_h(x_j - \alpha)\delta_h(x_j - \beta)h^2 \leq C\right)$

Uniquely determined: $C = \frac{3}{8}$.

$$\delta_h(x) = \begin{cases} \frac{1}{8h}\left(3 - 2\left|x\right|/h + \sqrt{1 + 4\left|x\right|/h - 4(\left|x\right|/h)^2}\right) & \left|x\right| \leq h, \\ \frac{1}{8h}\left(5 - 2\left|x\right|/h - \sqrt{-7 + 12\left|x\right|/h - 4(\left|x\right|/h)^2}\right) & h \leq \left|x\right| \leq 2h, \\ 0 & \text{otherwise} \end{cases}$$

Poisson equation with jump discontinuities

$$\Delta u(\mathbf{x}) = f(\mathbf{x}), \text{ in } \Omega,$$

$$[u](s) = g_0(s), \qquad \left[\frac{\partial u}{\partial \mathbf{n}}\right](s) = g_1(s) \text{ on } \Gamma,$$

$$u(\mathbf{x}) = u_b(\mathbf{x}) \text{ on } \partial\Omega,$$

where the jumps $[u](s) = u^+ - u^-$ and $\left[\frac{\partial u}{\partial \mathbf{n}}\right](s) = \frac{\partial u^+}{\partial \mathbf{n}} - \frac{\partial u^-}{\partial \mathbf{n}}$.

Motivation: Applying the projection method to solve the immersed boundary models

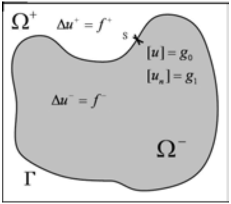

Different approaches

1. Peskin's immersed boundary method (1972): rewrite the equation by adding a delta function source on the righthand side when $g_0 = 0$. Approximating the delta source by the usual discrete delta function gives first-order accurate results.
2. A. Mayo's method (1984): incorporating the jumps in Cartesian directions, dimension by dimension approach
   - Fast Poisson solver on irregular regions
   - Rapid evaluation of volume integrals of potential theory
3. LeVeque & Li's immersed interface method (1994)
   - Elliptic equations with discontinuous coefficients and singular sources
   - Stokes (LeVeque & Li 1997) and Navier-Stokes (Li & Lai 2001) with interfaces, many applications
4. Russel & Wang's method (2003): incorporating the jumps in normal directions
5. Li, Wang, Chern & Lai (2003): removing the singularities by normal extension

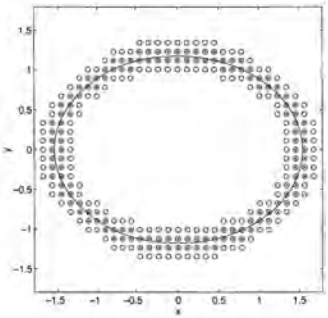

Figure: Irregular points and their stencils.

Idea:

1. Embedding the interface/irregular domain into a regular Cartesian domain so a fast direct Poisson solver can be applied
2. Incorporating the jump conditions into finite difference discretizations. The modification depending on the jumps only appear at those irregular points

$$\begin{cases} \Delta_h u = f + C_* \\ u\big|_{\partial\Omega} \text{ is given.} \end{cases} \qquad \textbf{Question: } C_* = ?$$

Finite difference corrections– 1D case

Lemma: Let $u(x)$ be a piecewise twice differentiable function. Assume that $u(x)$ and its derivatives have finite jumps $[u]$, $[u_x]$, and $[u_{xx}]$, at $x^* = x + \alpha h$, $-1 \leq \alpha \leq 1$, then the following relations hold:

$$\frac{u(x+h) - u(x-h)}{2h} = \begin{cases} u'(x) + \dfrac{C(x,\alpha)}{2h} + O(h^2), & \text{if } \alpha \geq 0, \\ u'(x) - \dfrac{\tilde{C}(x,\alpha)}{2h} + O(h^2), & \text{if } \alpha < 0, \end{cases}$$

$$\frac{u(x+h) - 2u(x) + u(x-h)}{h^2} = \begin{cases} u''(x) + \dfrac{C(x,\alpha)}{h^2} + O(h), & \text{if } \alpha \geq 0, \\ u''(x) + \dfrac{\tilde{C}(x,\alpha)}{h^2} + O(h), & \text{if } \alpha < 0, \end{cases}$$

where

$$\begin{aligned} C(x,\alpha) &= [u] + [u_x]\,(1-\alpha)\,h + [u_{xx}]\,\frac{(1-\alpha)^2\,h^2}{2}, \\ \tilde{C}(x,\alpha) &= [u] - [u_x]\,(1-|\alpha|)\,h + [u_{xx}]\,\frac{(1-|\alpha|)^2\,h^2}{2}, \end{aligned}$$

Proof: First, we assume that $0 < \alpha \leq 1$. Therefore, $x - h$ and x are on the same side while $x + h$ is on the other side. We use the Taylor expansion twice for $u(x+h)$ at x^*, then at x, as follows,

$$\begin{aligned}
u(x+h) &= u(x^* + (1-\alpha)h) \\
&= u^+(x^*) + u_x^+(x^*)(1-\alpha)h + u_{xx}^+(x^*)\frac{(1-\alpha)^2 h^2}{2} \\
&+ O(h^3) \\
&= u^-(x^*) + u_x^-(x^*)(1-\alpha)h + u_{xx}^-(x^*)\frac{(1-\alpha)^2 h^2}{2} \\
&+ C(x,\alpha) + O(h^3) \\
&= u(x) + u_x(x)\alpha h + u_{xx}(x)\frac{\alpha^2 h^2}{2} \\
&+ u_x(x)(1-\alpha)h + u_{xx}(x)\alpha(1-\alpha)h^2 \\
&+ u_{xx}(x)\frac{(1-\alpha)^2 h^2}{2} + C(x,\alpha) + O(h^3).
\end{aligned}$$

Thus, we have

$$u(x+h) = u(x) + u_x(x)\,h + u_{xx}(x)\,\frac{h^2}{2} + C(x,\alpha) + O(h^3).$$

$$u(x-h) = u(x) - u_x(x)\,h + u_{xx}(x)\,\frac{h^2}{2} + O(h^3).$$

Then, we assume that $0 > \alpha \geq -1$. Therefore, $x+h$ and x are on the same side while $x-h$ is on the other side. We use the Taylor expansion twice for $u(x-h)$ at x^*, then at x, as follows,

$$\begin{aligned} u(x-h) &= u(x^* - (1-|\alpha|)h) \\ &= u^-(x^*) - u_x^-(x^*)(1-|\alpha|)h \\ &+ u_{xx}^-(x^*)\frac{(1-|\alpha|)^2h^2}{2} + O(h^3) \\ &= u^+(x^*) - u_x^+(x^*)(1-|\alpha|)h \\ &+ u_{xx}^+(x^*)\frac{(1-|\alpha|)^2h^2}{2} + \tilde{C}(x,\alpha) + O(h^3) \\ &= u(x) - u_x(x)|\alpha|h + u_{xx}(x)\frac{|\alpha|^2h^2}{2} \\ &- (u_x(x) - u_{xx}(x)|\alpha|h)(1-|\alpha|)h \\ &+ u_{xx}(x)\frac{(1-|\alpha|)^2h^2}{2} + \tilde{C}(x,\alpha) + O(h^3). \end{aligned}$$

$$u(x-h) = u(x) - u_x(x)\,h + u_{xx}(x)\,\frac{h^2}{2} + \tilde{C}(x,\alpha) + O(h^3).$$

$$u(x+h) = u(x) + u_x(x)\,h + u_{xx}(x)\,\frac{h^2}{2} + O(h^3).$$

In summary,

$$
\begin{aligned}
u_i' &= \frac{u_{i+1} - u_{i-1}}{2h} - \frac{[u]}{2h} - \frac{[u_x](x_{i+1} - x^*)}{2h} \\
&- \frac{[u_{xx}](x_{i+1} - x^*)^2}{4h} + O(h^2) \\
u_{i+1}' &= \frac{u_{i+2} - u_i}{2h} - \frac{[u]}{2h} - \frac{[u_x](x_i - x^*)}{2h} \\
&- \frac{[u_{xx}](x_i - x^*)^2}{4h} + O(h^2) \\
u_i'' &= \frac{u_{i-1} - 2u_i + u_{i+1}}{h^2} - \frac{[u]}{h^2} - \frac{[u_x](x_{i+1} - x^*)}{h^2} \\
&- \frac{[u_{xx}](x_{i+1} - x^*)^2}{2h^2} + O(h) \\
u_{i+1}'' &= \frac{u_i - 2u_{i+1} + u_{i+2}}{h^2} + \frac{[u]}{h^2} + \frac{[u_x](x_i - x^*)}{h^2} \\
&+ \frac{[u_{xx}](x_i - x^*)^2}{2h^2} + O(h)
\end{aligned}
$$

2D case– dimension by dimension

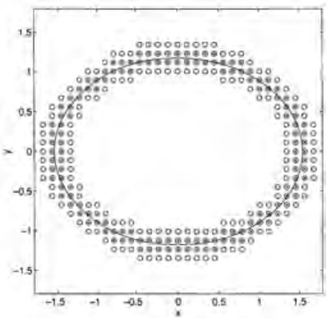

$$\Gamma : (\boldsymbol{X}(s), \boldsymbol{Y}(s)) \qquad s: \text{ parameter (arc length)}$$

$$\boldsymbol{\tau} = (\dot{X}(s), \dot{Y}(s)) \qquad \boldsymbol{n} = (\dot{Y}(s), -\dot{X}(s))$$

$$[u](s) = g_0(s) \quad \Rightarrow \quad [u_x]\dot{X} + [u_y]\dot{Y} = \dot{g_0}$$

$$\left[\frac{\partial u}{\partial n}\right](s) = g_1(s) \quad \Rightarrow \quad [u_x]\dot{Y} - [u_y]\dot{X} = g_1$$

$$[u_x] = \dot{X}\dot{g_0} + \dot{Y}g_1, \qquad [u_y] = \dot{Y}\dot{g_0} - \dot{X}g_1$$

Question: How to find $[u_{xx}]$, $[u_{yy}]$?
Differentiating the jump conditions w.r.t. s, we obtain

$$[u_{xx}]\,(\dot{X})^2+[u_{xy}]\,\dot{X}\dot{Y}+[u_x]\,\ddot{X}+[u_{yx}]\,\dot{X}\dot{Y}+[u_{yy}]\,(\dot{Y})^2+[u_y]\,\ddot{Y}=\ddot{g}_0$$
$$[u_{xx}]\,\dot{X}\dot{Y}+[u_{xy}]\,(\dot{Y})^2+[u_x]\,\ddot{Y}-[u_{yx}]\,(\dot{X})^2-[u_{yy}]\,\dot{X}\dot{Y}-[u_y]\,\ddot{X}=\dot{g}_1$$

$$[u_{xy}]=[u_{yx}]$$
$$[u_{xx}]+[u_{yy}]=[f]$$

$$[u_{xx}]=g_2+(\dot{Y})^2[f], \qquad [u_{yy}]=-g_2+(\dot{X})^2[f],$$

where

$$g_2=2\kappa\dot{X}\dot{Y}\dot{g}_0+((\dot{X})^2-(\dot{Y})^2)(\ddot{g}_0-\kappa g_1)+2\dot{X}\dot{Y}\dot{g}_1$$

and $\kappa=\ddot{X}\dot{Y}-\dot{X}\ddot{Y}$ is the curvature.

An IIM to incorporate the jumps in the normal direction, Russel & Wang, 2003

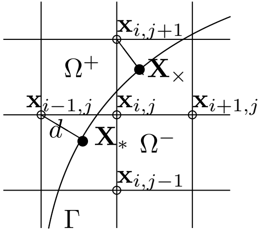

Figure: The five-point Laplacian at the irregular point $\mathbf{x}_{i,j}$.

Let $\mathbf{X}_*$ and $\mathbf{X}_\times$ be the orthogonal projections of the grid points $\mathbf{x}_{i-1,j}$ and $\mathbf{x}_{i,j+1}$ on the interface, respectively.

$$
\begin{aligned}
\Delta_h u &= \frac{u_{i-1,j} - 2u_{i,j} + u_{i+1,j}}{h^2} + \frac{u_{i,j+1} - 2u_{i,j} + u_{i,j-1}}{h^2} \\
&= \frac{u^+_{i-1,j} - 2u^-_{i,j} + u^-_{i+1,j}}{h^2} + \frac{u^+_{i,j+1} - 2u^-_{i,j} + u^-_{i,j-1}}{h^2} \\
&= \frac{u^-_{i-1,j} - 2u^-_{i,j} + u^-_{i+1,j}}{h^2} + \frac{u^-_{i,j+1} - 2u^-_{i,j} + u^-_{i,j-1}}{h^2} \\
&\quad + \frac{u^+_{i-1,j} - u^-_{i-1,j}}{h^2} + \frac{u^+_{i,j+1} - u^-_{i,j+1}}{h^2} \\
&= (u^-_{xx})_{i,j} + (u^-_{yy})_{i,j} + \mathcal{O}(h^2) + \frac{u^c_{i-1,j}}{h^2} + \frac{u^c_{i,j+1}}{h^2} \\
&= f^-_{i,j} + \frac{1}{h^2}\left(u^c_{i-1,j} + u^c_{i,j+1}\right) + \mathcal{O}(h^2).
\end{aligned}
$$

$$
\begin{aligned}
u^c_{i-1,j} &= u^+_{i-1,j} - u^-_{i-1,j} \\
&= \left(u^+_* + d\frac{\partial u^+_*}{\partial \mathbf{n}} + \frac{d^2}{2}\frac{\partial^2 u^+_*}{\partial \mathbf{n}^2} + \mathcal{O}(h^3) \right) \\
&\quad - \left(u^-_* + d\frac{\partial u^-_*}{\partial \mathbf{n}} + \frac{d^2}{2}\frac{\partial^2 u^-_*}{\partial \mathbf{n}^2} + \mathcal{O}(h^3) \right) \\
&= [u]_{\mathbf{X}_*} + d\left[\frac{\partial u}{\partial \mathbf{n}}\right]_{\mathbf{X}_*} + \frac{d^2}{2}\left[\frac{\partial^2 u}{\partial \mathbf{n}^2}\right]_{\mathbf{X}_*} + \mathcal{O}(h^3).
\end{aligned}
$$

d: the signed distance between the grid point $\mathbf{x}_{i-1,j}$ and the projection $\mathbf{X}_*$. Notice that, $d < 0$ if the grid point $\mathbf{x}_{i-1,j}$ is inside the interface.

Question: How to find the second normal derivative at the interface $\left[\frac{\partial^2 u}{\partial \mathbf{n}^2}\right]_{\mathbf{X}_*}$?

The Laplace operator on the interface

$$\frac{\partial^2 u}{\partial \mathbf{n}^2}(\mathbf{X}(s)) + \kappa(\mathbf{X}(s))\, \frac{\partial u}{\partial \mathbf{n}}(\mathbf{X}(s)) + \frac{\partial^2 u}{\partial s^2}(\mathbf{X}(s)) = f(\mathbf{X}(s)),$$

where the value $\kappa(\mathbf{X}(s))$ is the local curvature of the interface.

$$\left[\frac{\partial^2 u}{\partial \mathbf{n}^2}\right]_{\mathbf{X}_*} = [f]_{\mathbf{X}_*} - \kappa_{\mathbf{X}_*} \left[\frac{\partial u}{\partial \mathbf{n}}\right]_{\mathbf{X}_*} - \frac{\partial^2}{\partial s^2}\, [u]_{\mathbf{X}_*}\,.$$

$$\begin{aligned} u^c_{i-1,j} &= [u]_{\mathbf{X}_*} + d \left[\frac{\partial u}{\partial \mathbf{n}}\right]_{\mathbf{X}_*} + \frac{1}{2}\, d^2 \left[\frac{\partial^2 u}{\partial \mathbf{n}^2}\right]_{\mathbf{X}_*} \\ &= [u]_{\mathbf{X}_*} + d \left[\frac{\partial u}{\partial \mathbf{n}}\right]_{\mathbf{X}_*} + \frac{1}{2}\, d^2 \left([f]_{\mathbf{X}_*} - \kappa_{\mathbf{X}_*} \left[\frac{\partial u}{\partial \mathbf{n}}\right]_{\mathbf{X}_*} - \frac{\partial^2}{\partial s^2}\, [u]_{\mathbf{X}_*} \right). \end{aligned}$$

The correction term $u^c_{i,j+1}$ can be computed in a similar way.

An interpolation (grid to interface) formula for non-smooth functions, Lai & Tseng 2008

Question: Given a non-smooth (with known jumps) function on the grid, how to interpolate the value of u_I^- at $\mathbf{X}_I = (X_I, Y_I) = (x_{i,j} + \alpha h, y_{i,j} + \beta h)$ from surrounding values $u_{i,j}, u_{i+1,j}, u_{i,j+1}$ and $u_{i+1,j+1}$?

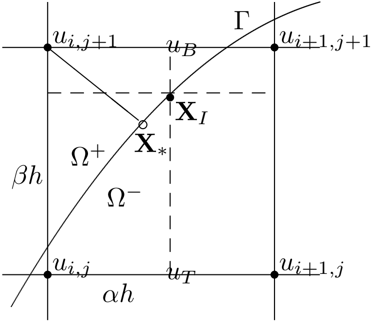

Figure: An interpolation of the values from surrounding grid points to the interface.

Let

$$u_I^- = \beta\, u_T + (1-\beta)\, u_B + C_I^- + \mathcal{O}(h^2).$$

What is C_I^-?

$$\begin{aligned}
& \beta\, u_T + (1-\beta)\, u_B \\
= \;& \beta\, \left((1-\alpha) u_{i,j+1}^{+} + \alpha u_{i+1,j+1}^{-}\right) + (1-\beta)\, \left((1-\alpha)\, u_{i,j}^{-} + \alpha\, u_{i+1,j}^{-}\right) \\
= \;& \beta\, \left((1-\alpha)\, u_{i,j+1}^{-} + \alpha\, u_{i+1,j+1}^{-}\right) \\
& +(1-\beta)\, \left((1-\alpha)\, u_{i,j}^{-} + \alpha u_{i+1,j}^{-}\right) + \beta\,(1-\alpha)\, u_{i,j+1}^{c} \\
= \;& u_I^- + \beta\,(1-\alpha)\, u_{i,j+1}^{c}
\end{aligned}$$

where the correction $u_{i,j+1}^{c}$ can be derived exactly same procedure except neglecting the second-order term. That is,

$$u_{i,j+1}^{c} = u_{i,j+1}^{+} - u_{i,j+1}^{-} = [u]_{\mathbf{X}_*} + d\, \left[\frac{\partial u}{\partial \mathbf{n}}\right]_{\mathbf{X}_*} + \mathcal{O}(h^2),$$

where $\mathbf{X}_*$ is the orthogonal projection of the grid point $\mathbf{x}_{i,j+1}$ on the interface. Therefore, the correction term can be written as

$$C_I^- = -\beta\,(1-\alpha)\, \left([u]_{\mathbf{X}_*} + d\, \left[\frac{\partial u}{\partial \mathbf{n}}\right]_{\mathbf{X}_*}\right).$$

Numerical results

We consider three different exact solutions for Poisson equation in $\Omega = [-1, 1] \times [-1, 1]$ with jump discontinuities on an elliptical interface $\Gamma = \{\frac{x^2}{a^2} + \frac{y^2}{b^2} = 1\}$ with $a = 0.8$, and $b = 0.2$. Interface markers $(X_k, Y_k) = (0.8 \cos\theta_k, 0.2 \sin\theta_k)$, $k = 0, 1, \ldots, N-1$ with $\theta_k = k\Delta\theta$, $\Delta\theta = 2\pi/N$

	Example 1	Example 2	Example 3
u_-	1	$\exp(x)\cos(y)$	$x^2 - y^2$
u_+	$1 + \ln(2\sqrt{x^2+y^2})$	$\exp(x^2)\cos(y)$	0
f_-	0	0	0
f_+	0	$(1+4x^2)\exp(x^2)\cos(y)$	0

	N	$\|u-u_e\|_\infty$	ratio	CPU time
Example 1	40	2.1577E-03	-	0.015
	80	6.3698E-04	3.39	0.016
	160	1.7153E-04	3.71	0.046
	320	4.0663E-05	4.22	0.219
Example 2	40	1.1909E-03	3.71	0.015
	80	3.0901E-04	3.85	0.016
	160	7.8497E-05	3.94	0.078
	320	1.9776E-05	3.97	0.235
Example 3	40	5.5511E-16	-	0.015
	80	7.9797E-16	-	0.016
	160	2.6749E-15	-	0.047
	320	1.5377E-14	-	0.172

Table: The maximum errors for the examples of Poisson problem on the $N \times N$ grid points.

N	$\|u^- - u_e^-\|_{\infty,\Gamma}$	ratio
40	1.6036E-03	-
80	4.7394E-04	3.38
160	1.2650E-04	3.75
320	4.0435E-05	3.13

Table: The interpolation errors for Example 2 of Poisson problem on the interface markers $(X_k, Y_k) = (0.8 \cos\theta_k, 0.2 \sin\theta_k)$, $k = 0, 1, \ldots, N-1$ with $\theta_k = k\Delta\theta$, $\Delta\theta = 2\pi/N$.

Stokes flow with singular forces, Lai & Tseng, 2008

The steady Stokes equations with singular forces along the interface Γ are of the form

$$\begin{aligned} -\nabla p + \mu \Delta \mathbf{u} + \mathbf{f} + \mathbf{g} &= 0 && \text{in } \Omega, \\ \nabla \cdot \mathbf{u} &= 0 && \text{in } \Omega, \\ \mathbf{u} &= \mathbf{u}_b && \text{on } \partial\Omega, \end{aligned}$$

where

$$\mathbf{f}(\mathbf{x}) = \int_\Gamma \mathbf{F}(s)\delta(\mathbf{x} - \mathbf{X}(s))\, ds,$$

$$\mathbf{F} = (F_1, F_2) = (\mathbf{F} \cdot \mathbf{n})\mathbf{n} + (\mathbf{F} \cdot \tau)\tau = F_{\mathbf{n}}\, \mathbf{n} + F_\tau\, \tau,$$

$\mathbf{g}$: the external force

$$
\begin{aligned}
-\nabla p + \mu\, \Delta \mathbf{u} + \mathbf{g} &= 0 \qquad \text{in } \Omega, \\
\nabla \cdot \mathbf{u} &= 0 \qquad \text{in } \Omega, \\
[\mathbf{u}] = 0, \qquad \mu \left[\frac{\partial \mathbf{u}}{\partial \mathbf{n}} \right] &= -F_\tau\, \tau, \qquad \text{on } \Gamma \\
[p] = F_{\mathbf{n}}, \qquad \left[\frac{\partial p}{\partial \mathbf{n}} \right] &= \frac{\partial F_\tau}{\partial s} + [\mathbf{g}] \cdot \mathbf{n}, \qquad \text{on } \Gamma \\
\mathbf{u} &= \mathbf{u}_b \qquad \text{on } \partial\Omega,
\end{aligned}
$$

Other works:

- LeVeque & Li 1997, Stokes flow with interface
- Cortez 2001, The regularized Stokeslets
- Beale & Strain 2008, Layton 2008

Solution procedure

$$\begin{aligned} \Delta p &= \nabla \cdot \mathbf{g} && \text{in } \Omega, \\ [p] = F_{\mathbf{n}}, \quad \left[\frac{\partial p}{\partial \mathbf{n}}\right] &= \frac{\partial F_\tau}{\partial s} + [\mathbf{g}] \cdot \mathbf{n} && \text{on } \Gamma. \end{aligned}$$

$$\begin{aligned} \Delta \mathbf{u} &= \frac{1}{\mu}\,(\nabla p - \mathbf{g}), && \text{in } \Omega, \\ [\mathbf{u}] = 0, \quad \left[\frac{\partial \mathbf{u}}{\partial \mathbf{n}}\right] &= -\frac{1}{\mu}\,F_\tau\,\tau, && \text{on } \Gamma \\ \mathbf{u} &= \mathbf{u}_b && \text{on } \partial\Omega. \end{aligned}$$

$$\left[\frac{\partial p}{\partial \mathbf{n}}\right] = [p_x]\;n_1 + [p_y]\;n_2 = \frac{\partial F_\tau}{\partial s} + [\mathbf{g}] \cdot \mathbf{n},$$

$$\frac{\partial\,[p]}{\partial s} = [p_x]\;\tau_1 + [p_y]\;\tau_2 = -\,[p_x]\;n_2 + [p_y]\;n_1 = \frac{\partial F_{\mathbf{n}}}{\partial s},$$

$$[\nabla p] = ([p_x]\,, [p_y])$$

Summary

Step 1: Solve the pressure Poisson equation

$$\Delta_h p = \nabla \cdot \mathbf{g} + \frac{p^c}{h^2}, \qquad \text{in}\,\Omega$$

with modified righthand side functions at those irregular points which the modifications are based on the jump conditions of the pressure. More precisely, the correction terms at those irregular points can be computed as

$$\begin{aligned} p^c &= [p] + d\left[\frac{\partial p}{\partial \mathbf{n}}\right] + \frac{1}{2}d^2\left([\Delta p] - \kappa\left[\frac{\partial p}{\partial \mathbf{n}}\right] - \frac{\partial^2 [p]}{\partial s^2}\right) \\ &= F_{\mathbf{n}} + d\left(\frac{\partial F_\tau}{\partial s} + [\mathbf{g}]\cdot\mathbf{n}\right) + \frac{1}{2}d^2\left([\nabla\cdot\mathbf{g}] - \kappa(\frac{\partial F_\tau}{\partial s} + [\mathbf{g}]\cdot\mathbf{n}) - \frac{\partial^2 F_{\mathbf{n}}}{\partial s^2}\right). \end{aligned}$$

Step 2: Solve the velocity equations

$$
\begin{aligned}
\Delta_h \mathbf{u} &= \frac{1}{\mu}(\nabla_h p - \mathbf{g}) + \frac{\mathbf{u}^c}{h^2} \qquad \text{in}\,\Omega, \\
\mathbf{u} &= \mathbf{u}_b \qquad \text{on}\ \partial\Omega,
\end{aligned}
$$

where the corrections are made only at irregular points as

$$
\begin{aligned}
\mathbf{u}^c &= [\mathbf{u}] + d\,\left[\frac{\partial \mathbf{u}}{\partial \mathbf{n}}\right] + \frac{1}{2}\,d^2\,\left([\Delta \mathbf{u}] - \kappa\,\left[\frac{\partial \mathbf{u}}{\partial \mathbf{n}}\right] - \frac{\partial^2\,[\mathbf{u}]}{\partial s^2}\right) \\
&= \frac{1}{\mu}\left(-dF_\tau \tau + \frac{1}{2}\,d^2\,([\nabla p] - [\mathbf{g}] + \kappa\,F_\tau \tau)\right).
\end{aligned}
$$

Note that, the above pressure gradient jump has been derived previously.

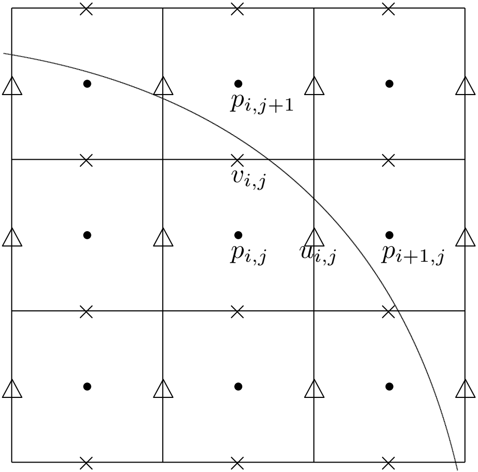

Figure: A diagram of the interface cutting through a staggered grid with a uniform mesh width h in Ω. The pressure is located at the center of the cell, the velocity component u is at the left-right face, and v is at the top-bottom face of a cell.

Remark:

Modifications of computing p_x and p_y near the interface

1. Suppose the locations of $p_{i,j}$ and $u_{i,j}$ fall in the same side of the interface while the location of $p_{i+1,j}$ falls in another side of the interface, then we need to add a correction term $p^c_{i+1,j}$ of $p_{i+1,j}$ so that the approximation of p_x at $u_{i,j}$ grid can be computed by $((p_{i+1,j} + p^c_{i+1,j}) - p_{i,j})/h$.
2. If the locations of $p_{i+1,j}$ and $u_{i,j}$ fall in the same side of the interface while the location of $p_{i,j}$ falls in another side of the interface, then the approximation of p_x at $u_{i,j}$ grid can be computed by $(p_{i+1,j} - (p_{i,j} + p^c_{i,j}))/h$, where a correction term $p^c_{i,j}$ of $p_{i,j}$ must be added.
3. p_y can be approximated similarly

Numerical results

- $\Omega = [-2, 2] \times [-2, 2]$
- $\Gamma = \{\mathbf{X}(\theta) = (\cos(\theta), \sin(\theta)), 0 \leq \theta < 2\pi\}$
- Staggered grid for fluid variables
- Examples were taken from the paper of Cortez in 2001.

Example 1: Normal forces on an interface Let

$$\mathbf{F}(\theta) = 2\,\sin(3\,\theta)\mathbf{X}(\theta).$$

The exact solution is

$$p(r,\theta) = \begin{cases} -r^3\sin(3\theta), & r < 1 \\ r^{-3}\sin(3\theta), & r > 1 \end{cases}$$

$$u(r,\theta) = \begin{cases} \frac{3}{8}r^2\sin(2\theta) + \frac{1}{16}r^4\sin(4\theta) - \frac{1}{4}r^4\sin(2\theta), & r < 1 \\ \frac{1}{8}r^{-2}\sin(2\theta) - \frac{3}{16}r^{-4}\sin(4\theta) + \frac{1}{4}r^{-2}\sin(4\theta), & r \geq 1 \end{cases}$$

$$v(r,\theta) = \begin{cases} \frac{3}{8}r^2\cos(2\theta) - \frac{1}{16}r^4\cos(4\theta) - \frac{1}{4}r^4\cos(2\theta), & r < 1 \\ \frac{1}{8}r^{-2}\cos(2\theta) + \frac{3}{16}r^{-4}\cos(4\theta) - \frac{1}{4}r^{-2}\cos(4\theta), & r \geq 1. \end{cases}$$

Example 2: Tangential forces on an interface Let

$$\mathbf{F}(\theta) = 2\,\sin(3\theta)\mathbf{X}'(\theta).$$

The exact solution is

$$p(r,\theta) = \begin{cases} -r^3\cos(3\theta), & r < 1 \\ -r^{-3}\cos(3\theta), & r > 1 \end{cases}$$

$$u(r,\theta) = \begin{cases} \frac{1}{8}r^2\cos(2\theta) + \frac{1}{16}r^4\cos(4\theta) - \frac{1}{4}r^4\cos(2\theta), & r < 1 \\ -\frac{1}{8}r^{-2}\cos(2\theta) + \frac{5}{16}r^{-4}\cos(4\theta) - \frac{1}{4}r^{-2}\cos(4\theta), & r \geq 1 \end{cases}$$

$$v(r,\theta) = \begin{cases} -\frac{1}{8}r^2\sin(2\theta) + \frac{1}{16}r^4\sin(4\theta) + \frac{1}{4}r^4\sin(2\theta), & r < 1 \\ \frac{1}{8}r^{-2}\sin(2\theta) + \frac{5}{16}r^{-4}\sin(4\theta) - \frac{1}{4}r^{-2}\sin(4\theta), & r \geq 1. \end{cases}$$

Example 3: Normal and tangential forces on an interface In this example, we consider the boundary force that has both normal and tangential components as

$$\mathbf{F}(\theta) = 2\,\sin(3\theta)\mathbf{X}'(\theta) - \cos^3(\theta)\,\mathbf{X}(\theta).$$

The velocity components u and v are chosen exactly the same as in Example 2 while the pressure written in Cartesian coordinates $(x = r\cos\theta, y = r\sin\theta)$ is

$$p(x,y) = \begin{cases} x^3 + \cos(\pi x)\cos(\pi y) & r < 1 \\ \cos(\pi x)\cos(\pi y) & r \geq 1. \end{cases}$$

The velocity and the pressure satisfy the Stokes equations with a nonzero external force $\mathbf{g} \neq 0$ which can be calculated analytically. Here, we use the zero Neumann boundary condition (easily to be checked) for the pressure and the Dirichlet boundary conditions for the velocity.

	N	$\|u-u_e\|_\infty$	ratio	$\|v-v_e\|_\infty$	ratio	$\|p-p_e\|_\infty$	ratio
Ex1	32	2.9955E-03	-	9.5555E-03	-	1.4625E-02	-
	64	7.4576E-04	4.02	2.1775E-03	4.39	3.2027E-03	4.57
	128	2.1442E-04	3.48	5.4344E-04	4.01	8.2001E-04	3.91
	256	4.8445E-05	4.43	1.3800E-04	3.94	1.9358E-04	4.24
Ex2	32	9.3164E-03	-	5.5489E-03	-	1.7579E-02	-
	64	2.2334E-03	4.17	9.8214E-04	5.65	3.5421E-03	4.96
	128	4.5329E-04	4.93	2.6948E-04	3.64	9.5814E-04	3.70
	256	1.2100E-04	3.75	6.8943E-05	3.91	2.1994E-04	4.36
Ex3	32	9.9654E-03	-	9.3837E-03	-	2.5682E-02	-
	64	2.7483E-03	3.63	1.8844E-03	4.98	7.2394E-03	3.55
	128	5.2897E-04	5.20	4.4803E-04	4.21	1.8827E-03	3.85
	256	1.4410E-04	3.67	1.2263E-04	3.65	4.7359E-04	3.98

Table: The maximum errors for the examples of Stokes problem on $N \times N$ grid points.

N	$\|u-u_e\|_{\infty,\Gamma}$	ratio	$\|v-v_e\|_{\infty,\Gamma}$	ratio
32	1.0035E-02	-	1.0923E-02	-
64	2.3020E-03	4.36	2.9853E-03	3.66
128	4.5430E-04	5.07	6.8889E-04	4.33
256	1.2788E-04	3.55	1.8553E-04	3.71

Table: The interpolation errors for Example 3 of Stokes problem on the interface markers $(X_k, Y_k) = (\cos\theta_k, \sin\theta_k)$, $k = 0, 1, \ldots, N-1$, $\theta_k = k\Delta\theta$, $\Delta\theta = 2\pi/N$.

Poisson equation on an irregular domain

Consider the 2D Poisson equation on a domain Ω with irregular boundary Γ.

$$\begin{cases} \Delta u = f & x \in \Omega^- \\ u = g & x \text{ on } \Gamma \end{cases}$$

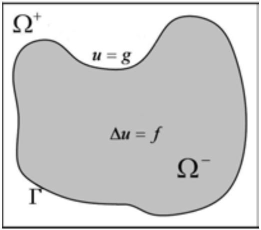

Different embedding approaches

1. Capacitance matrix method, Widlund, Golub et. al. 1970s
2. Integral equation formulation and fast Poisson solver
   - Double layer potential and jump conditions(depending on layer density function), Mayo, 1984-1985
   - Double layer potential with fast multipole accelerated integral equation solver, McKenney, Greengard & Mayo, 1995
   - Nearly singular integrals at irregular points, Beale & Lai 2001
3. Finite volume discretization with adaptive mesh refinement, Johansen & Colella, 1998
4. Augmented IIM approach, Li 2006
5. Boundary extrapolation methods
   - Second-order schemes, Gibou et. al. 2002, Macklin & Lowengrub 2005, Jomaa & Macaskill 2005
   - Fourth-order scheme (5-point stencil), Gibou & Fedkiw 2005
   - Compact high-order scheme

Integral equation formulation approach

Consider the 2D Laplace's equation

$$\begin{cases} \Delta u = 0 & x \in \Omega^- \\ u = g & x \in \Gamma \end{cases}$$

Then the solution can be written as a double layer potential

$$u(\mathbf{x}) = \frac{1}{2\pi} \int_\Gamma \frac{\partial r(\mathbf{z}(s), \mathbf{x})}{\partial \mathbf{n}_s} \mu(s)\, ds, \qquad \mathbf{x} \in \Omega^-,$$

where

$$r(\mathbf{z}(s), \mathbf{x}) = |\mathbf{z}(s) - \mathbf{x}|$$

$$\mu(t) + \frac{1}{\pi} \int_\Gamma \frac{\partial r(\mathbf{z}(s), \mathbf{z}(t))}{\partial \mathbf{n}_s} \mu(s)\, ds = 2g(t).$$

Outside Ω^-, we define a harmonic function extension

$$\tilde{u}(\mathbf{x}) = \frac{1}{2\pi} \int_\Gamma \frac{\partial r(\mathbf{z}(s), \mathbf{x})}{\partial \mathbf{n}_s} \mu(s)\, ds, \qquad \mathbf{x} \in \Omega^+.$$

So, we have $[u] = \mu(s)$ and $[u_n] = 0$.

$$
\begin{aligned}
\Delta u(\mathbf{x}) &= 0, &\qquad \text{in} \quad \Omega^- \cup \Omega^+, \\
[u](s) &= \mu(s), &\qquad [u_n] = 0 \text{ on } \Gamma
\end{aligned}
$$

Numerical procedures:

1. Solve an integral equation for the dipole strength $\mu(s)$, well-conditioned integral equation
2. Modify the discrete Laplacian at those irregular points
   - by using the Taylor's expansions and jump discontinuities, Mayo 1984
   - by computing nearly singular integrals, Beale & Lai 2001
3. Apply the fast Poisson solver

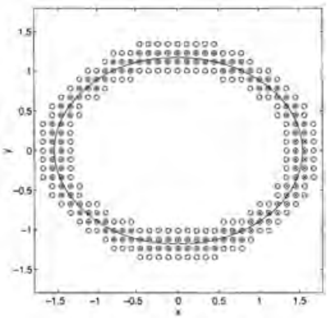

N	$\|u - u_e\|_\infty$	ratio
32	8.84E-04	-
64	2.29E-04	3.86
128	5.89E-05	3.89
256	1.50E-05	3.93

Table: The errors for the Dirichlet problem.
$\Gamma = \{x^2/\cosh(1)^2 + y^2/\sinh(1)^2 = 1\}$.
The solution is $exp(x + \sqrt{3}y)/2\ \cos((-\sqrt{3}x + y)/2)$.

Boundary extrapolation method–1D case

Consider the 1D Poisson equation

$$u_{xx} \;=\; f, \qquad x \in \Omega^- \;= [a, x_I), \qquad u_{x_I} = u_I.$$

Embedding Ω^- into a uniform domain on $[a, b]$, and set $u = 0$ in $\Omega^+ = [a, b] \backslash \Omega^-$, we have

$$\begin{cases} u_{xx} = f & x \in \Omega^- \\ u_{x_I} = u_I & \\ u = 0 & x \in \Omega^+ \end{cases}$$

Fourth-order compact discretization

Compute the Poisson equation at the grid point, and write $u_i = u(x_i)$. Compact fourth-order discretization at regular point x_i:

$$\frac{u_{i+1} - 2u_i + u_{i-1}}{\Delta x^2} = (u_{xx})_i + \frac{\Delta x^2}{12}(u_{xxxx})_i + O(\Delta x^4).$$

Since $u_{xxxx} = f_{xx}$ and approximate it by second-order difference, we have

$$\frac{u_{i+1} - 2u_i + u_{i-1}}{\Delta x^2} \approx \frac{f_{i+1} + 10 f_i + f_{i-1}}{12}$$

At irregular point x_i,

$$\frac{u^G_{i+1} - 2u_i + u_{i-1}}{\Delta x^2} \approx \frac{f^G_{i+1} + 10 f_i + f_{i-1}}{12}$$

Question: How to construct the ghost values to preserve the compact structure?

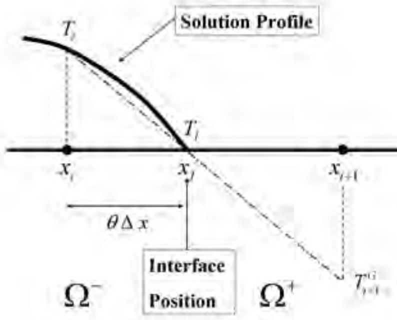

Goal: to construct an interpolant $\tilde{u}(x)$ of $u(x)$ such that $\tilde{u}(0) = u_i$, $\tilde{u}(\theta\Delta x) = u_I$ and $\tilde{u}(\Delta x) = u^G_{i+1}$.

Different boundary value extrapolations

- Constant extrapolation: $\tilde{u}(x) = u_I$
- Linear extrapolation: $\tilde{u}(x) = cx + d$ with $\tilde{u}(0) = u_i$, $\tilde{u}(\theta\Delta x) = u_I$
- Quadratic extrapolation: $\tilde{u}(x) = bx^2 + cx + d$ with $\tilde{u}(-\Delta x) = u_{i-1}$, $\tilde{u}(0) = u_i$, $\widetilde{u}(\theta\Delta x) = u_I$
- Cubic extrapolation: $\tilde{u}(x) = ax^3 + bx^2 + cx + d$ with $\tilde{u}(-\Delta x) = u_{i-1}$, $\tilde{u}(0) = u_i$, $\tilde{u}(\theta\Delta x) = u_I$, $\tilde{u_{xx}}(\theta\Delta x) = f_I$.

The extrapolation for f is similar except the cubic extrapolation $\tilde{f}(-2\Delta x) = f_{i-2}$.

Summary

Degree of extrapolation	Order of accuracy	Linear system
Constant	First	Symmetric
Linear	Second	Symmetric
Quadratic	Third	Non-symmetric
Cubic	Fourth	Non-symmetric

Linear extrapolation. $u = \sin(\pi x), x_I = 2/3, \Omega = [0, 1]$

N	FD2 error	ratio	CP4 error	ratio
16	3.9813E-03		3.5300E-03	
32	9.7994E-04	2.02	9.0770E-04	1.96
64	2.4681E-04	1.99	2.2899E-04	1.99
128	6.1471E-05	2.01	5.7650E-05	1.99
256	1.5396E-05	2.00	1.4446E-05	2.00

Quadratic extrapolation. $u = \sin(\pi x), x_I = 2/3, \Omega = [0, 1]$

N	CD2 error	ratio	CP4 error	ratio
16	1.2973E-03		1.8028E-04	
32	3.3837E-04	1.94	2.2010E-05	3.03
64	8.5905E-05	1.98	3.4392E-06	2.68
128	2.1751E-05	1.98	3.5976E-07	3.26
256	5.4567E-06	1.99	5.6212E-08	2.68

Cubic extrapolation. $u = \sin(\pi x), x_I = 2/3, \Omega = [0, 1]$

N	CD2 error	ratio	CP4 error	ratio
16	1.4134E-03		4.7210E-06	
32	3.5114E-04	2.01	6.4784E-07	2.87
64	8.7817E-05	2.00	1.8597E-08	5.12
128	2.1950E-05	2.00	2.5700E-09	2.86
256	5.4876E-06	2.00	7.2334E-11	5.15

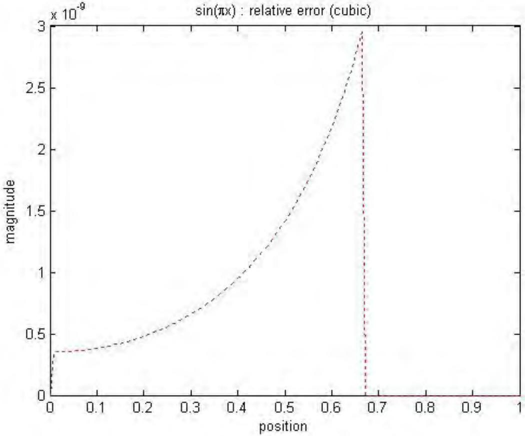

x 10^-9
sin(πx) : relative error (cubic)
magnitude
position
0
0.5
1
1.5
2
2.5
3
0
0.1
0.2
0.3
0.4
0.5
0.6
0.7
0.8
0.9
1

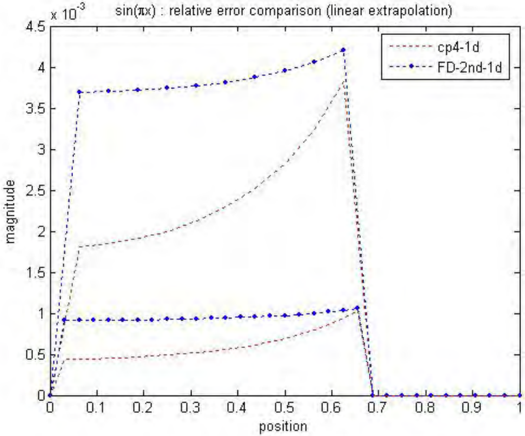
sin(πx) : relative error comparison (linear extrapolation)
x 10^-3
4.5
4
3.5
3
2.5
2
1.5
1
0.5
0
magnitude
0
0.1
0.2
0.3
0.4
0.5
0.6
0.7
0.8
0.9
1
position
cp4-1d
FD-2nd-1d

Compact scheme– 2D case

Standard compact 9-points stencil: $h = \Delta x = \Delta y$

$$
\begin{aligned}
\Delta_9 u_{i,j} &= \frac{1}{6\,h^2}(4u_{i-1,j} + 4u_{i+1,j} + 4u_{i,j-1} + 4u_{i,j+1} \\
&\quad + u_{i-1,j-1} + u_{i-1,j+1} + u_{i+1,j-1} + u_{i+1,j+1} - 20u_{i,j}) \\
&= \Delta u_{i,j} + \frac{h^2}{12}[(u_{xxxx})_{i,j} + 2(u_{xxyy})_{i,j} + (u_{yyyy})_{i,j}] + O(h^4) \\
&= f_{i,j} + \frac{h^2}{12}\Delta f_{i,j} + O(h^4) \\
&= f_{i,j} + \frac{h^2}{12}\Delta_5 f_{i,j} + O(h^4)
\end{aligned}
$$

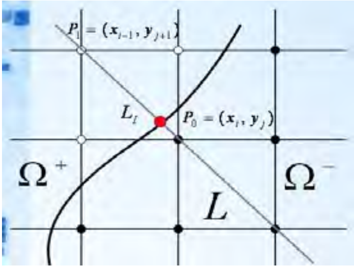

Figure: A diagram of an irregular point P_0

The discretization at the irregular point $P_0 = (x_i, y_i)$ is

$$
\begin{aligned}
&\frac{1}{6h^2}[4u^G_{i-1,j} + 4u_{i+1,j} + 4u_{i,j-1} + 4u^G_{i,j+1} + u_{i-1,j-1} \\
&\quad + u^G_{i-1,j+1} + u_{i+1,j-1} + u_{i+1,j+1} - 20u_{i,j}] \\
&= \frac{f^G_{i-1,j} + f_{i+1,j} + f^G_{i,j-1} + f_{i,j+1} + 8f_{i,j}}{12}.
\end{aligned}
$$

Question: How to construct the ghost value $u^G_{i-1,j+1}$?

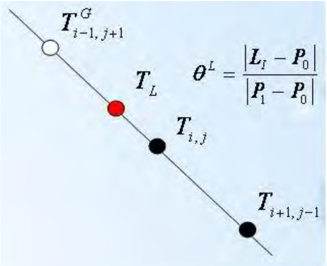

1. Use the line segment, L to connect (x_{i-1}, y_{j+1}) and (x_i, y_j).
2. Locate the interface L_I, by solving a nonlinear equation.
3. Define $\theta^L = \frac{|L_I - P_0|}{|P_1 - P_0|}$.
4. Construct the linear/quadratic extrapolation $\tilde{u}$ using the values $u_{i,j}, u_{i+1,j-1}, u_I$ and their associated positions.
5. Extrapolate the ghost value $u^G_{i-1,j+1}$.

Example 1

The exact solution $u = \cos(x + y)$ inside a unit circle. The domain is embedded in a square. Outside the unit circle we set $u = 0$.

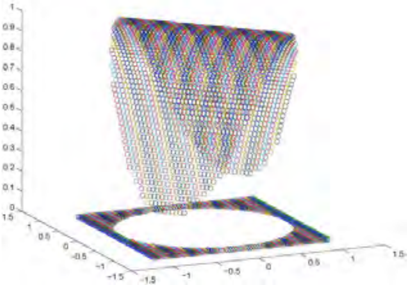

	Linear		Quadratic	
N	L^∞ error	ratio	L^∞ error	ratio
16	1.5867E-03		3.2722E-04	
32	3.3722E-04	2.23	2.9732E-05	3.46
64	9.2690E-05	1.81	4.2617E-06	2.80
128	2.2966E-05	2.07	4.8286E-07	3.14

Example 2

The exact solution $u = \cos(x+y)$ inside an elliptical domain $\frac{x^2}{0.9^2} + \frac{y^2}{0.4^2} = 1$. The domain is embedded in a square. Outside the ellipse, we set $u = 0$.

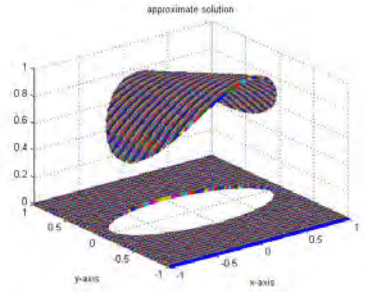

	Linear		Quadratic	
N	L^∞ error	ratio	L^∞ error	ratio
16	5.1891E-02		3.4991E-02	
32	5.4063E-04	6.58	7.1812E-05	8.91
64	1.3898E-04	1.96	3.7956E-06	4.24
128	3.6658E-05	1.92	4.7220E-07	3.01
256	8.8252E-06	2.05	6.2963E-08	2.91

Example 3

The exact solution
$u = \sin(\pi x) + \cos(\pi x) + \sin(\pi y) + \cos(\pi y) + x^6 + y^6$ inside an asteroid interface. The domain is embedded in a square. Outside the asteroid, we set $u = 0$.

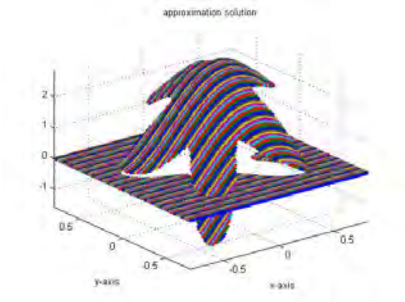

	Linear		Quadratic	
N	L^∞ error	ratio	L^∞ error	ratio
16	1.6856E-02	–	2.3293E-03	–
32	4.1630E-03	2.02	3.8621E-04	2.59
64	1.3166E-03	1.66	5.6038E-05	2.78
128	2.9076E-04	2.18	8.5473E-06	2.71
256	7.7409E-05	1.91	1.0385E-06	3.04

Some Numerical Issues on Interfacial Problems with Fluid Flows

Ming-Chih Lai
mclai@math.nctu.edu.tw

Department of Applied Mathematics
National Chiao Tung University
Taiwan

Interfacial Problems with Fluid Flows

A fluid droplet (material) immersed in another fluid (matrix) so there is an interface between those two phases

Droplet surface forces affect the fluid dynamics while the fluid velocity changes the droplet geometry

- The droplet surface (or interface) will deform (geometry change) due to the surrounding fluids
- How to represent the interface?
- How to track or capture the interface evolution?
- How to impose the stress force balance conditions at the interface? Those stress forces might depend on the mean curvature of the interface and its surface Laplacian

Two extra issues

- What if some surface material quantity (surfactant) exists along the interface? **Solving PDEs on an evolving surface**
- What if there exists some extra constraints such as the incompressibility (or inextensibility in 2D) on the interface? **Imposing PDE constraint on an evolving surface**

PDEs on surfaces

Applications: Material science, biological modeling, computer graphics, and image processing

- Examine phase change of a material on a surface
- Study wound healing on a skin
- Place a texture (coating) on a surface
- Segment out objects defined in surface textures
- Restore a damaged pattern on a vase
- Evolve surfactant (**Surf**ace **act**iv **agent**) on interfaces to change the surface tension, surface tension is no more a constant, reduced capillary force and induced Marangoni force

3D surfactant transport equation on an interface

Consider a 2D interfacial element $\Sigma(t)$ in a 3D domain, where

$$\Sigma(t) := \{\boldsymbol{X}(\alpha, \beta, t) | (\alpha, \beta) \in S_0\}.$$

- Two independent parameters (α, β) to label a fixed material point of initial configuration ($\Sigma(0) := \{\boldsymbol{X}_0(\alpha, \beta) | (\alpha, \beta) \in S_0\}$, S_0 is a fixed domain)
- Two tangential and normal vectors

$$\boldsymbol{\tau}_1 = \frac{\frac{\partial \boldsymbol{X}}{\partial \alpha}}{\left|\frac{\partial \boldsymbol{X}}{\partial \alpha}\right|}, \qquad \boldsymbol{\tau}_2 = \frac{\frac{\partial \boldsymbol{X}}{\partial \beta}}{\left|\frac{\partial \boldsymbol{X}}{\partial \beta}\right|}, \qquad \boldsymbol{n} = \frac{\boldsymbol{\tau}_1 \times \boldsymbol{\tau}_2}{|\boldsymbol{\tau}_1 \times \boldsymbol{\tau}_2|} = \frac{\frac{\partial \boldsymbol{X}}{\partial \alpha} \times \frac{\partial \boldsymbol{X}}{\partial \beta}}{\left|\frac{\partial \boldsymbol{X}}{\partial \alpha} \times \frac{\partial \boldsymbol{X}}{\partial \beta}\right|}.$$

Assume no diffusion along the interface, then the surfactant mass satisfies

$$\frac{d}{dt} \int_{\Sigma(t)} \Gamma(x, y, z, t)\, dS = 0,$$

where dS is the surface area element.

Law of mass conservation

$$
\begin{aligned}
0 &= \frac{d}{dt}\int_{\Sigma(t)} \Gamma(x,y,z,t)\ dS \\
&= \frac{d}{dt}\int_{\Sigma(0)} \Gamma(\boldsymbol{X}(\alpha,\beta,t),t)\left|\frac{\partial \boldsymbol{X}}{\partial \alpha}\times\frac{\partial \boldsymbol{X}}{\partial \beta}\right|\ d\alpha\, d\beta \\
&= \int_{\Sigma(0)} \frac{D\Gamma}{Dt}\left|\frac{\partial \boldsymbol{X}}{\partial \alpha}\times\frac{\partial \boldsymbol{X}}{\partial \beta}\right|\ d\alpha\, d\beta \ + \ \int_{\Sigma(0)} \Gamma\frac{d}{dt}\left|\frac{\partial \boldsymbol{X}}{\partial \alpha}\times\frac{\partial \boldsymbol{X}}{\partial \beta}\right|\ d\alpha\, d\beta, \\
&= \int_{\Sigma(0)} \left(\frac{\partial \Gamma}{\partial t} + \boldsymbol{u}\cdot\nabla_s\Gamma + \Gamma(\nabla_s\cdot\boldsymbol{u})\right)\left|\frac{\partial \boldsymbol{X}}{\partial \alpha}\times\frac{\partial \boldsymbol{X}}{\partial \beta}\right|\ d\alpha\, d\beta, \\
&= \int_{\Sigma(t)} \left(\frac{\partial \Gamma}{\partial t} + \boldsymbol{u}\cdot\nabla_s\Gamma + \Gamma(\nabla_s\cdot\boldsymbol{u})\right) dS.
\end{aligned}
$$

Since the material element is arbitrary, we have

$$
\frac{\partial \Gamma}{\partial t} + \boldsymbol{u}\cdot\nabla_s\Gamma + \Gamma\nabla_s\cdot\boldsymbol{u} = 0.
$$

If we add the diffusion, we have

$$\frac{\partial \Gamma}{\partial t} + \boldsymbol{u} \cdot \nabla_s \Gamma + \Gamma \nabla_s \cdot \boldsymbol{u} = \frac{1}{Pe_s} \nabla_s^2 \Gamma, \quad \text{on } \Sigma(t)$$

Computational issue: Given a velocity $\boldsymbol{u}$ and an initial surface $\Sigma(0)$ with initial surfactant distribution $\Gamma(0)$, how to compute the above surfactant equation accurately and efficiently? Note that, $\frac{d\Sigma}{dt} = \boldsymbol{u}$.

- Solve directly on the surface: surface FEM, FDM, FVM, surface mesh, mesh stretching and distortion, mass conservation
- Extend the PDE to the Cartesian space: regular Cartesian method can be applied, normal extension, concave surface, level set, phase field method, no mass conservation
- A point cloud method: construct local mesh based on the data points

A more challenging soluble surfactant problem: Coupled surface-bulk PDEs on an evolving surface and an irregular domain

$$\frac{D\Gamma}{Dt} + (\nabla_s \cdot \boldsymbol{u})\,\Gamma = \frac{1}{Pe_s}\,\nabla_s^2\Gamma + S_a C_s(1-\Gamma) - S_d\Gamma \qquad \text{on } \Sigma$$

$$\frac{\partial C}{\partial t} + \boldsymbol{u}\cdot\nabla C = \frac{1}{Pe}\nabla^2 C \qquad \text{in } \Omega_1$$

$$\frac{1}{Pe}\frac{\partial C}{\partial \boldsymbol{n}}|_{\Sigma} = S_a C_s(1-\Gamma) - S_d\Gamma \qquad \frac{\partial C}{\partial \boldsymbol{n_1}}|_{\partial\Omega_1} = 0$$

- $\nabla_s = (\boldsymbol{I} - \boldsymbol{n}\otimes\boldsymbol{n})\nabla = \nabla - \frac{\partial}{\partial \boldsymbol{n}}\boldsymbol{n}$ and $\nabla_s^2 = \nabla_s \cdot \nabla_s$ are the surface gradient and surface Laplacian operators
- Pe_s and Pe are surface and bulk Peclet numbers, S_a and S_d are the absorption and desorption Stanton number
- C_s is the bulk concentration adjacent to the interface ($C_s = C$ on the interface)
- $\boldsymbol{n}$ is the unit normal vector to Σ pointing into Ω_1
- $\boldsymbol{n_1}$ is the unit outward normal to the boundary $\partial\Omega_1 = \partial\Omega$.

Surface and volume charges in electrohydrodynamics

- $q_v = \nabla \cdot (\varepsilon \mathbf{E})$: volume-charge density in Ω;
- $q_s = [\varepsilon \mathbf{E} \cdot \mathbf{n}]$: surface charge on Σ, $[\cdot]$ denotes the jump of the quantity across the interface Σ
- $\mathbf{E} = -\nabla \phi$ where ϕ is the electric potential
- Coupled volume and surface charge concentration equations

$$\frac{\partial q_v}{\partial t} + \boldsymbol{u} \cdot \nabla q_v + \nabla \cdot (\sigma \mathbf{E}) = 0 \qquad \text{in } \Omega$$

$$\frac{\partial q_s}{\partial t} + \boldsymbol{u}_s \cdot \nabla_s q_s - q_s \mathbf{n} \cdot (\mathbf{n} \cdot \nabla) \boldsymbol{u} + [\sigma \mathbf{E} \cdot \mathbf{n}] + (\boldsymbol{u} \cdot \mathbf{n})[q_v] = 0 \qquad \text{on } \Sigma$$

- The velocity $\boldsymbol{u}$ here is determined by Navier-Stokes flow. The interface Σ moves along with the velocity $\boldsymbol{u}$

Review: D. A. Saville (1997) Electrohydrodynamics: The Taylor-Melcher leaky dielectric model

Computational challenges:

1. How to solve the above coupled surface-bulk convection-diffusion equation efficiently?
2. Since Σ (surface) is moving, we need to solve surface concentration and Ω_1 is an evolutional domain, we need to solve convection-diffusion PDEs on a moving (time-dependent) interface and an irregular domain, respectively.
3. Can we preserve the total surfactant mass (surface + bulk)?
4. How to avoid the insolubility of surfactant on Ω_0, i.e. $C = 0$ in Ω_0 ?
5. 2D insoluble surfactant (Lai, Tseng, & Huang, JCP 2008), surfactant with moving contact line (Lai, Tseng, & Huang, CiCP 2010), 3D axisymmetric case (Lai, Huang & Huang, IJNAM 2011), phase-field model (Teng, Chern & Lai, DCDS-B, 2012), level set with IIM (Xu, Huang, Lai & Li, CiCP 2014), soluble surfactant (Chen & Lai, JCP 2014), droplet collision (Pan et. al. & Lai, JFM 2016)
6. Total surfactant mass conservation and Lagrangian markers control with equi-arclength parametrization (Seol & Lai, 2016)

How to track the interface?

- Front-tracking method (Peskin 1972, Unverdi and Tryggvason 1992): Lagrangian method, follow the interface markers; easy to implement, complex topological change, PDEs on surfaces can be explicitly defined
- Level set method (Osher and Sethian 1988): Eulerian method, zero level set function as the interface, geometrical quantities can be easily found, can handle topological change, surface is implicitly defined
- Phase field (diffuse interface) method (Anderson, McFadden and Wheeler 1998): Eulerian method, phase field function, with physical meaning, can handle topological change, surface is implicitly defined
- Volume-of-fluid (VOF) method (Hirt and Nichols 1981): Eulerian method, volume fraction of different fluids, hard to reconstruct the interface

Droplets collision: Experiment and IB 3D axis-symmetric Computation (Pan et. al. & Lai, JFM 2016)

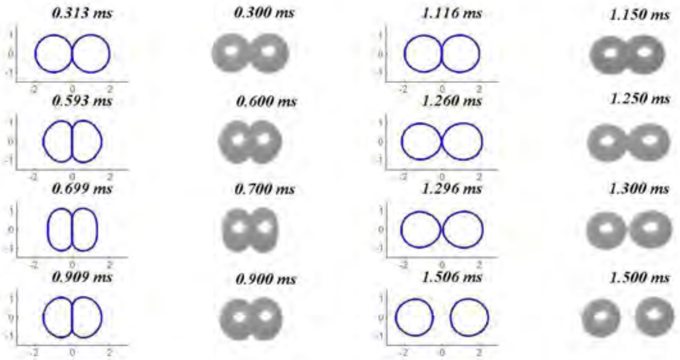

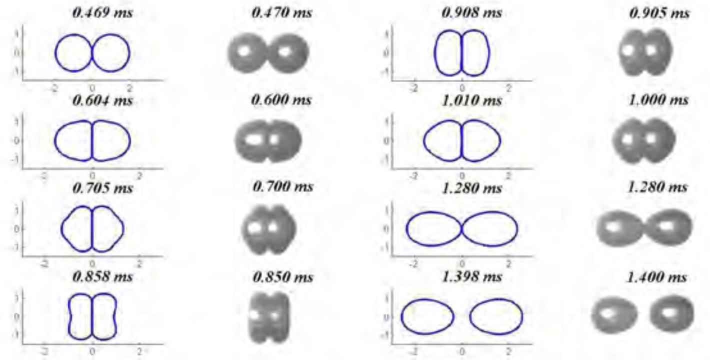
0.469 ms
0.470 ms
0.908 ms
0.905 ms
0.604 ms
0.600 ms
1.010 ms
1.000 ms
0.705 ms
0.700 ms
1.280 ms
1.280 ms
0.858 ms
0.850 ms
1.398 ms
1.400 ms

3D Interfacial flows with insoluble surfactant, Seol & Lai 2016

$$
\begin{aligned}
&\frac{\partial \mathbf{u}}{\partial t} + (\mathbf{u}\cdot\nabla)\mathbf{u} = -\nabla p + \frac{1}{Re}\nabla\cdot\left(\mu\left(\nabla\mathbf{u} + (\nabla\mathbf{u})^T\right)\right) + \frac{\mathbf{f}}{Re\,Ca} \quad \text{in } \Omega,\\
&\nabla\cdot\mathbf{u} = 0 \quad \text{in } \Omega,\\
&\mathbf{f}(\mathbf{x},t) = \int_\Sigma \mathbf{F}(\alpha,\beta,t)\,\delta(\mathbf{x}-\mathbf{X}(\alpha,\beta,t))\,\mathrm{d}A,\\
&\frac{\partial \mathbf{X}}{\partial t}(\alpha,\beta,t) = \mathbf{U}(\alpha,\beta,t) = \int_\Omega \mathbf{u}(\mathbf{x},t)\,\delta(\mathbf{x}-\mathbf{X}(\alpha,\beta,t))\,dx,\\
&\mathbf{F}(\alpha,\beta,t) = \nabla_s\sigma - 2\sigma H\mathbf{n}, \qquad \sigma(\alpha,\beta,t) = \sigma_0(1-\eta\Gamma(\alpha,\beta,t)) \quad \text{on } \Sigma,\\
&\frac{D\Gamma}{Dt} + (\nabla_s\cdot\mathbf{U})\Gamma = \frac{1}{Pe_s}\Delta_s\Gamma \text{ on } \Sigma,
\end{aligned}
$$

- Re: Reynolds number, Ca: capillary number
- σ: surface tension, Pe_s: surface Peclet number
- μ: fluid viscosity, H: mean curvature
- η: dimensionless elasticity number.

Classical differential geometry

For the interface $\mathbf{X}(\alpha, \beta)$, define the first fundamental form as

$$E = \mathbf{X}_\alpha \cdot \mathbf{X}_\alpha, \quad F = \mathbf{X}_\alpha \cdot \mathbf{X}_\beta, \quad \text{and} \quad G = \mathbf{X}_\beta \cdot \mathbf{X}_\beta,$$

then

- $\nabla_s \sigma = \dfrac{G\sigma_\alpha - F\sigma_\beta}{EG - F^2}\mathbf{X}_\alpha + \dfrac{E\sigma_\beta - F\sigma_\alpha}{EG - F^2}\mathbf{X}_\beta$
- $\nabla_s \cdot \mathbf{U} = \dfrac{G\mathbf{U}_\alpha - F\mathbf{U}_\beta}{EG - F^2} \cdot \mathbf{X}_\alpha + \dfrac{E\mathbf{U}_\beta - F\mathbf{U}_\alpha}{EG - F^2} \cdot \mathbf{X}_\beta$
- For a surface vector field $\mathbf{U}^s = P\mathbf{X}_\alpha + Q\mathbf{X}_\beta$,
  $\nabla_s \cdot \mathbf{U}^s = \dfrac{1}{|\mathbf{X}_\alpha \times \mathbf{X}_\beta|}\left[\dfrac{\partial}{\partial \alpha}\left(|\mathbf{X}_\alpha \times \mathbf{X}_\beta| P\right) + \dfrac{\partial}{\partial \beta}\left(|\mathbf{X}_\alpha \times \mathbf{X}_\beta| Q\right)\right].$
- The surface Laplacian (or Laplace-Beltrami operator) of Γ:
  $\Delta_s \Gamma = \dfrac{1}{|\mathbf{X}_\alpha \times \mathbf{X}_\beta|}\left[\left(\dfrac{G\Gamma_\alpha - F\Gamma_\beta}{|\mathbf{X}_\alpha \times \mathbf{X}_\beta|}\right)_\alpha + \left(\dfrac{E\Gamma_\beta - F\Gamma_\alpha}{|\mathbf{X}_\alpha \times \mathbf{X}_\beta|}\right)_\beta\right].$

An equi-arclength parameterization

We modify the surface evolutional equation by adding two tangential velocities as

$$\mathbf{X}_t = \mathbf{U} + V_1 \boldsymbol{\tau}^1 + V_2 \boldsymbol{\tau}^2,$$

where $\boldsymbol{\tau}^1 = \mathbf{X}_\alpha / |\mathbf{X}_\alpha|$ and $\boldsymbol{\tau}^2 = \mathbf{X}_\beta / |\mathbf{X}_\beta|$ are the unit tangent vectors. Assume that the velocities $\mathbf{U}, V_1, V_2$ are all doubly 2π-periodic. The equi-arclength parametrization satisfies

$$\frac{\partial}{\partial \alpha} |\mathbf{X}_\alpha| = 0 \quad \text{and} \quad \frac{\partial}{\partial \beta} |\mathbf{X}_\beta| = 0,$$

for all $(\alpha, \beta) \in [0, 2\pi] \times [0, 2\pi]$.

Thus, we have

$$|\mathbf{X}_\alpha| = \frac{1}{2\pi}\int_0^{2\pi} |\mathbf{X}_{\alpha'}|\,\mathrm{d}\alpha' \quad \text{and} \quad |\mathbf{X}_\beta| = \frac{1}{2\pi}\int_0^{2\pi} |\mathbf{X}_{\beta'}|\,\mathrm{d}\beta'. \qquad (1)$$

Taking the time derivative in Eq. (1), it yields

$$|\mathbf{X}_\alpha|_t = \frac{1}{2\pi}\int_0^{2\pi} |\mathbf{X}_{\alpha'}|_t\,\mathrm{d}\alpha' \quad \text{and} \quad |\mathbf{X}_\beta|_t = \frac{1}{2\pi}\int_0^{2\pi} |\mathbf{X}_{\beta'}|_t\,\mathrm{d}\beta', \qquad (2)$$

where $|\mathbf{X}_\alpha|_t$ can be expressed by

$$\begin{aligned} |\mathbf{X}_\alpha|_t &= \frac{\mathbf{X}_{\alpha t}\cdot\mathbf{X}_\alpha}{|\mathbf{X}_\alpha|} = \mathbf{X}_{\alpha t}\cdot\boldsymbol{\tau}^1 = (\mathbf{X}_t)_\alpha\cdot\boldsymbol{\tau}^1 \\ &= \frac{\partial\mathbf{U}}{\partial\alpha}\cdot\boldsymbol{\tau}^1 + \frac{\partial V_1}{\partial\alpha} + \frac{\partial V_2}{\partial\alpha}\left(\boldsymbol{\tau}^2\cdot\boldsymbol{\tau}^1\right) + V_2\frac{\partial\boldsymbol{\tau}^2}{\partial\alpha}\cdot\boldsymbol{\tau}^1. \end{aligned}$$

Substituting the above equation into Eq. (2) and integrating with respect to α, we obtain

$$V_1(\alpha,\beta,t) = \frac{\alpha}{2\pi}\int_0^{2\pi} Q(\alpha',\beta,t)\,\mathrm{d}\alpha' - \int_0^{\alpha} Q(\alpha',\beta,t)\,\mathrm{d}\alpha',$$

where

$$Q(\alpha,\beta,t) = \frac{\partial \mathbf{U}}{\partial \alpha}\cdot \boldsymbol{\tau}^1 + \frac{\partial V_2}{\partial \alpha}\left(\boldsymbol{\tau}^2\cdot\boldsymbol{\tau}^1\right) + V_2\frac{\partial \boldsymbol{\tau}^2}{\partial \alpha}\cdot\boldsymbol{\tau}^1.$$

Similarly,

$$V_2(\alpha,\beta,t) = \frac{\beta}{2\pi}\int_0^{2\pi} R(\alpha,\beta',t)\,\mathrm{d}\beta' - \int_0^{\beta} R(\alpha,\beta',t)\,\mathrm{d}\beta',$$

where

$$R(\alpha,\beta,t) = \frac{\partial \mathbf{U}}{\partial \beta}\cdot \boldsymbol{\tau}^2 + \frac{\partial V_1}{\partial \beta}\left(\boldsymbol{\tau}^1\cdot\boldsymbol{\tau}^2\right) + V_1\left(\frac{\partial \boldsymbol{\tau}^1}{\partial \beta}\cdot\boldsymbol{\tau}^2\right).$$

In the above derivations, we additionally impose the boundary conditions for $V_1(0,\beta,t) = V_2(\alpha,0,t) = 0$.

Modified surfactant concentration equation

By taking the new surface parametrization

$$\mathbf{X}_t = \mathbf{U} + V_1\boldsymbol{\tau}^1 + V_2\boldsymbol{\tau}^2,$$

the material derivative $\frac{D}{Dt}$ now becomes

$$\frac{D\Gamma}{Dt} = \frac{\partial\Gamma}{\partial t} - (V_1\boldsymbol{\tau}^1 + V_2\boldsymbol{\tau}^2)\cdot\nabla_s\Gamma.$$

So the modified surfactant equation becomes

$$\frac{\partial\Gamma}{\partial t} - (V_1\boldsymbol{\tau}^1 + V_2\boldsymbol{\tau}^2)\cdot\nabla_s\Gamma + (\nabla_s\cdot\mathbf{U})\Gamma = \frac{1}{Pe_s}\Delta_s\Gamma.$$

Multiplying the surface stretching factor $|\mathbf{X}_\alpha\times\mathbf{X}_\beta|$ on both sides of the above equation and using the following identity,

$$\frac{\partial|\mathbf{X}_\alpha\times\mathbf{X}_\beta|}{\partial t} = |\mathbf{X}_\alpha\times\mathbf{X}_\beta|\nabla_s\cdot\left(\frac{\partial\mathbf{X}}{\partial t}\right) = |\mathbf{X}_\alpha\times\mathbf{X}_\beta|\nabla_s\cdot\left(\mathbf{U} + V_1\boldsymbol{\tau}^1 + V_2\boldsymbol{\tau}^2\right),$$

we obtain

$$\frac{\partial \Gamma}{\partial t}|\mathbf{X}_\alpha \times \mathbf{X}_\beta| - |\mathbf{X}_\alpha \times \mathbf{X}_\beta|(V_1\boldsymbol{\tau}^1 + V_2\boldsymbol{\tau}^2)\cdot\nabla_s\Gamma$$
$$+ \frac{\partial|\mathbf{X}_\alpha \times \mathbf{X}_\beta|}{\partial t}\Gamma - |\mathbf{X}_\alpha \times \mathbf{X}_\beta|\left[\nabla_s\cdot\left(V_1\boldsymbol{\tau}^1 + V_2\boldsymbol{\tau}^2\right)\right]\Gamma = \frac{|\mathbf{X}_\alpha \times \mathbf{X}_\beta|}{Pe_s}\Delta_s\Gamma.$$

By applying the chain rule, one can simplify the above equation as

$$\frac{\partial\left(\Gamma|\mathbf{X}_\alpha \times \mathbf{X}_\beta|\right)}{\partial t} - |\mathbf{X}_\alpha \times \mathbf{X}_\beta|\nabla_s\cdot\left[\left(V_1\frac{\mathbf{X}_\alpha}{|\mathbf{X}_\alpha|} + V_2\frac{\mathbf{X}_\beta}{|\mathbf{X}_\beta|}\right)\Gamma\right] = \frac{|\mathbf{X}_\alpha \times \mathbf{X}_\beta|}{Pe_s}\Delta_s\Gamma.$$

By directly substituting the formulas for the surface divergence and the surface Laplacian, we have the modified surfactant concentration equation

$$\frac{\partial\left(\Gamma|\mathbf{X}_\alpha \times \mathbf{X}_\beta|\right)}{\partial t} - \left[\left(\frac{|\mathbf{X}_\alpha \times \mathbf{X}_\beta|V_1\Gamma}{\sqrt{E}}\right)_\alpha + \left(\frac{|\mathbf{X}_\alpha \times \mathbf{X}_\beta|V_2\Gamma}{\sqrt{G}}\right)_\beta\right]$$
$$= \frac{1}{Pe_s}\left[\left(\frac{G\Gamma_\alpha - F\Gamma_\beta}{|\mathbf{X}_\alpha \times \mathbf{X}_\beta|}\right)_\alpha + \left(\frac{E\Gamma_\beta - F\Gamma_\alpha}{|\mathbf{X}_\alpha \times \mathbf{X}_\beta|}\right)_\beta\right].$$

Grid layouts for Eulerian and Lagrangian variables

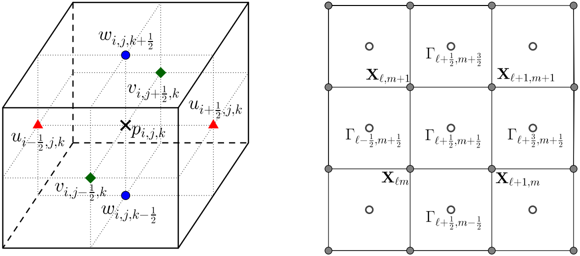

Figure: Fluid variables on a staggered MAC grid in 3D (left). The Lagrangian markers $\mathbf{X}$ and the surfactant concentration Γ (right).

We use a Fourier representation to discretize the interface as $\mathbf{X}(\alpha, \beta, t) = (\alpha, \beta, 0)^T + \mathbf{Y}(\alpha, \beta, t)$, where

$$\mathbf{Y}(\alpha, \beta, t) = \sum_{k_1=-N_1/2}^{N_1/2-1} \sum_{k_2=-N_2/2}^{N_2/2-1} \widehat{\mathbf{Y}}(k_1, k_2, t) e^{i(\alpha k_1 + \beta k_2)}.$$

Numerical algorithm

A conservative scheme for the modified surfactant equation

$$
\begin{aligned}
&\frac{\Gamma^{n+1}_{l+\frac12,m+\frac12}(S_{\alpha\beta})^{n+1}_{l+\frac12,m+\frac12}-\Gamma^{n}_{l+\frac12,m+\frac12}(S_{\alpha\beta})^{n}_{l+\frac12,m+\frac12}}{\Delta t}\\
&-\frac{1}{\Delta\alpha}\left(\frac{(S_{\alpha\beta})^{n}_{l+1,m+\frac12}(V_1)^{n+1}_{l+1,m+\frac12}\Gamma^{n}_{l+1,m+\frac12}}{\sqrt{E^{n}_{l+1,m+\frac12}}}-\frac{(S_{\alpha\beta})^{n}_{l,m+\frac12}(V_1)^{n+1}_{l,m+\frac12}\Gamma^{n}_{l,m+\frac12}}{\sqrt{E^{n}_{l,m+\frac12}}}\right)\\
&-\frac{1}{\Delta\beta}\left(\frac{(S_{\alpha\beta})^{n}_{l+\frac12,m+1}(V_2)^{n+1}_{l+\frac12,m+1}\Gamma^{n}_{l+\frac12,m+1}}{\sqrt{G^{n}_{l+\frac12,m+1}}}-\frac{(S_{\alpha\beta})^{n}_{l+\frac12,m}(V_2)^{n+1}_{l+\frac12,m}\Gamma^{n}_{l+\frac12,m}}{\sqrt{G^{n}_{l+\frac12,m}}}\right)\\
=&\frac{1}{Pe_s\Delta\alpha}\left[\frac{1}{\left(S_{\alpha\beta}\right)^{n}_{l+1,m+\frac12}}\left(G^{n}_{l+1,m+\frac12}\frac{\Gamma^{n}_{l+\frac32,m+\frac12}-\Gamma^{n}_{l+\frac12,m+\frac12}}{\Delta\alpha}-F^{n}_{l+1,m+\frac12}\frac{\Gamma^{n}_{l+1,m+1}-\Gamma^{n}_{l+1,m}}{\Delta\beta}\right)\right.\\
&\left.-\frac{1}{\left(S_{\alpha\beta}\right)^{n}_{l,m+\frac12}}\left(G^{n}_{l,m+\frac12}\frac{\Gamma^{n}_{l+\frac12,m+\frac12}-\Gamma^{n}_{l-\frac12,m+\frac12}}{\Delta\alpha}-F^{n}_{l,m+\frac12}\frac{\Gamma^{n}_{l,m+1}-\Gamma^{n}_{lm}}{\Delta\beta}\right)\right]\\
&+\frac{1}{Pe_s\Delta\beta}\left[\frac{1}{\left(S_{\alpha\beta}\right)^{n}_{l+\frac12,m+1}}\left(E^{n}_{l+\frac12,m+1}\frac{\Gamma^{n}_{l+\frac12,m+\frac32}-\Gamma^{n}_{l+\frac12,m+\frac12}}{\Delta\beta}-F^{n}_{l+\frac12,m+1}\frac{\Gamma^{n}_{l+1,m+1}-\Gamma^{n}_{l,m+1}}{\Delta\alpha}\right)\right.\\
&\left.-\frac{1}{\left(S_{\alpha\beta}\right)^{n}_{l+\frac12,m}}\left(E^{n}_{l+\frac12,m}\frac{\Gamma^{n}_{l+\frac12,m+\frac12}-\Gamma^{n}_{l+\frac12,m-\frac12}}{\Delta\beta}-F^{n}_{l+\frac12,m}\frac{\Gamma^{n}_{l+1,m}-\Gamma^{n}_{lm}}{\Delta\alpha}\right)\right],
\end{aligned}
$$

$S_{\alpha\beta} = |\mathbf{X}_\alpha \times \mathbf{X}_\beta| = \sqrt{EG - F^2}$, is the local stretching factor on the interface

$$(S_{\alpha\beta})_{l+\frac{1}{2},m} = \frac{(S_{\alpha\beta})_{lm} + (S_{\alpha\beta})_{l+1,m}}{2}$$

$$(S_{\alpha\beta})_{l+\frac{1}{2},m+\frac{1}{2}} = \frac{(S_{\alpha\beta})_{lm} + (S_{\alpha\beta})_{l+1,m} + (S_{\alpha\beta})_{l,m+1} + (S_{\alpha\beta})_{l+1,m+1}}{4}.$$

Total surfactant mass conservation:

$$\begin{aligned} & \sum_{l=0}^{N_1-1} \sum_{m=0}^{N_2-1} \Gamma^{n+1}_{l+\frac{1}{2},m+\frac{1}{2}} (S_{\alpha\beta})^{n+1}_{l+\frac{1}{2},m+\frac{1}{2}} \Delta\alpha\Delta\beta \\ = \quad & \sum_{l=0}^{N_1-1} \sum_{m=0}^{N_2-1} \Gamma^{n}_{l+\frac{1}{2},m+\frac{1}{2}} (S_{\alpha\beta})^{n}_{l+\frac{1}{2},m+\frac{1}{2}} \Delta\alpha\Delta\beta. \end{aligned}$$

Time-stepping scheme

1. Compute the tension by $\sigma_{lm} = \sigma_0(1 - \eta\Gamma^n_{lm})$ and then the interfacial tension force by

$$\mathbf{F}(\mathbf{X}^n_{lm})\mathrm{d}A(\mathbf{X}^n_{lm}) = \left(\nabla_s\sigma_{lm} - 2\sigma_{lm}H_{lm}\mathbf{n}_{lm}\right)\mathrm{d}A(\mathbf{X}^n_{lm}),$$

   where $\mathrm{d}A(\mathbf{X}^n_{lm})$ is the surface area element computed by $\mathrm{d}A(\mathbf{X}^n_{lm}) = (S_{\alpha\beta})^n_{lm}\Delta\alpha\Delta\beta$.
2. Distribute the tension force acting on Lagrangian markers into the Eulerian grid by using the smoothed Dirac delta function δ_h as

$$\mathbf{f}^n(\mathbf{x}) = \sum_{l=0}^{N_1-1}\sum_{m=0}^{N_2-1}\mathbf{F}(\mathbf{X}^n_{lm})\,\delta_h(\mathbf{x} - \mathbf{X}^n_{lm})\,\mathrm{d}A(\mathbf{X}^n_{lm}),$$

   where $\mathbf{x} = (x, y, z)$ is the Eulerian grid point and $\delta_h(\mathbf{x}) = \frac{1}{h^3}\phi\left(\frac{x}{h}\right)\phi\left(\frac{y}{h}\right)\phi\left(\frac{z}{h}\right)$ employing the 4-point supported function ϕ.

3. Find the indicator function $I(\mathbf{x})$, where $I(\mathbf{x})$ is set by 1 in the lower fluid and 0 elsewhere, so the dimensionless viscosity can be defined by $\mu = 1 + (\lambda - 1)I(\mathbf{x})$. Then solve the fluid equation

$$\frac{3\mathbf{u}^* - 4\mathbf{u}^n + \mathbf{u}^{n-1}}{2\Delta t} + 2\left(\mathbf{u}^n \cdot \nabla_h\right)\mathbf{u}^n - \left(\mathbf{u}^{n-1} \cdot \nabla_h\right)\mathbf{u}^{n-1}$$
$$= -\nabla_h p^n + \frac{1}{Re}\left[\lambda \Delta_h \mathbf{u}^* - \lambda \Delta_h \mathbf{u}^n + \nabla_h \cdot \left(\mu\left(\nabla_h \mathbf{u}^n + (\nabla_h \mathbf{u}^n)^T\right)\right)\right] + \frac{\mathbf{f}^n}{Re\,Ca},$$
$$\Delta_h p^\star = \frac{3}{2\Delta t}\nabla_h \cdot \mathbf{u}^\star, \quad \frac{\partial p^\star}{\partial \mathbf{n}} = 0 \text{ on } \partial\Omega_D, \quad \mathbf{u}^\star = \mathbf{u}^{n+1} \text{ on } \partial\Omega_D,$$
$$\mathbf{u}^{n+1} = \mathbf{u}^\star - \frac{2\Delta t}{3}\nabla_h p^\star, \quad \nabla_h p^{n+1} = \nabla_h p^\star + \nabla_h p^n - \frac{2\lambda\Delta t}{3Re}\Delta_h(\nabla_h p^\star).$$

4. Update the new position

$$\mathbf{X}_{lm}^{n+1} = \mathbf{X}_{lm}^n + \Delta t\left((V_1)_{lm}^{n+1}\left(\boldsymbol{\tau}^1\right)_{lm}^n + (V_2)_{lm}^{n+1}\left(\boldsymbol{\tau}^2\right)_{lm}^n + \sum_{\mathbf{x}} \mathbf{u}^{n+1}(\mathbf{x})\delta_h(\mathbf{x} - \mathbf{X}_{lm}^n)h^3\right).$$

5. After computing $(S_{\alpha\beta})_{l+\frac{1}{2},m+\frac{1}{2}}^{n+1}$, update the surfactant concentration distribution $\Gamma_{l+\frac{1}{2},m+\frac{1}{2}}^{n+1}$, and then apply the linear interpolation to obtain Γ_{lm}^{n+1}.

Numerical results

Numerical tests

- Effect of Lagrangian mesh control
- Convergence study for interfacial configuration, fluid velocity, and surfactant concentration
- Physical examples
  - Self-healing dynamics (inward and outward spreading)
  - Two-layer fluids in Couette flow

Numerical parameters

Unless otherwise stated, we use

- $Re = 1$, $Ca = 0.1$, $\sigma_0 = 1$, $Pe_s = 100$, and $\eta = 0.5$
- Fluid mesh size 128^3 in $[0, 2\pi]^3$, and interfacial mesh size 256^2
- Fluid meshwidth $h = 2\pi/128$ and interfacial meshwidth $\Delta\alpha = \Delta\beta = 2\pi/256$
- The time step size $\Delta t = h/4$ and the initial surfactant concentration distribution $\Gamma = 0.5$

Effect of mesh control

The initial surfactant concentration distribution is $\Gamma(\alpha,\beta,0) = \dfrac{1-\tanh(20(1-r))}{2}$, where r is the distance of Lagrangian marker from the center of the given flat interface.

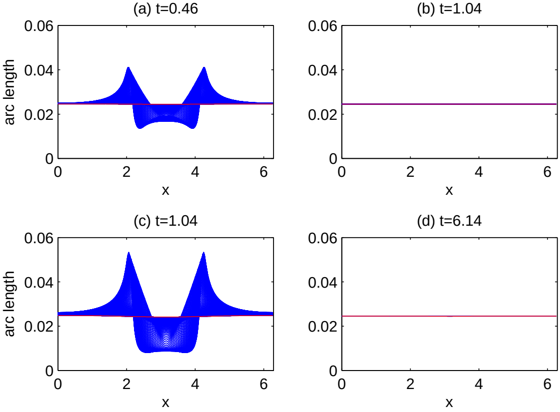

Figure: The plots of arclength $|\mathbf{X}_\alpha|\Delta\alpha$. The straight red line is the initial uniform arclength.

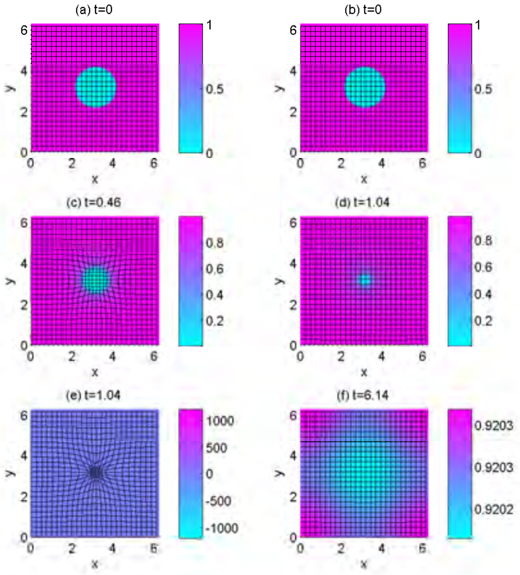

Figure: The underlying Lagrangian mesh and the corresponding surfactant concentration at different times. Left panel (without mesh control); right panel (with mesh control).

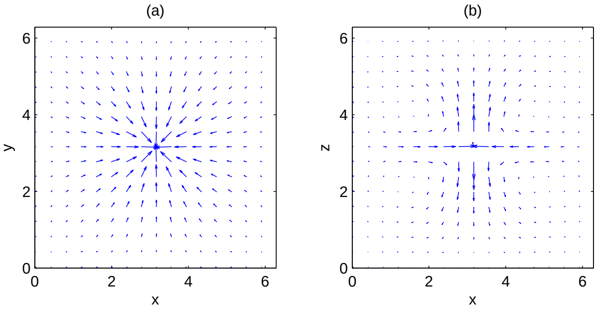

Figure: At $t = 1.04$ with mesh control. (a) the velocity field on the plane $z = \pi$; (b) the velocity field on the plane $y = \pi$.

Convergence study

- Set $Re = 1$, $Ca = 0.01$, $Pe_s = 1$, and $\eta = 0.8$
- The grid size $N = 32, 64, 128, 256$
- $h = 2\pi/N$ and $\Delta t = h/256$
- Rate $= \log_2(\|u_N - u_{2N}\|_\infty / \|u_{2N} - u_{4N}\|_\infty)$
- When $N = 32$, we use $(2N)^2 = 64^2$ number of Lagrangian markers.
- The initial surfactant concentration distribution is

$$\Gamma(\alpha, \beta, 0) = \frac{1 - \tanh(20(2 - r))}{2}$$

- The solutions are taken up to $t = 2.4$

N	$\|u_N - u_{2N}\|_\infty$	Rate	$\|v_N - v_{2N}\|_\infty$	Rate	$\|w_N - w_{2N}\|_\infty$	Rate
$T = 1.5$						
32	5.112E-02	-	5.734E-02	-	4.694E-02	-
64	2.463E-02	1.05	2.758E-02	1.06	1.933E-02	1.28
128	1.181E-02	1.06	1.287E-02	1.10	8.954E-03	1.11
$T = 2.4$						
32	3.302E-02	-	3.472E-02	-	2.109E-02	-
64	1.219E-02	1.44	1.300E-02	1.42	8.910E-03	1.24
128	5.792E-03	1.07	5.981E-03	1.12	4.433E-03	1.01

N	$\|\mathbf{X}_N - \mathbf{X}_{2N}\|_\infty$	Rate	$\|\Gamma_N - \Gamma_{2N}\|_\infty$	Rate
$T = 1.5$				
32	9.935E-02	-	1.601E-02	-
64	5.581E-02	0.83	5.973E-03	1.42
128	2.863E-02	0.96	2.635E-03	1.18
$T = 2.4$				
32	1.061E-01	-	1.028E-02	-
64	5.654E-02	0.91	3.674E-03	1.48
128	2.875E-02	0.98	1.559E-03	1.24

Table: Convergence rates of the fluid velocity $\mathbf{u} = (u, v, w)$, the Lagrangian markers $\mathbf{X}$, and the surfactant concentration Γ at time $T = 1.5$ and 2.4.

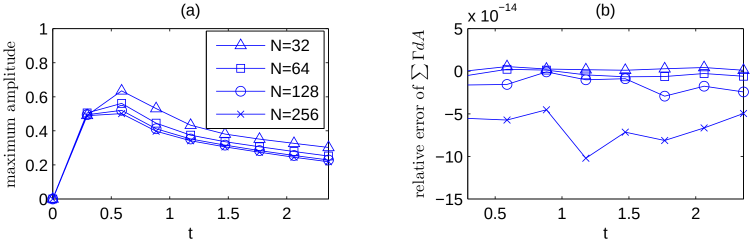

Figure: (a) the maximum amplitude of the deforming interface in the z-direction; (b) the relative error of total surfactant mass.

$$\text{error} = \left(\sum_{\ell m} \Gamma^n_{\ell+\frac{1}{2},m+\frac{1}{2}} (S_{\alpha\beta})^n_{\ell+\frac{1}{2},m+\frac{1}{2}} \Big/ \sum_{\ell m} \Gamma^0_{\ell+\frac{1}{2},m+\frac{1}{2}} (S_{\alpha\beta})^0_{\ell+\frac{1}{2},m+\frac{1}{2}} \right) - 1$$

Self-healing dynamics: inward spreading of surfactant

- Set $Re = 10^{-5}$, $Ca = 0.1$, $Pe_s = 1000$, and $\eta = 0.5$
- The dimensionless viscosity contrast $\lambda = 2$ (more viscous lower layer)
- Grid size $128 \times 128 \times 64$ in $[0, 2\pi] \times [0, 2\pi] \times [0, \pi]$
- The initially flat interface is located at $z = \pi/10$
- The initial surfactant concentration distribution is

$$\Gamma(\alpha, \beta, 0) = \frac{1 - \tanh(20(1.8 - r))}{2}$$

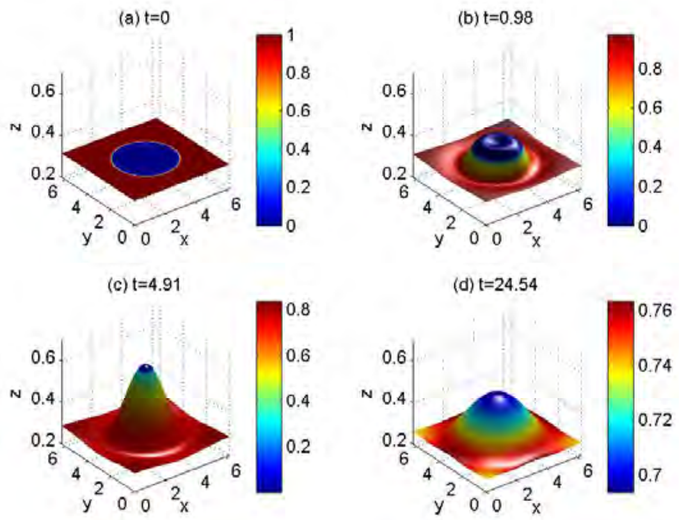

Figure: Interfacial deformations due to inward spreading of surfactant at different times. The color represents the surfactant concentration Γ.

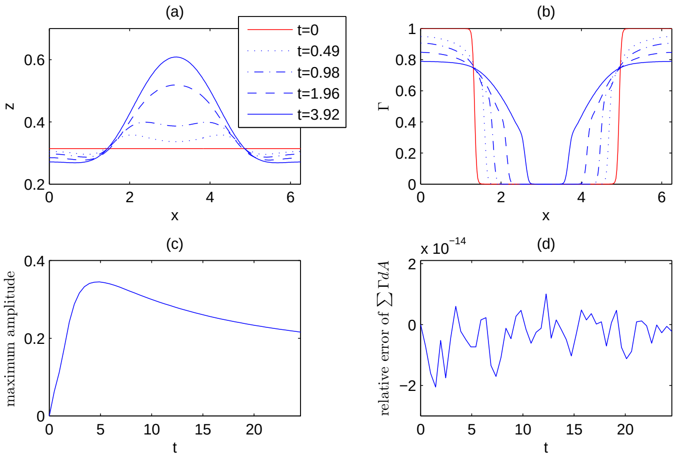

Figure: Inward spreading of surfactant. (a) the sectional view of evolving interface at $y = \pi$; (b) the corresponding surfactant concentration Γ on those curves in (a); (c) the time evolutional plot of the maximum amplitude of the deforming interface in the z-direction; (d) the relative error of total surfactant mass.

Self-healing dynamics: outward spreading of surfactant

- The initially flat interface is located at $z = 9\pi/10$
- The initial surfactant concentration distribution is

$$\Gamma(\alpha, \beta, 0) = \frac{1 + \tanh(20(1.8 - r))}{2}$$

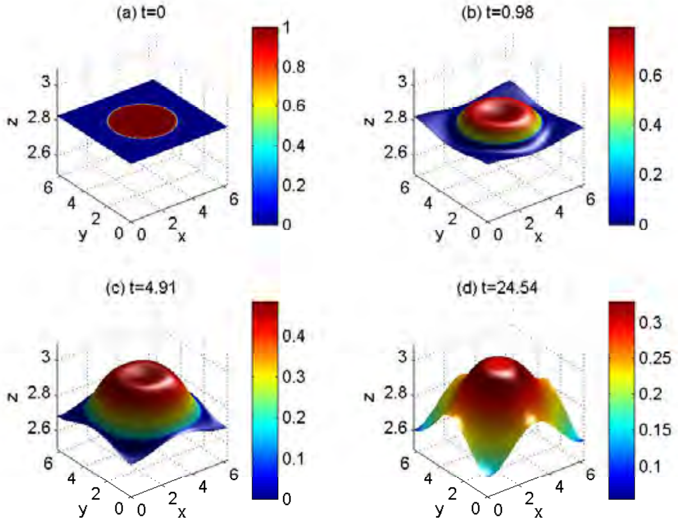

Figure: Interfacial deformations due to outward spreading of surfactant at different times. The color represents the surfactant concentration Γ.

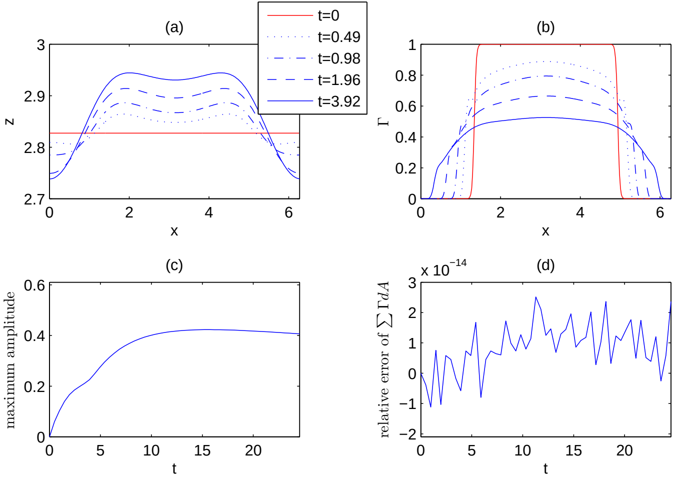

Figure: Outward spreading of surfactant. (a) the sectional view of evolving interface at $y = \pi$; (b) the corresponding surfactant concentration Γ on those curves in (a); (c) the time evolutional plot of the maximum amplitude of the deforming interface in the z-direction; (d) the relative error of total surfactant mass.

Two-layer fluids in Couette flow

- Set $Re = 1$, $Pe_s = 1000$, $\eta = 0.5$, and $\Delta t = h/32$
- The viscosity contrast $\lambda = 4$ (more viscous lower layer)
- The initial surfactant concentration distribution is $\Gamma = 0.5$
- The initially perturbed interface is configured by

$$\mathbf{X} = \left(\alpha, \beta, 2\pi/10 + 0.1 \sum_{k=1}^{3} (\sin k\alpha \sin k\beta) \right).$$

- The boundary condition is $\mathbf{u} = (z, 0, 0)$ in $[0, 2\pi]^3$
- We vary Ca from 0.2 to 0.6 to study how the different capillary number affects the interfacial deformation.

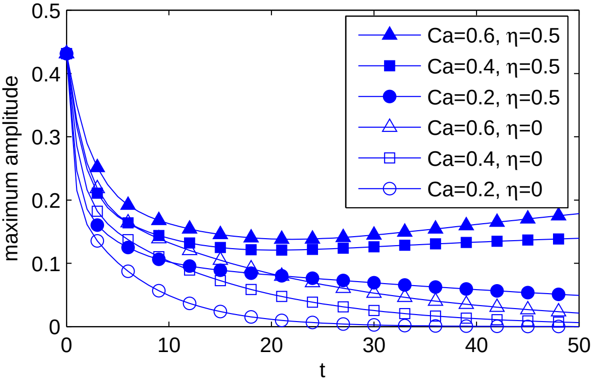

Figure: Two-layer fluids in Couette flow. The time evolutional plots of the interface maximum amplitudes for different capillary numbers $Ca = 0.2, 0.4, 0.6$. The parameter $\eta = 0$ represents the case of without surfactant while $\eta = 0.5$ represents the one with surfactant.

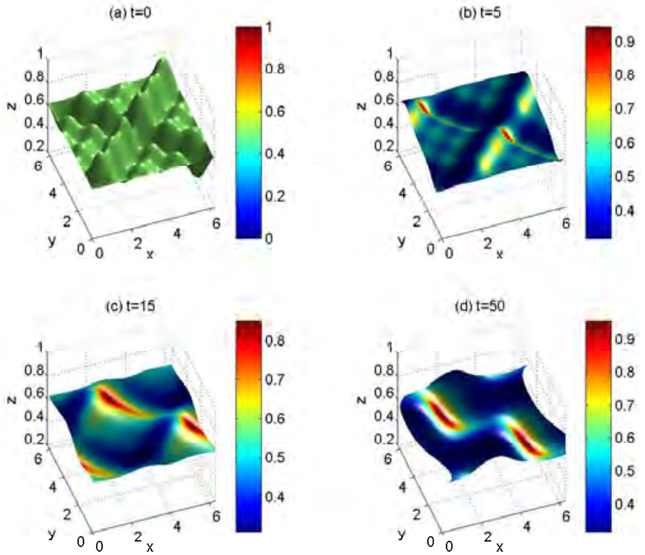

Figure: In the presence of surfactant $(\eta = 0.5, Ca = 0.6)$, the initially perturbed interface under Couette flow tends to amplify and develops into a wavy surface. The color represents the surfactant concentration Γ.

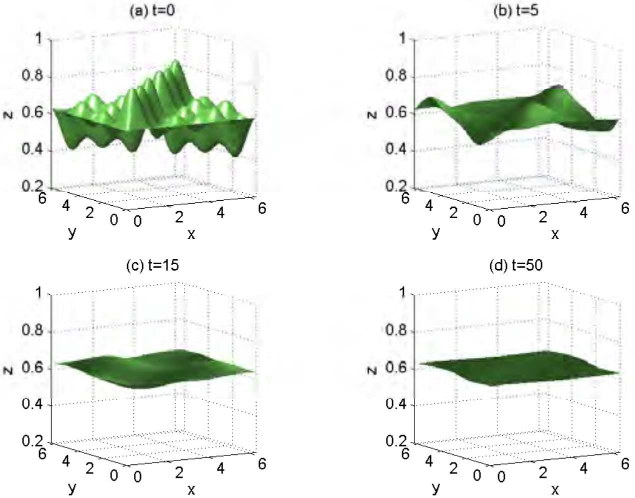

Figure: In the absence of surfactant ($\eta = 0, Ca = 0.6$), the initially perturbed interface under Couette flow tends to damp out and becomes a flat surface eventually.

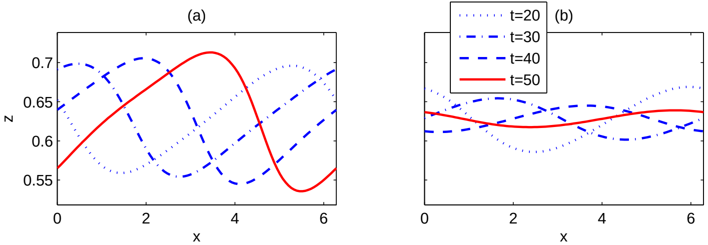

Figure: The sectional views of interface with fixed $y = \pi/2$ at different times. (a) and (b) correspond to Figures 11 and 12, respectively.

Vesicle problem: Navier-Stokes + PDE constraint on the evolving surface

- Vesicle can be visualized as a bubble of liquid within another liquid with a closed lipid membrane suspended in aqueous solution, size is about $10\mu m$
- Lipid membrane consists of tightly packed lipid molecules with hydrophilic heads facing the exterior and interior fluids and hydrophobic tails hiding in the middle, thickness is about $6nm$ so we treat the membrane as a surface (3d) or a curve (2d)
- Lipid membrane (or vesicle boundary) can deform but resist area dilation, that is surface incompressible

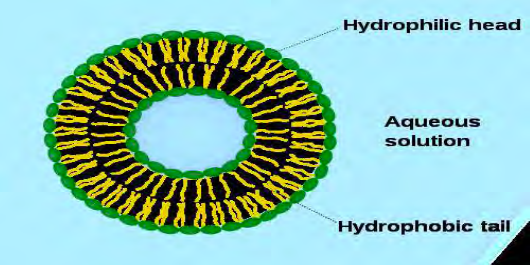

Questions: How the vesicle behaves in fluid flows?

- To mimic some mechanical behavior of red blood cells (RBC), drug carrying capsules in capillary
- Amoeboid motion (active vesicle swimmer) in confined geometry, Wu et. al. Lai & Misbah, PRE-Rapid 2015, Soft Matter 2016
- In shear flow: Tank-treading (TT), Tumbling (TU), Trembling (TR), depend on the viscosity contrast $\lambda = \mu_{in}/\mu_{out}$; Keller & Skalak JFM, 1982 (theory), Deschamps et. al. PNAS, 2009 (experiment)

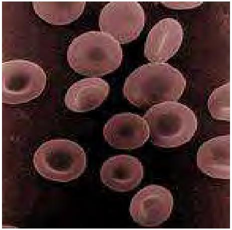

Figure: Red blood cells: flexible biconcave disks

Mathematical formulation for vesicle problem

- Vesicle: A liquid drop within another liquid with a closed lipid membrane
- Vesicle boundary Σ: fluid membrane can deform, but resist area dilation, i.e. Σ is surface incompressible
- The fluid-structure interaction is formulated by the stress balance condition on Σ

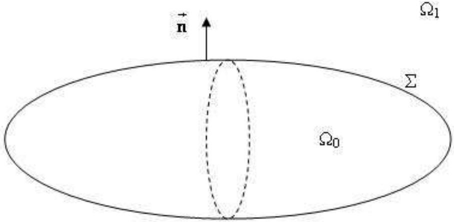

Immersed Boundary (IB) formulation: treat the vesicle boundary as a force generator

$$
\begin{aligned}
\rho\left(\frac{\partial \boldsymbol{u}}{\partial t} + \boldsymbol{u}\cdot\nabla\boldsymbol{u}\right) + \nabla p &= \mu\Delta\boldsymbol{u} + \boldsymbol{f} \qquad \text{in } \Omega \\
\nabla\cdot\boldsymbol{u} &= 0 \qquad \text{in } \Omega \\
\nabla_s\cdot\boldsymbol{U} &= 0 \qquad \text{on } \Sigma \\
\frac{\partial \mathbf{X}}{\partial t} &= \boldsymbol{U} = \int_\Omega \mathbf{u}(\mathbf{x},t)\delta(\mathbf{x}-\mathbf{X})d\mathbf{x}
\end{aligned}
$$

where the immersed boundary force

$$
\begin{aligned}
\boldsymbol{f} &= \int_\Sigma \boldsymbol{F}(\boldsymbol{X})\,\delta(\boldsymbol{x}-\boldsymbol{X})\,d\boldsymbol{X} \\
\boldsymbol{F} &= \boldsymbol{F}_b + \boldsymbol{F}_\sigma \qquad \text{on } \Sigma \\
\boldsymbol{F}_b &= c_b\left(\Delta_s H + 2H(H^2-K)\right)\,\boldsymbol{n} \\
\boldsymbol{F}_\sigma &= \nabla_s\sigma - 2\,H\,\sigma\boldsymbol{n}
\end{aligned}
$$

- H: mean curvature, K: Gaussian curvature,

$$\nabla_s = \nabla - \frac{\partial}{\partial \boldsymbol{n}}\boldsymbol{n}, \qquad \Delta_s = \nabla_s \cdot \nabla_s$$

- c_b: bending rigidity
- σ: unknown elastic tension to be introduced to enforce $\nabla_s \cdot \boldsymbol{U} = 0$
- It can be shown that the tension doesn't do extra work to the fluid; i.e. $< S(\sigma), \mathbf{u} >_\Omega = - < \sigma, \nabla_s \cdot \boldsymbol{U} >_\Gamma$
- The pressure and elastic tension have the same roles as Lagrange multipliers

Question: Where does the boundary force $\boldsymbol{F}$ come from?

Answer: Variational derivative of Helfrich energy

$$\begin{aligned} E &= \frac{c_b}{2}\int_\Sigma H^2 \, d\boldsymbol{S} + \int_\Sigma \sigma \, d\boldsymbol{S} \\ \Rightarrow \boldsymbol{F} &= -\frac{\delta E}{\delta \boldsymbol{X}} = \boldsymbol{F}_b + \boldsymbol{F}_\sigma \end{aligned}$$

Some differential geometry

Let the surface be denoted by $\Sigma(t) = \{\mathbf{X}(\alpha, \beta, t) | 0 \le \alpha \le \ell_\alpha, 0 \le \beta \le \ell_\beta\}$. Two linearly independent tangent vectors on the surface are $\mathbf{X}_\alpha = \frac{\partial \mathbf{X}}{\partial \alpha}$ and $\mathbf{X}_\beta = \frac{\partial \mathbf{X}}{\partial \beta}$, and the outward normal is $\mathbf{n} = (\mathbf{X}_\alpha \times \mathbf{X}_\beta) / |\mathbf{X}_\alpha \times \mathbf{X}_\beta|$.

$$\nabla_s \sigma = \frac{(\mathbf{X}_\beta \times \mathbf{n})\sigma_\alpha + (\mathbf{n} \times \mathbf{X}_\alpha)\sigma_\beta}{|\mathbf{X}_\alpha \times \mathbf{X}_\beta|},$$

$$\nabla_s \cdot \mathbf{U} = \frac{(\mathbf{X}_\beta \times \mathbf{n}) \cdot \mathbf{U}_\alpha + (\mathbf{n} \times \mathbf{X}_\alpha) \cdot \mathbf{U}_\beta}{|\mathbf{X}_\alpha \times \mathbf{X}_\beta|}.$$

Lemma

$$(i) \quad -2H\mathbf{n} = \frac{\mathbf{X}_\beta \times \mathbf{n}_\alpha + \mathbf{n}_\beta \times \mathbf{X}_\alpha}{|\mathbf{X}_\alpha \times \mathbf{X}_\beta|},$$

$$(ii) \quad \nabla_s \sigma - 2\sigma H\mathbf{n} = \frac{(\sigma(\mathbf{X}_\beta \times \mathbf{n}))_\alpha + (\sigma(\mathbf{n} \times \mathbf{X}_\alpha))_\beta}{|\mathbf{X}_\alpha \times \mathbf{X}_\beta|}.$$

Skew-adjoint operators, Lai & Seol, AML 2016

$$\langle \mathbf{u}, \mathbf{v} \rangle_\Omega = \int_\Omega \mathbf{u}(\mathbf{x}) \cdot \mathbf{v}(\mathbf{x})\,\mathrm{d}\mathbf{x},$$
$$\langle f, g \rangle_\Gamma = \int_\Gamma f(S)\, g(S)\,\mathrm{d}S,$$

Define $S(\sigma) = \int_\Gamma (\nabla_s \sigma - 2\sigma H \mathbf{n})\, |\mathbf{X}_\alpha \times \mathbf{X}_\beta|\, \delta(\mathbf{x} - \mathbf{X}(\alpha,\beta,t))\,\mathrm{d}\alpha\mathrm{d}\beta$, then

$$\begin{aligned}
& \langle S(\sigma), \mathbf{u} \rangle_\Omega \\
= \; & \int_\Omega \left[\int_\Gamma (\nabla_s \sigma - 2\sigma H \mathbf{n})\, |\mathbf{X}_\alpha \times \mathbf{X}_\beta|\, \delta(\mathbf{x} - \mathbf{X}(\alpha,\beta,t))\,\mathrm{d}\alpha\mathrm{d}\beta\right] \cdot \mathbf{u}(\mathbf{x})\,\mathrm{d}\mathbf{x} \\
= \; & \int_\Gamma (\nabla_s \sigma - 2\sigma H \mathbf{n}) \cdot \mathbf{U}(\alpha,\beta,t)\, |\mathbf{X}_\alpha \times \mathbf{X}_\beta|\ \mathrm{d}\alpha\mathrm{d}\beta \\
= \; & \int_\Gamma \sigma_\alpha (\mathbf{X}_\beta \times \mathbf{n}) \cdot \mathbf{U} + \sigma_\beta (\mathbf{n} \times \mathbf{X}_\alpha) \cdot \mathbf{U} - 2\sigma H \mathbf{n} \cdot \mathbf{U}\, |\mathbf{X}_\alpha \times \mathbf{X}_\beta|\ \mathrm{d}\alpha\mathrm{d}\beta \\
= \; & \int_\Gamma (\sigma(\mathbf{X}_\beta \times \mathbf{n}))_\alpha \cdot \mathbf{U} + (\sigma(\mathbf{n} \times \mathbf{X}_\alpha))_\beta \cdot \mathbf{U} \\
& - [\sigma(\mathbf{X}_\beta \times \mathbf{n})_\alpha + \sigma(\mathbf{n} \times \mathbf{X}_\alpha)_\beta + 2\sigma H \mathbf{n}\, |\mathbf{X}_\alpha \times \mathbf{X}_\beta|] \cdot \mathbf{U}\,\mathrm{d}\alpha\mathrm{d}\beta \\
= \; & -\int_\Gamma \sigma(\mathbf{X}_\beta \times \mathbf{n}) \cdot \mathbf{U}_\alpha + \sigma(\mathbf{n} \times \mathbf{X}_\alpha) \cdot \mathbf{U}_\beta\,\mathrm{d}\alpha\mathrm{d}\beta \\
& (\text{since } \sigma(\mathbf{X}_\beta \times \mathbf{n})_\alpha + \sigma(\mathbf{n} \times \mathbf{X}_\alpha)_\beta + 2\sigma H \mathbf{n}\, |\mathbf{X}_\alpha \times \mathbf{X}_\beta| = 0) \\
= \; & -\int_\Gamma \sigma(\nabla_s \cdot \mathbf{U})\, |\mathbf{X}_\alpha \times \mathbf{X}_\beta|\ \mathrm{d}\alpha\mathrm{d}\beta = -\langle \sigma, \nabla_s \cdot \mathbf{U} \rangle_\Gamma
\end{aligned}$$

Remark: Tension does not do extra work to the fluid. Similar to the pressure in incompressible fluid!

Numerical issues:

1. Coupled with fluid dynamics which vesicle boundary is moving with fluid and whose shape is not known *a priori*
2. Both the volume and the surface area of the vesicle are conserved. How to maintain fluid and vesicle boundary incompressible simultaneously?
3. Need to find H, $\Delta_s H$, $\boldsymbol{n}$, K on a moving surface Σ
4. In additional to the fluid incompressibility, we need extra constraint (surface incompressibility) on the surface
5. The role of pressure p on fluid equations is the same as the role of tension σ on $\nabla_s \cdot \boldsymbol{U} = 0$. Both conditions are local!
6. How to solve the above governing equations efficiently?
7. Boundary integral method, Immersed boundary (Front-tracking), Level-set, or Phase field method?

IB and IIM simulations for vesicle problems

- Kim & Lai JCP 2010, 2D penalty IB method
- Li & Lai EAJAM 2011, IIM for 2D inextensible interface
- Kim & Lai PRE 2012, study the inertial effect on tumbling inhibition
- Lai, Hu & Lin SISC 2012, a compound inextensible interface with a solid particle, skew-adjoint operators
- Hu, Kim & Lai JCP 2014, 3D axis-symmetric case, nearly incompressible approach
- Hsieh, Lai, Yang & You JSC 2015, an unconditionally energy stable IB method for a compound inextensible interface with a solid particle
- Wu, Fai, Atzberger & Peskin SISC 2015, SIBM for osmotic swelling of vesicles
- Seol, Hu, Kim & Lai JCP 2016, 3D vesicle simulations under shear flow

Nearly surface incompressibility approach

- $\nabla_s \cdot \mathbf{U} = 0$ means that $\frac{\partial}{\partial t}|\mathbf{X}_r \times \mathbf{X}_s| = 0$
- To avoid solving the extra unknown tension $\sigma(r, s, t)$, we alternatively use a spring-like elastic tension

$$\sigma = \sigma_0 \left(|\mathbf{X}_r \times \mathbf{X}_s| - |\mathbf{X}_r^0 \times \mathbf{X}_s^0|\right)$$

  where $\sigma_0 \gg 1$ and $|\mathbf{X}_r^0 \times \mathbf{X}_s^0|$ is the initial surface dilating factor
- Similar idea has been used in level set framework by Maitre, Misbah, Peyla & Raoult, Physica D 2012
- The modified elastic energy by

$$E_\sigma(\mathbf{X}) = \frac{\sigma_0}{2} \iint \left(|\mathbf{X}_r \times \mathbf{X}_s| - |\mathbf{X}_r^0 \times \mathbf{X}_s^0|\right)^2 \, drds$$

Derivation of modified elastic force by variational derivative

$$
\begin{aligned}
&\frac{d}{d\varepsilon}E_\sigma(\mathbf{X}+\varepsilon\mathbf{Y})\Big|_{\varepsilon=0} \\
&= \iint \sigma_0\left(|\mathbf{X}_r\times\mathbf{X}_s| - |\mathbf{X}_r^0\times\mathbf{X}_s^0|\right)\frac{\mathbf{X}_r\times\mathbf{X}_s}{|\mathbf{X}_r\times\mathbf{X}_s|}\cdot(\mathbf{Y}_r\times\mathbf{X}_s+\mathbf{X}_r\times\mathbf{Y}_s)\,drds \\
&= \iint \sigma\mathbf{n}\cdot(\mathbf{Y}_r\times\mathbf{X}_s+\mathbf{X}_r\times\mathbf{Y}_s)\,drds \quad \left(\text{by } \mathbf{n}=\frac{\mathbf{X}_r\times\mathbf{X}_s}{|\mathbf{X}_r\times\mathbf{X}_s|}\right) \\
&= \iint \sigma(\mathbf{X}_s\times\mathbf{n})\cdot\mathbf{Y}_r+\sigma(\mathbf{n}\times\mathbf{X}_r)\cdot\mathbf{Y}_s\,drds \quad (\text{by the scalar triple product formula}) \\
&= -\iint(\sigma\mathbf{X}_s\times\mathbf{n})_r\cdot\mathbf{Y}+(\sigma\mathbf{n}\times\mathbf{X}_r)_s\cdot\mathbf{Y}\,drds \quad (\text{by integration by parts}) \\
&= -\iint\left[\sigma_r\mathbf{X}_s\times\mathbf{n}+\sigma_s\mathbf{n}\times\mathbf{X}_r+\sigma(\mathbf{X}_s\times\mathbf{n})_r+\sigma(\mathbf{n}\times\mathbf{X}_r)_s\right]\cdot\mathbf{Y}\,drds \\
&= -\iint(\sigma_r\mathbf{X}_s\times\mathbf{n}+\sigma_s\mathbf{n}\times\mathbf{X}_r+\sigma\mathbf{X}_s\times\mathbf{n}_r+\sigma\mathbf{n}_s\times\mathbf{X}_r)\cdot\mathbf{Y}\,drds \\
&= -\iint(\nabla_s\sigma-2\sigma H\mathbf{n})\cdot\mathbf{Y}\,|\mathbf{X}_r\times\mathbf{X}_s|\,drds \\
&= -\int_\Gamma(\nabla_s\sigma-2\sigma H\mathbf{n})\cdot\mathbf{Y}\,\mathrm{d}A \quad (\text{since } \mathrm{d}A=|\mathbf{X}_r\times\mathbf{X}_s|\,drds) \\
&= -\int_\Gamma\mathbf{F}_\sigma\cdot\mathbf{Y}\,\mathrm{d}A \qquad \mathbf{F}_\sigma\ \text{are exactly identical !}
\end{aligned}
$$

Numerical algorithm

1. Compute the tension force $\mathbf{F}_\sigma^n$ associated with the spring-like tension and the bending force $\mathbf{F}_b^n$
2. Distribute the interfacial force terms $\mathbf{F}_\sigma^n$ and $\mathbf{F}_b^n$ from the Lagrangian markers to the fluid grid points by using the discrete delta function as in traditional IB method
3. Solve the Navier-Stokes equations by the pressure-increment projection method to obtain new velocity field $\mathbf{u}^{n+1}$
4. Interpolate the new velocity on the fluid grid point to the marker points and then move the marker points to new positions $\mathbf{X}^{n+1}$

Axis-symmetric case, Hu, Kim & Lai, JCP 2014

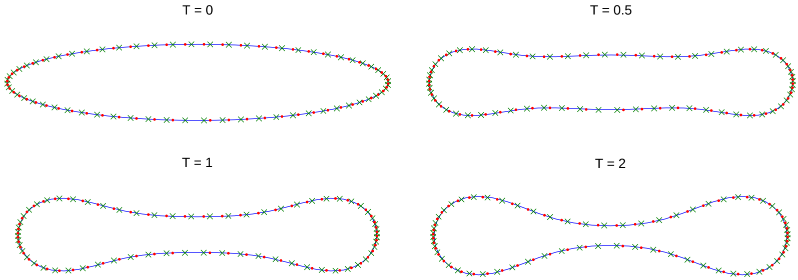

Figure: Freely suspended vesicles with different penalty number σ_0. Blue solid line: $\sigma_0 = 2 \times 10^3$; green marker "×": $\sigma_0 = 2 \times 10^4$; red marker "·": $\sigma_0 = 2 \times 10^5$.

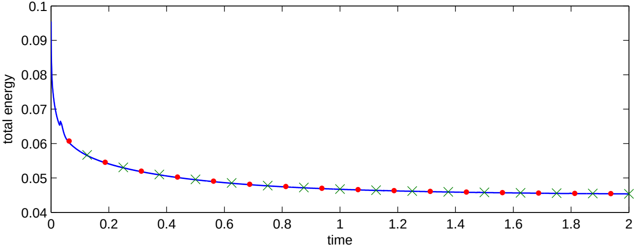

Figure: The corresponding evolution of total energy. Blue solid line: $\sigma_0 = 2 \times 10^3$; green marker "$\times$": $\sigma_0 = 2 \times 10^4$; red marker "$\cdot$": $\sigma_0 = 2 \times 10^5$

σ_0	$\\|R\,\lvert\mathbf{X}_s\rvert - R^0\,\lvert\mathbf{X}_s\rvert^0\\|_\infty$	$\lvert A_h - A_0\rvert/A_0$	$\lvert V_h - V_0\rvert/V_0$
2×10^3	2.988E-04	2.431E-03	9.391E-04
2×10^4	6.551E-05	2.060E-04	2.865E-04
2×10^5	2.903E-05	2.105E-05	2.657E-04

Table: The errors of the area dilating factor, the total surface area, and the volume.

Full 3D case: Seol, Hu, Kim & Lai JCP 2016

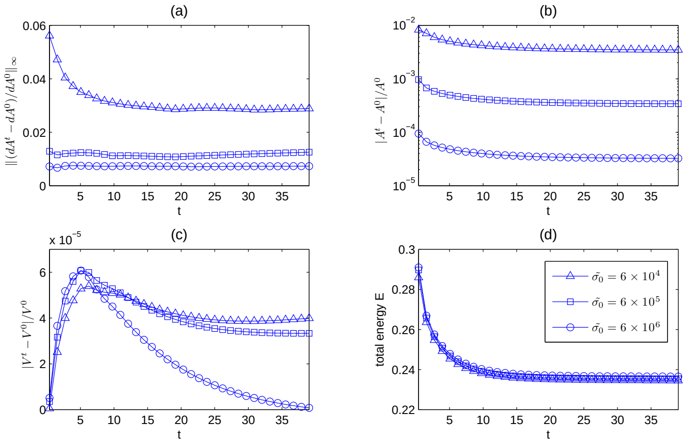

Figure: The comparison for three different stiffness parameters: $\tilde{\sigma_0} = 6 \times 10^4(\triangle)$, $6 \times 10^5(\square)$, and $6 \times 10^6(\bigcirc)$. (a) the maximum relative error of the local surface area; (b) the relative error of the global surface area; (c) the relative error of the global volume; (d) the total energy.

Vesicle under shear flow

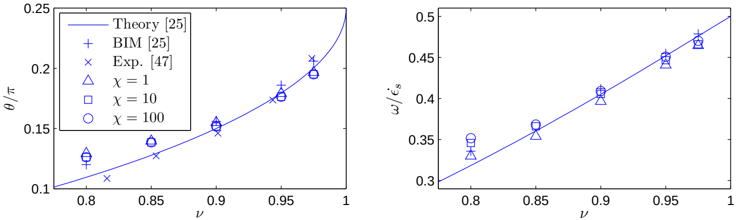

Figure: The plot of the inclination angle (left) and the scaled mean angular frequency (right) as functions of reduced volume ν for different dimensionless shear rate χ.

- The frequency ω can be computed using $\omega = \frac{1}{N_v}\sum_{i=1}^{N_v}\frac{|\mathbf{r}\times\mathbf{v}|}{|\mathbf{r}|^2}$, where $\mathbf{r}$ and $\mathbf{v}$ are the position and velocity of the vertices projected on the xz-plane, respectively.